

Water Quality Modeling and Monitoring in the California North Delta Area

BY

Raffi Jirair Moughamian

THESIS

Submitted in partial satisfaction of the requirements of the degree of

MASTER OF SCIENCE

in

CIVIL AND ENVIRONMENTAL ENGINEERING

In the

OFFICE OF GRADUATE STUDIES

Of the

UNIVERISTY OF CALIFORNIA, DAVIS

Approved:

S.G. Schladow

Wm. E. Fleenor

J. F. Mount

Committee in Charge

2005

## **ABSTRACT**

A water quality model, including salinity and temperature, has been linked to a one-dimensional, MIKE 11 hydraulic model of the northern part of the Sacramento-San Joaquin Delta (the North Delta). It was produced to examine any water quality effects that the restoration might have on the region, the effect of regional scale changes on the restoration area and to produce local boundary conditions for future multi-dimensional modeling of the restoration area.

Temperature and electrical conductivity data were collected at the boundaries of the North Delta model to facilitate the calibration and verification of the water quality model. Continuous water quality data was collected in order to create a database used in this study and possibly in future studies in the North Delta. The model was used to examine various restoration alternatives involving McCormack-Williamson Tract and the Delta Cross channel during the summer low flow periods. The results from the model illustrate that the restoration alternatives which change flow also alter the water quality. It was discovered that the restoration alternatives involving McCormack-Williamson Tract produce highly localized changes in water temperature and electrical conductivity around the altered tract while only slight changes occur upstream and downstream. Furthermore we found that the MIKE 11 water temperature model can only capture general trends, neglecting smaller events that can occur.

## TABLE OF CONTENTS

<b>Introduction.....</b>	<b>1</b>
<b>Background.....</b>	<b>3</b>
<i>Study Area.....</i>	3
<i>Previous Studies.....</i>	4
<b>Model Study Area.....</b>	<b>12</b>
<b>Data Correlations.....</b>	<b>16</b>
<i>Water Temperature.....</i>	16
<i>Electrical Conductance.....</i>	17
<b>Model Description.....</b>	<b>20</b>
<i>Hydrodynamics.....</i>	20
<i>Electrical Conductivity Modeling.....</i>	21
<i>Water Temperature Modeling.....</i>	22
<b>Calibration.....</b>	<b>23</b>
<i>Electrical Conductivity Model Calibration.....</i>	28
<i>Water Temperature Model Calibration .....</i>	30
<b>Sensitivity Analysis.....</b>	<b>36</b>
<i>Electrical Conductivity Model Sensitivity Analysis.....</i>	36
<i>Water Temperature Model Sensitivity Analysis.....</i>	42
<b>Scenarios.....</b>	<b>50</b>
<b>Scenario Results.....</b>	<b>55</b>
<b>Discussion and Conclusions.....</b>	<b>64</b>
<b>References.....</b>	<b>66</b>

<b>Appendix A</b>	<b>68</b>
<b>Appendix B</b>	<b>72</b>
<b>Appendix C</b>	<b>79</b>
<b>Appendix D</b>	<b>86</b>
<b>Appendix E</b>	<b>90</b>
<b>Appendix F</b>	<b>95</b>
<b>Appendix G</b>	<b>105</b>
<b>Appendix H</b>	<b>113</b>

## LIST OF FIGURES

<b>Figure 1:</b> Study area of Cosumnes-Mokelumne-North Delta modeling effort.....	6
<b>Figure 2:</b> McCormack-Williamson Tract and the Delta Cross Channel location map, showing the locations of New Hope and Benson's Ferry. The McCormack-Williamson Tract is bordered by Lost Slough to the north, the Mokelumne River to the southeast, and Snodgrass Slough to the west. The Delta Cross Channel (DCC) hydraulically connects the Sacramento River to Snodgrass Slough when DCC gates are open.....	7
<b>Figure 3:</b> Aerial photograph of the Delta Cross Channel.....	8
<b>Figure 4:</b> The extent of the MIKE 11 model with boundary condition and internal comparison locations. Six upstream boundary conditions are present located at Michigan Bar on the Cosumnes River (MB), Wilton Road on Deer Creek (WR), Galt on Dry Creek (GA), Woodbridge on the Mokelumne River (WB), Lambert Road on Stone Lakes Outlet (SN), and above the Delta Cross Channel on the Sacramento River (US). Five downstream boundary conditions located below Georgiana Slough divergence on the Sacramento River (LS), on the San Joaquin River at San Andres Landing (SA), Venice Island (VI), Turner Cut (TC), and Rindle Pump (RP). Three internal comparison locations at Bensons Ferry (BF), New Hope (NH) and South Staten Island (SS) used to calibrate and validate model.....	13
<b>Figure 5:</b> An of Onset Optic StowAway Temp water temperature probe.....	15
<b>Figure 6:</b> A Richard Brancker Research (RBR) data logger with two D cell batteries... <td>15</td>	15
<b>Figure 7:</b> Benson's Ferry, looking downstream along the Mokelumne River during construction of new bridge.....	18
<b>Figure 8:</b> New Hope, looking downstream from Wimpy's Marina along the South Fork of the Mokelumne River.....	19
<b>Figure 9:</b> Comparison of measured and modeled water stage at Benson's Ferry in 2003 and 2004.....	24
<b>Figure 10:</b> Comparison of measured and modeled water stage at New Hope in 2003 and 2004.....	25
<b>Figure 11:</b> Comparison of measured and modeled water stage at Benson's Ferry in 2000.....	27
<b>Figure 12:</b> Comparison of measured and modeled water stage at Benson's Ferry in 1986.....	27

<b>Figure 13:</b> 2004 Observed and modeled electrical conductivity data at New Hope and South Staten.....	29
<b>Figure 14:</b> Daily averaged air temperature at Woodbridge Dam for summer of 2003 and 2004. Data were measured by East Bay Municipal Utility District.....	31
<b>Figure 15:</b> Mokelumne River just downstream of Benson's Ferry, looking upstream....	32
<b>Figure 16:</b> South Fork Mokelumne River near Sycamore Slough.....	32
<b>Figure 17:</b> Comparison of observed and modeled water temperature data for 2003 at both Benson's Ferry and New Hope.....	33
<b>Figure 18:</b> Comparison of observed and modeled water temperature data for 2004 at both Benson's Ferry and New Hope.....	34
<b>Figure 19:</b> Discharge of the Mokelumne River for measured at Woodbridge Dam during the summer months of 2003 and 2004.....	35
<b>Figure 20:</b> Calibrated 2004 electrical conductivity run plotted with the 2004 electrical conductivity run with a 20% increase of Mokelumne flow at Benson's Ferry....	38
<b>Figure 21:</b> Calibrated 2004 electrical conductivity run plotted with 2004 electrical conductivity run with a 20% increase in Sacramento flow at New Hope.....	38
<b>Figure 22:</b> Calibrated 2004 electrical conductivity run plotted with 2004 electrical conductivity run with a 20% increase in Sacramento flow at South Staten.....	38
<b>Figure 23:</b> Calibrated 2004 electrical conductivity run plotted with 2004 electrical conductivity run at New Hope with doubled dispersion coefficient values in all reaches.....	41
<b>Figure 24:</b> Calibrated 2004 electrical conductivity run plotted with 2004 electrical conductivity run at South Staten with doubled dispersion coefficient values in all reaches.....	41
<b>Figure 25:</b> Calibrated 2003 water temperature run plotted with 2003 water temperature run with a 20% increase of Mokelumne flow at Benson's Ferry.....	47
<b>Figure 26:</b> Calibrated 2003 water temperature run plotted with 2003 water temperature run with a 20% increase of Mokelumne flow at New Hope.....	47
<b>Figure 27:</b> Calibrated 2004 water temperature run plotted with 2004 water temperature run with a 20% increase of Mokelumne flow at Benson's Ferry.....	49

<b>Figure 28:</b> Calibrated 2004 water temperature run plotted with 2004 water temperature run with a 20% increase of Mokelumne flow at New Hope.....	49
<b>Figure 29:</b> Scenario one: minimum control and maximum fluvial flow.....	52
<b>Figure 30:</b> Scenario two: maximum control of water in and out of tract.....	53
<b>Figure 31:</b> Scenario three: a hybrid of subsidence reversal and season floodplain.....	54
<b>Figure 32:</b> Comparison of calibrated base case plotted with the application of scenario 1 to 2003 at New Hope.....	57
<b>Figure 33:</b> Comparison of calibrated base case plotted with the application of scenario 1 to 2004 at New Hope.....	57
<b>Figure 34:</b> Comparison of calibrated base case plotted with scenario 1 for 2004 electrical conductivity at Benson's Ferry.....	59
<b>Figure 35:</b> Comparison of calibrated base case plotted with scenario 1 for 2004 electrical conductivity at South Staten.....	59
<b>Figure 36:</b> Comparison of calibrated base case plotted with scenario 1 for 2004 electrical conductivity at New Hope.....	59
<b>Figure 37:</b> Comparison of water temperatures at New Hope when DCC is open (calibrated base case) to when DCC is closed in 2004.....	61
<b>Figure 38:</b> Comparison of at New Hope when DCC is open (calibrated base case) to when DCC is closed in 2003.....	61
<b>Figure 39:</b> Scenario four at Benson's Ferry where the Delta Cross Channel (DCC) is closed with the calibrated base case that has the DCC open.....	63
<b>Figure 40:</b> Scenario four at New Hope where the Delta Cross Channel (DCC) is closed with the calibrated base case that has the DCC open.....	63
<b>Figure 41:</b> Scenario four at South Staten where the Delta Cross Channel (DCC) is closed with the calibrated base case that has the DCC open.....	63

## LIST OF TABLES

<b>Table 1:</b> Correlation coefficients of the water and air temperature at Benson's Ferry and New Hope during the summer of 2003 and 2004. Refer to Appendix A for the data and trend lines of the correlations.....	17
<b>Table 2:</b> Correlation coefficients of the tidal exchange and water temperature at Benson's Ferry and New Hope during the summer of 2003 and 2004. Refer to Appendix A for the data and trend lines of the correlations.....	17
<b>Table 3:</b> Correlation coefficients of the tidal exchange with electrical conductivity and air temperature with electrical conductivity at New Hope during the summer of 2004. Refer to Appendix A for the data and trend lines of the correlations.....	18
<b>Table 4:</b> 2003 water temperature model variables (lower reaches refer to reaches below New Hope, while the middle reaches are between Benson's Ferry and New Hope).....	30
<b>Table 5:</b> 2004 water temperature model variables (lower reaches refer to reaches below New Hope, while the middle reaches are between Benson's Ferry and New Hope).....	30
<b>Table 6:</b> Average and maximum percent difference between calibrated model electrical conductivity results and increase flow model results. Appendix E has all graphical plots of this sensitivity analysis.....	37
<b>Table 7:</b> The average and maximum percent difference found in the varied dispersion coefficient runs with the calibrated 2004 runs for electrical conductivity. Appendix D has all the graphical plots of this sensitivity analysis.....	39
<b>Table 8:</b> Average and maximum percent difference of 2003 runs where maximum absorbed solar radiation was changed by 20%, compared to the calibrated 2003 runs. Appendix B and C have all the graphical plots of this sensitivity analysis.....	43
<b>Table 9:</b> Average and maximum percent difference of 2004 runs where maximum absorbed solar radiation was changed by 20% compared to the calibrated 2004 runs. Appendix B and C have all the graphical plots of this sensitivity analysis.....	44
<b>Table 10:</b> Average and maximum percent difference of 2003 runs where emitted heat radiation was changed by 20% compared to the calibrated 2003 runs. Appendix B and C have all the graphical plots of this sensitivity analysis.....	44

<b>Table 11:</b> Average and maximum percent difference of 2004 runs where emitted heat radiation was changed by 20% compared to the calibrated 2004 runs. Appendix B and C have all the graphical plots of this sensitivity analysis.....	45
<b>Table 12:</b> Average and maximum percent difference between calibrated model water temperature results and increase flow model results for 2003. Appendix E has all the graphical plots of this sensitivity analysis.....	46
<b>Table 13:</b> Average and maximum percent difference between calibrated water temperature model with and increase flow model results for 2004 at Benson's Ferry and New Hope. Appendix E has all the graphical plots of this sensitivity analysis.....	48

## INTRODUCTION

Over 90% of the tidal freshwater wetlands of the Delta regions have been isolated by levees, removing them from tidal and flood inundation (Simenstad et al., 2000). Currently there are efforts to try and restore some of these historical wetlands to their original tidal inundation state. The California-Federal Bay/Delta Program (CALFED) has proposed the restoration of tidal freshwater ecosystems by reconnecting regions currently managed for agricultural purposes to their adjacent rivers and sloughs (CALFED, 2000).

The effect of these proposed actions on water stage and discharge has been examined (Hammersmark, 2002), however their implications on water quality (e.g. water temperature and electrical conductivity) upstream and downstream of the changes are not known. This study is a first attempt at addressing this issue. Water quality data have been collected and are used to calibrate and validate a water quality model. The model is then used to examine the effects of the proposed management scenarios for a north Delta island (McCormack-Williamson Tract) on two water quality parameters, water temperature and electrical conductivity. Since almost two thirds of California residents depend on the Delta for their water supply, a high water quality standard is required (California Department of Water Resources, 1991). These management scenarios can alter the water temperature and salinity levels in the water which in turn alters the metabolic rates and food demands of fish that depend on this water for survival (Beschta et al., 1987). A one-dimensional hydraulic model coupled with water quality capabilities was the main tool used to explore the scenarios' effects. The management scenarios were developed based on input from various stakeholder groups, including The Nature

Conservancy, CALFED, the California Department of Water Resources, and the Cosumnes Research Group. Most of these scenarios involved degrading levees, or creating new channels on McCormack-Williamson Tract. Another management scenario involved examination of alternatives to the regular operation of the Delta Cross Channel, a gate structure that connect the Sacramento River to the north Delta area.

## BACKGROUND

### *Study Area*

The McCormack-Williamson Tract is a 652-ha (1,612-acre) island in the North Sacramento-San Joaquin Delta of California (Figure 1). The McCormack-Williamson Tract is demarcated by the Mokelumne River on its southeast side, Snodgrass Slough on the west side, and a dredged canal, Lost Slough, along the north side. Around the McCormack-Williamson Tract a semi-diurnal tidal pattern is present with the average tidal range during low river flow conditions ~1m (NOAA, 2002).

Historically, the McCormack-Williamson Tract supported tidal freshwater marsh and riverine floodplain habitats (USGS, 1911; Brown and Pasternack, 2004). However, with the agricultural boom at the turn of the 20<sup>th</sup> century that changed. In 1934 the levees that surround the McCormack-Williamson Tract were raised to reclaim the land for agricultural use (State of California Reclamation Board, 1941). Creating these levees has resulted in most of the land on the tract being below mean sea level, due to the subsidence associated with oxidation of peat soils (Rojstaczer et al., 1991). The current topography of the McCormack-Williamson Tract ranges in elevation from -0.9m to 1.5m (-3ft to +5 ft) NGVD 29 (California Department of Water Resources, 1992; California Department of Water Resources, 2002).

The McCormack-Williamson Tract is about 2.4 km downstream of the confluence of the Cosumnes and Mokelumne Rivers at Benson's Ferry (Figure 2). It is also 1.3 km east of the Delta Cross Channel (DCC). The Delta Cross Channel, Figure 3, is a gate structure that hydraulically connects the Delta to the Sacramento River when open. The Bureau of Reclamation built the structure in 1953. Originally the gates were

closed only when high Sacramento River flows threatened to flood the Delta. However, now it is only open during the summertime and also during the weekends leading up to the summer. It not only allows Sacramento River water to travel into the Delta, but is an important connection for recreational boaters. The Delta Cross Channel gates stand 4.3m above mean sea level (msl) (14 ft) of the Sacramento River when in the open position. When the Delta Cross Channel is open, it greatly alters the flow of the Sacramento River and the Delta. Over a single 25 day period the flow upstream of the Cross Channel along the Sacramento River decreased by 2,000cfs, when the gates were open (Oltmann et al., 1999).

Upstream of McCormack-Williamson Tract and the Delta Cross Channel there are two very different rivers feeding the north delta: the Cosumnes and Mokelumne. The Mokelumne is a heavily regulated river with three major dams controlling its flow. The most-downstream is the Woodbridge Dam which is approximately 30 km upstream of Benson's Ferry, and is operated by the local Woodbridge Irrigation District. The next is Camanche Dam, which is operated by East Bay Municipal Utility District, and is located about 60 km upstream of Benson's Ferry. The third is Pardee dam, also operated by East Bay Municipal Utility District approximately 10km upstream from Camanche Dam. The Cosumnes River, by contrast, is largely unregulated, except for one dam in the upper watershed, and is therefore prone to high flood peaks during the wet season and no flow during the summertime. During the two most-recent floods events in the Delta, the Cosumnes River had a peak flow of 2630cms (92800cfs) in 1997 and 1170cms (41300cfs) in 1986. Both flows were recorded at Michigan Bar far upstream in the North

Delta area, while the Mokelumne River had a constant 150cms (5300cfs) flowing out of Woodbridge Dam during both those events.

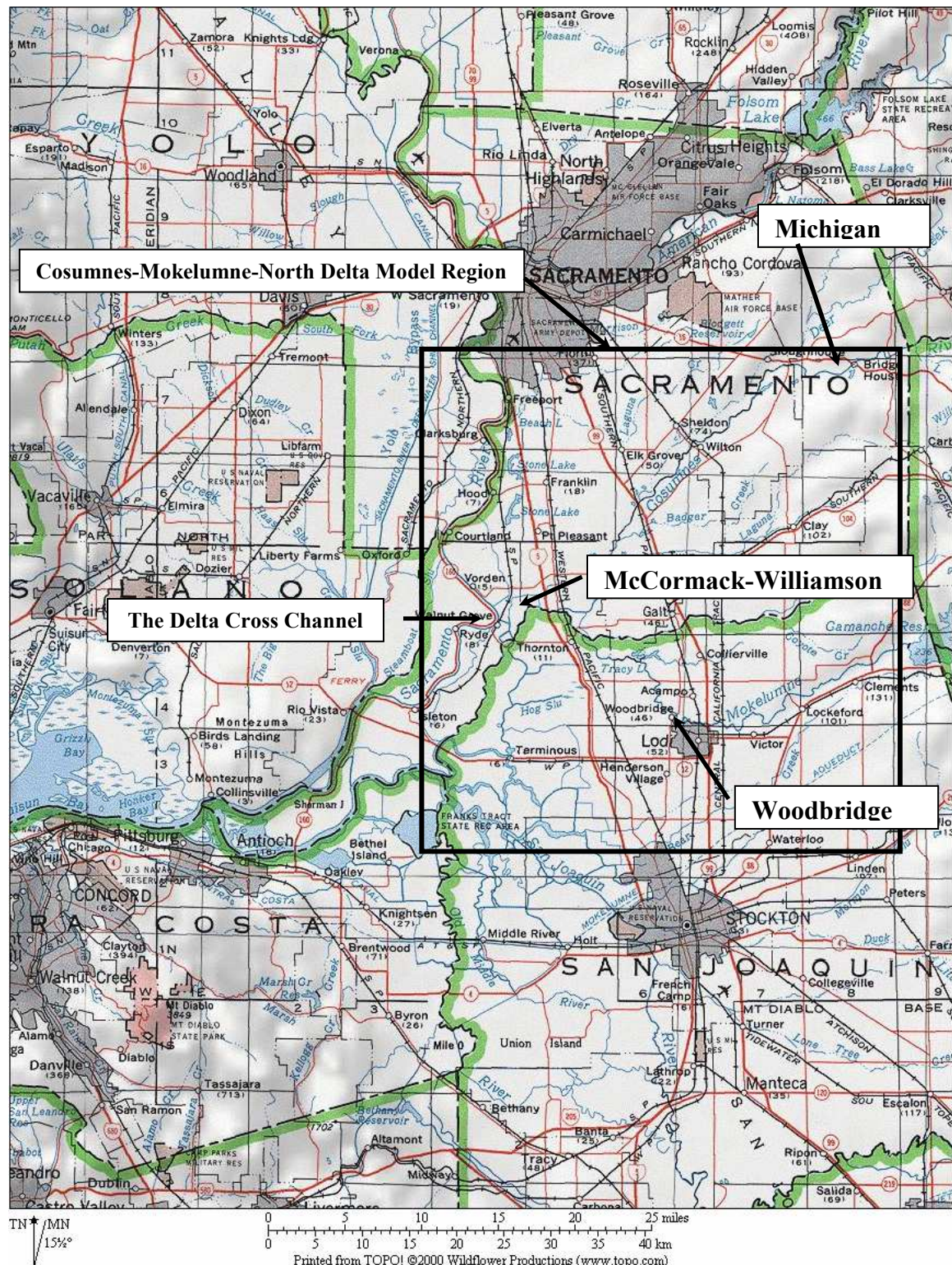


**Figure 1.** Study area of Cosumnes-Mokelumne-North Delta modeling effort.

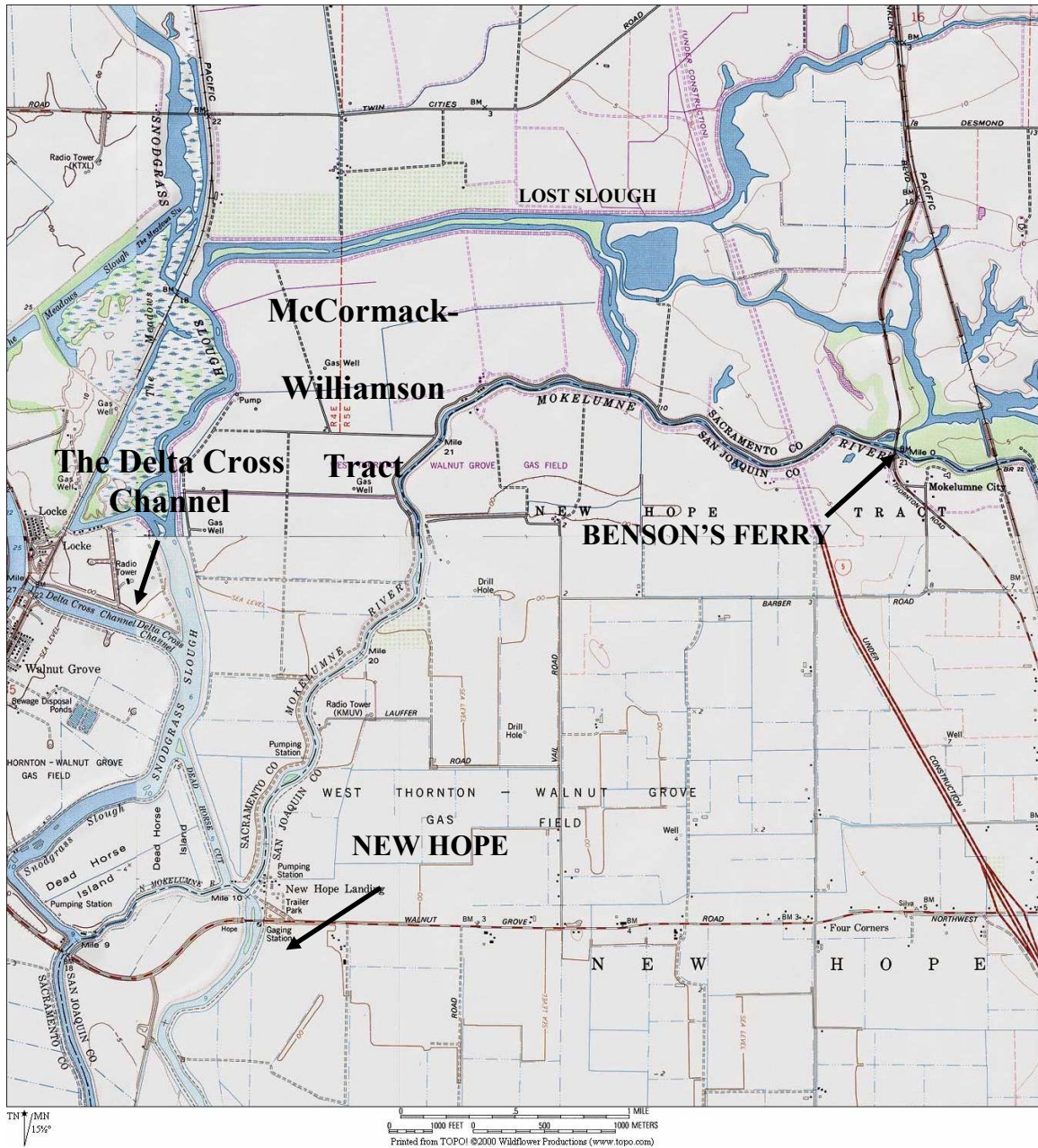


**Figure 2:** McCormack-Williamson Tract and the Delta Cross Channel location map, showing the locations of New Hope and Benson's Ferry. The McCormack-Williamson Tract is bordered by Lost Slough to the north, the Mokelumne River to the southeast, and Snodgrass Slough to the west. The Delta Cross Channel (DCC) hydraulically connects the Sacramento River to Snodgrass Slough when DCC gates are open.

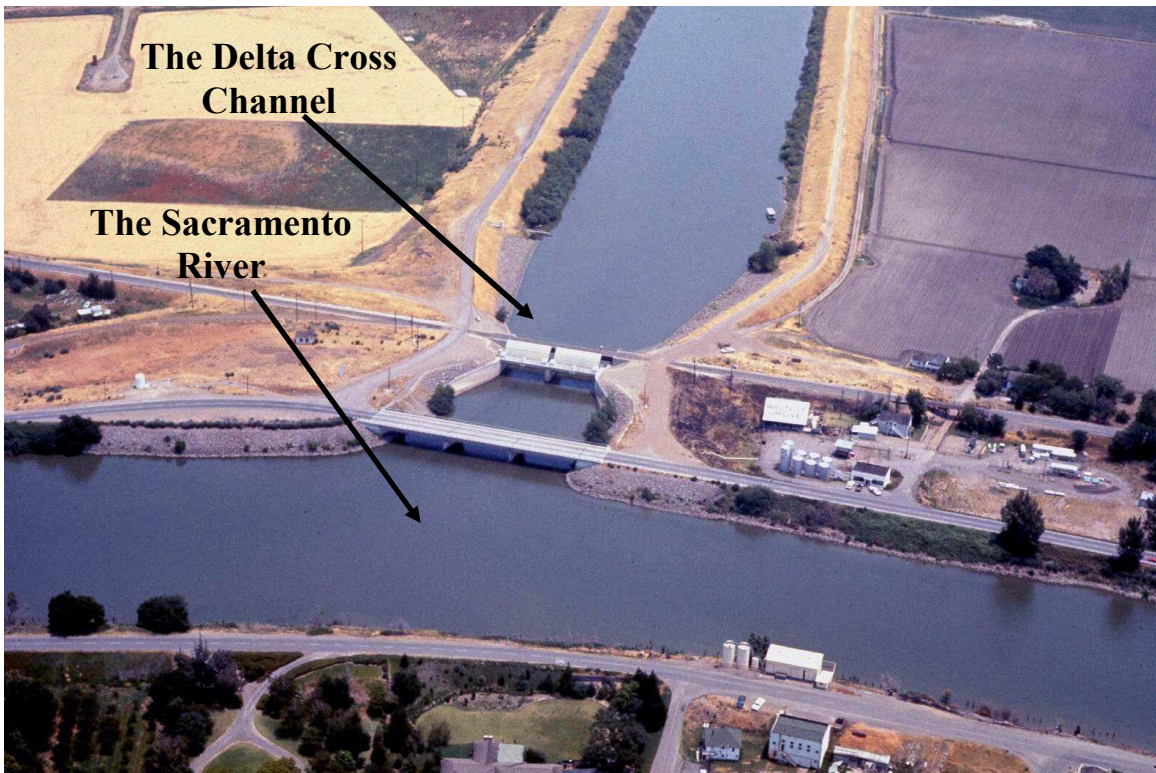


**Figure 3:** Aerial photograph of the Delta Cross Channel

### *Previous Studies*

With advancements in computers and commercial modeling software, using a mathematical water quality model has become an accepted part of the process of establishing and evaluating alternative scenarios for water-quality management (Orlob, 1992). The modeling approach to management and design issues is vital in identifying the important variables that account for the dominant mechanisms controlling system behavior (Whithead, 1980).

There have been several studies that have used models to explore the Sacramento San-Joaquin Delta, although most of the studies focused on hydraulics of the system. The California Department of Water Resources developed a DWOPER model of its North Delta Program focusing on the hydraulics of the system. In addition, DWR has modeled part of the region with its DSM2 model that contains limited water quality parameters. The U.S. Army Corp of Engineers has studied this region extensively in the context of flood control, to evaluate the flood impact of modifications to the hydraulic system (U.S. Army Corps of Engineers, 1988).

In the area of water quality modeling, a new, branched mass transport model was used to simulate salt transport in the Sacramento-San Joaquin Delta. The model uses a two-step procedure to determine the salt transport in a branch system. At the interior grid point, transport was determined by solving a one-dimensional advection-dispersion equation using an Euler-Lagrangian method (ELM). Salt transport at the junctions is then determined by an extension of the ELM and applying conservation of mass equation (Wong, 1990). In another water quality study two mathematical models were constructed to address the problems of nitrogen and algal cycles in the Sacramento-San Joaquin Delta

system. The steady-state, multi-dimensional models were used for analyzing nitrification and algal utilization of available nitrogen. The dynamic model incorporated the growth and death of phytoplankton and herbivorous zooplankton and the utilization of inorganic nitrogen, (Thomann, 1970). Another model developed used a linear programming approach within a simulation model to manage water quality for an urban water supply agency through blending reservoir and a raw water source of variable quality. Inputs to the simulation model include schedules of source water quality and availability in addition to the physical storage and conveyance constraints, regulatory restrictions, raw water demand, and urban water management priorities (Campbell et al., 2002). Temporal patterns of stream water quality were analyzed across the Cosumnes River watershed for three years to quantify the dynamics of the watershed. Many grab samples were taken to develop patterns and the data were also input into GIS to gain further water quality information about the watershed (Ahearn et al., 2004).

The hydraulic modeling foundation for the work conducted in the present study was first created by Blake (2001), where the floodplain dynamics of the Cosumnes River Preserve were studied. In this study the hydrodynamic model was initially set up and run with medium flow events. The next study that furthers Blake's modeling efforts was Hammersmark (2002) where management scenarios on McCormack-Williamson Tract, very similar to the ones that will be examined in the present study, were investigated in relation to water levels. Both high and low flow water events were examined. This study will use the hydraulic model developed by Blake and Hammersmark and add the capability to simulate water temperature and electrical conductivity in the North Delta,

exploring the effect different management scenarios have on the two water quality parameters.

## MODEL STUDY AREA

The model presented here spans the entire California North Delta area. It is possible that different restoration scenarios can be applied to different parts of the North Delta using this model. The specific extent of the model is illustrated in Figure 4. This model is bounded by eleven geographic locations. There are three northern boundary points. The first is on the Cosumnes River at Michigan Bar. The second is a small tributary that flows into the Cosumnes River, Deer Creek. The third northern boundary point is along Lambert Slough. The four southern boundary points are all along the San Joaquin River. They are San Andreas Landing, Venice Island, Turner Cut and Rindle Pump. There are two boundary points that are north and south of the Delta Cross Channel, along the Sacramento River, that form the western edge of the model. The eastern boundary points of the model are located along the Mokelumne River, just downstream of Woodbridge Dam, and at Dry Creek.

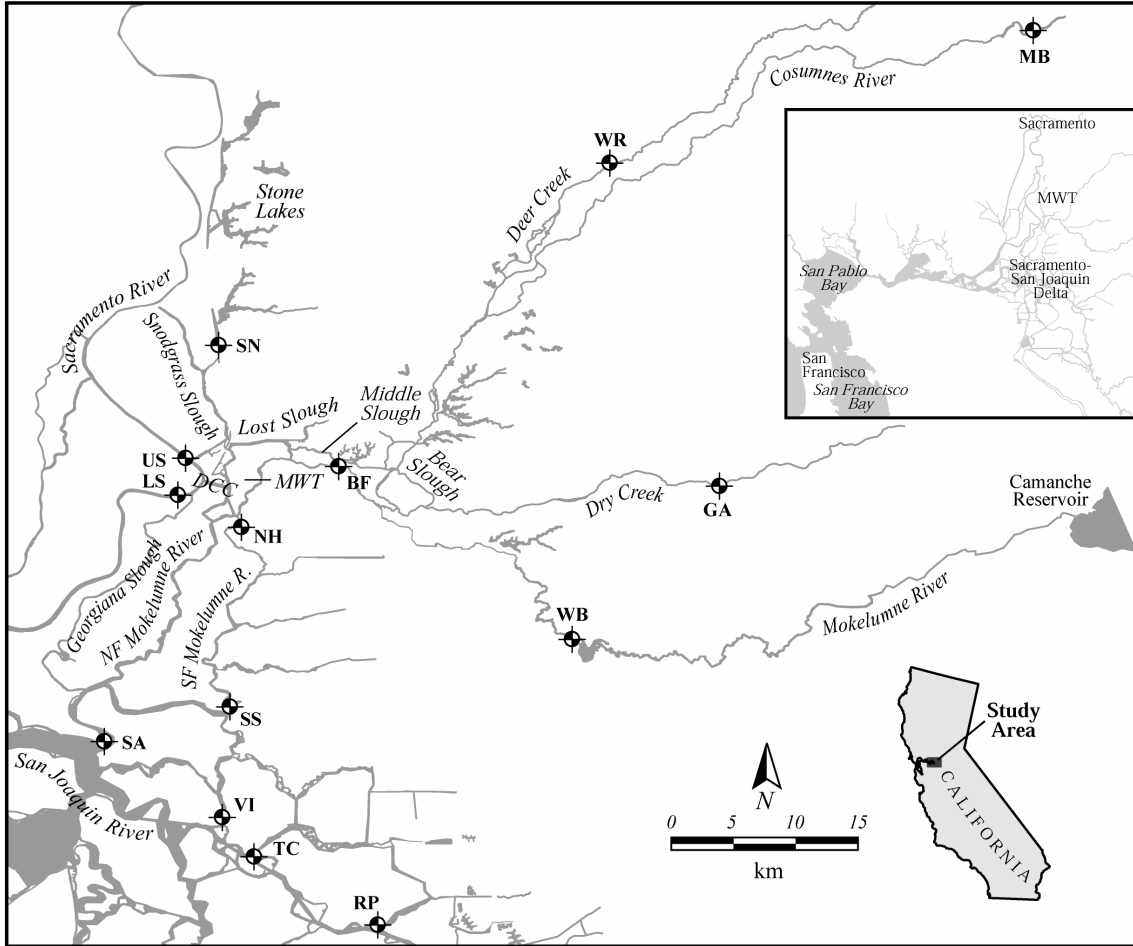


**Figure 4:** The extent of the MIKE 11 model with boundary condition and internal comparison locations. Six upstream boundary conditions are present located at Michigan Bar on the Cosumnes River (MB), Wilton Road on Deer Creek (WR), Galt on Dry Creek (GA), Woodbridge on the Mokelumne River (WB), Lambert Road on Stone Lakes Outlet (SN), and above the Delta Cross Channel on the Sacramento River (US). Five downstream boundary conditions located below Georgiana Slough divergence on the Sacramento River (LS), on the San Joaquin River at San Andres Landing (SA), Venice Island (VI), Turner Cut (TC), and Rindle Pump (RP). Three internal comparison locations at Bensons Ferry (BF), New Hope (NH) and South Staten Island (SS) used to calibrate and validate model.

The present study concentrated on the summer low-flow time period of 2003 and 2004, and not the flood events. The low flow time period is when water quality parameters are the most variable and susceptible to change. During low-flow periods, the Cosumnes River at Michigan Bar and Dry Creek have no flow through them. In the model these points were treated as no flow boundary conditions, meaning there is no flux

of water or water quality constituents at these points. All the other boundary conditions were treated as open, meaning that the flux of flow and concentration were present at these locations.

Discharge, water temperature, and electrical conductance data were required at all the boundary conditions and at internal model points that were selected to compare modeled and measured results. This task not only required the use of databases, created by the Interagency Ecology Program (IEP), California Data Exchange Center (CDEC) and Sacramento County Department of Water Resources, but extensive field measurements. Much of the stage and discharge data for calibrating the hydrodynamic were taken from the data bases of the above agencies while a large majority of the water temperature and electrical conductivity data were collected with field instruments.

All of the water temperature data required for the boundary conditions and internal points were measured with *in situ* instruments. Only two internal points, Benson's Ferry and New Hope, were used as comparison locations to calibrate the water temperature model. Continuous temperature measurements were made with Optic StowAway Temp loggers produced by Onset Computer Corporation (see Figure 5). The StowAway loggers have a range of -4 °C to +37°C and have dimensions of 132mm long x 20mm high x 25mm wide. Loggers were placed in a PVC casing with holes in the casing to ensure adequate water flow through it. The casings prevented the sun from skewing the reading of the water temperature. Since this system was hydraulically well mixed, the loggers were placed near the banks of the rivers or on a stationary structure in the channel flow like a harbor or a marina.

Only a few electrical conductivity data sets were available to download from the web database of CDEC. Available data sets were located at South Staten Island (SS), San Andreas Landing (SA), Venice Island (VI), Turner Cut (TC), above and below the Delta Cross Channel on the Sacramento River (US and DS), while the rest of the required data was supplemented by in situ instrument measurements. New Hope and South Staten Island are the only two internal locations used to calibrate the electrical conductivity model. Continuous electrical conductivity was measured with a Richard Brancker Research (RBR) data logger, Figure 6. The RBR sensors are cylindrical with dimensions of 1m long and 8 cm in diameter. The factory range for electrical conductivity was 0 to 100 mS/cm. However, this range did not produce sufficient resolution, since a typical reading of electrical conductivity for this area is in the range of 0.1 to 0.3 mS/cm. Resistors were changed so the range was reduced to 0 to 1 mS/cm. These instruments where either anchored at the bottom of the channel or hung from a piling in the channel flow.



**Figure 5:** An of Onset Optic StowAway Temp water temperature probe.



**Figure 6:** A Richard Brancker Research (RBR) data logger with two D cell batteries

## DATA CORRELATIONS

The collected water temperature and electrical conductivity data were correlated with stage and meteorological data downloaded from the CDEC website database. These correlations provide insight into factors that create the present water quality conditions and how closely related other parameters are to water temperature and electrical conductivity.

### *Water Temperature*

To help determine the primary driving factors for the water temperature, meteorological data were correlated with the measured water temperature at two internal points: Benson's Ferry and New Hope shown in photographs in Figures 7 and 8. Air temperature, which was measured by East Bay Municipal Utility District (EBMUD) below the Woodbridge Dam, and stage, which was measured by the Interagency Ecological Program (IEP), were the only two parameters that were correlated with the water temperature.

There was a very strong correlation between the air and water temperatures at both Benson's Ferry and New Hope. The correlation coefficients for these variables at each location for 2003 and 2004 are presented in Table 1. The strength of these correlations indicates that air temperature is a driving factor that has great influence on the water temperature of this system. It is interesting to note that Benson's Ferry has a higher correlation coefficient compared to New Hope in both time periods, illustrating the stronger relationship between air and water temperature at the more upstream location.

<b><i>Correlation Coefficients (<math>R^2</math>)</i></b>		
<b>Locations</b>	<b>2003</b>	<b>2004</b>
Benson's Ferry	0.89	0.96
New Hope	0.71	0.65

**Table 1:** Correlation coefficients of the water and air temperature at Benson's Ferry and New Hope during the summer of 2003 and 2004. Refer to Appendix A for the data and trend lines of the correlations.

Replication of the correlation analysis to stage (an indicator of tidal influence) and water temperature produced very weak correlation coefficients, shown in Table 2. It is evident from the coefficients that the water temperature does not have a strong relation with the tidal action at either location.

<b><i>Correlation Coefficients (<math>R^2</math>)</i></b>		
<b>Locations</b>	<b>2003</b>	<b>2004</b>
Benson's Ferry	0.04	0.01
New Hope	0.28	0.15

**Table 2:** Correlation coefficients of the tidal exchange and water temperature at Benson's Ferry and New Hope during the summer of 2003 and 2004. Refer to Appendix A for the data and trend lines of the correlations.

### *Electrical Conductance*

Correlations between air temperature and electrical conductivity were also examined. Only 2004 data at New Hope could be analyzed due to the lack of electrical conductivity probes and instrumentation failure at some sites in 2003. However, a correlation of 2004 electrical conductivity data with stage and air temperature still assisted in determining the dominant factors. A fairly weak correlation exists between

electrical conductivity and air temperature, while another weak, though slightly stronger correlation exists between the electrical conductivity and tidal exchange data, Table 3

<i><b>Correlation Coefficients (<math>R^2</math>)</b></i>	
<b>Electrical Conductivity and Stage</b>	<b>Electrical Conductivity and Air Temperature</b>
New Hope      0.4	0.31

**Table 3:** Correlation coefficients of the tidal exchange with electrical conductivity and air temperature with electrical conductivity at New Hope during the summer of 2004. Refer to Appendix A for the data and trend lines of the correlations



**Figure 7:** Benson's Ferry, looking downstream along the Mokelumne River during construction of new bridge.



**Figure 8:** New Hope, looking downstream from Wimpy's Marina along the South Fork of the Mokelumne River.

## MODEL DESCRIPTION

The MIKE 11 software package created by the Danish Hydraulic Institute was used to model the water quality constituents. MIKE 11 was selected as it was the only software package at the time that could model unsteady one-dimensional flow and had water quality modeling capabilities with a GIS interface. The MIKE 11 package has several modules that have the ability to model various hydrodynamic, and water quality parameters (DHI, 2004). For modeling water temperature, the Mike 11 water quality module was utilized and to model electrical conductivity, the advection-dispersion module was used. For both cases, the hydrodynamic model also needed to be run.

### *Hydrodynamics*

MIKE 11 solves for the vertically and laterally integrated equations of conservation of mass and momentum, better know as the St Venant Equations. The equations are:

$$\frac{\partial Q}{\partial x} + \frac{\partial A}{\partial t} = q$$

$$\frac{\partial Q}{\partial t} + \frac{\partial}{\partial x} \left( \alpha \frac{Q^2}{A} \right) + gA \frac{\partial h}{\partial x} + \frac{gQ|Q|}{C^2 AR} = 0$$

where:  $Q$  is the discharge,  $A$  is the flow area,  $q$  is the lateral inflow,  $h$  is the stage above datum,  $C$  is the Chezy resistance coefficient,  $R$  is the hydraulic or resistance radius,  $\alpha$  is the momentum distribution coefficient,  $g$  is the gravitational acceleration term,  $x$  the space coordinate, and  $t$  the time coordinate.

The equations assume that water is incompressible and homogenous, the bottom slope is small, the wave lengths are small compared with the water depth, and the flow is sub-critical (DHI, 2004). The calibration of the hydrodynamics of the system was facilitated by previous investigators using MIKE 11 in this region (Blake, 2001 and Hammersmark, 2002). Calibration is an important step due to the strong influence that the hydrodynamics have on the water quality parameters.

### *Electrical Conductivity Modeling*

In modeling electrical conductivity for the north delta study area the advection-dispersion (AD) module of MIKE 11 was used. The AD module solves the one dimensional, vertically and laterally integrated equation for conservation of mass of a substance in solution, also known as the one dimensional advection-dispersion equation (DHI, 2004). It takes the form of:

$$\frac{\partial AC}{\partial t} + \frac{\partial QC}{\partial x} - \frac{\partial}{\partial x} (AD \frac{\partial C}{\partial x}) = +AKC + C_2 q$$

where: C is the concentration of the substance being modeled , D the dispersion coefficient, K the linear decay coefficient, and C<sub>2</sub> the source/sink concentration. .

The advection-dispersion equation reflects two mechanisms of transport for a substance. The first is the advective transport with the mean flow and the second is dispersion transport due to the concentration gradients and shear flow. The main assumptions for the equation are: the substance is well mixed through the water column, the substance is conservative, and Fick's Law applies. The substance that is being modeled is required to be in units that describe a concentration. All the electrical conductivity measurements were in milli-Siemens per centimeter (mS/cm), so an

established conversion factor of 0.60 was multiplied by the measurements to convert the values to units of concentration, milli-grams per liter (mg/l).

### *Water Temperature Modeling*

For modeling water temperature, the MIKE 11 water quality (WQ) module was used. The WQ module uses a basic heat balance equation where  $T_{in} = T_{out}$  (DHI, 2004). The four parameters that control this balance are latitude, displacement from solar noon, maximum absorbed solar radiation, and emitted heat radiation. The latitude of the study area and the displacement of solar noon are globally applied variables, meaning they are applied to the entire model system and cannot be changed temporally or spatially. The maximum absorbed solar radiation and emitted heat radiation variables can be changed spatially, but not temporally. The MIKE 11 water quality editor takes these values and then applies a sine wave to simulate the diurnal fluctuations. Using the maximum absorbed solar radiation and emitted heat radiation makes it difficult to model over long time periods because these parameters would change due to the variations in the seasonal weather patterns. For this reason only the summer months were modeled.

## CALIBRATION

The hydrodynamic calibration process was based almost exclusively on previous model runs (Blake, 2001 and Hammersmark, 2002), for other low flow events. The hydrodynamic boundary conditions were either downloaded from the IEP website or the Sacramento County Department of Water Resources. The stage at Benson's Ferry and New Hope for the modeled and measured data for the two time periods (June, 2003-September, 2003 and June, 2004-September, 2004) in this study are shown in Figure 9 and Figure 10.

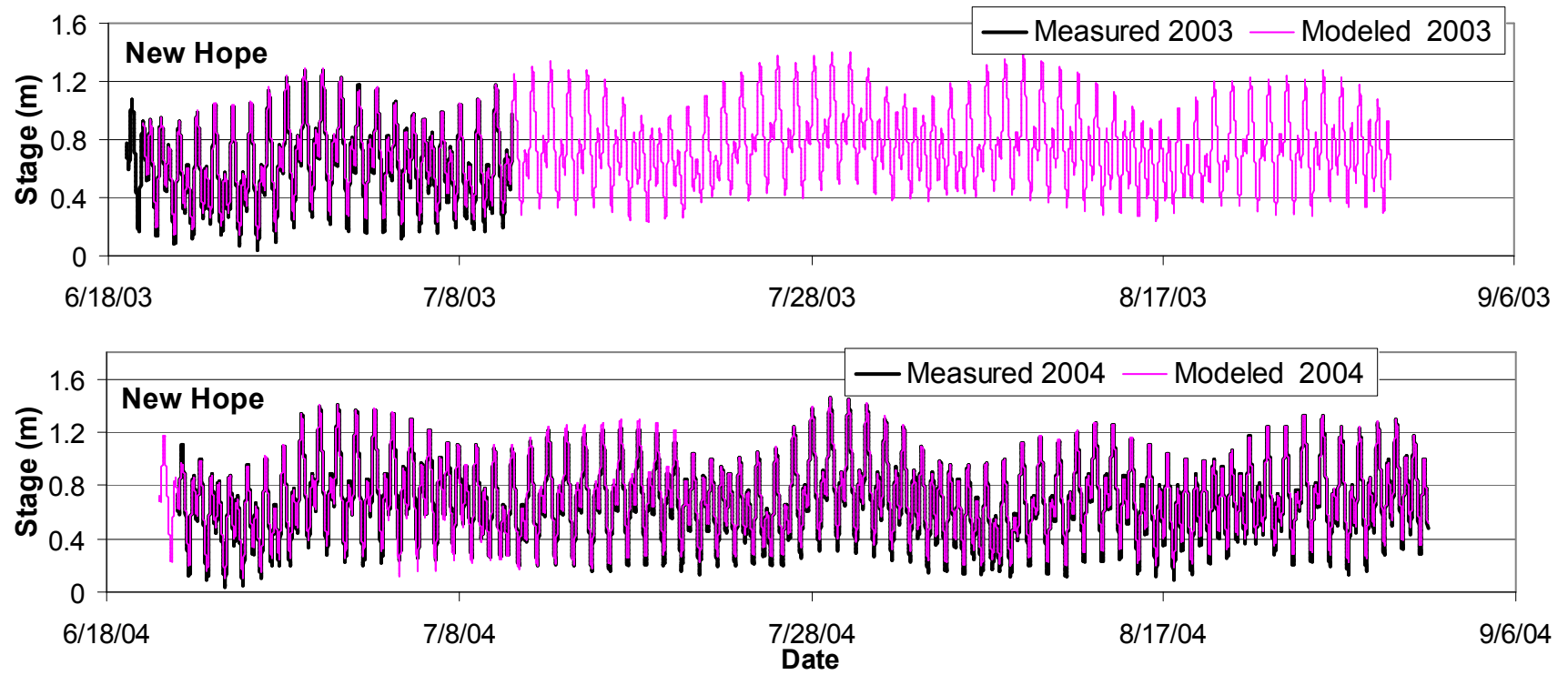


**Figure 9:** Comparison of measured and modeled water stage at Benson's Ferry in 2003 and 2004

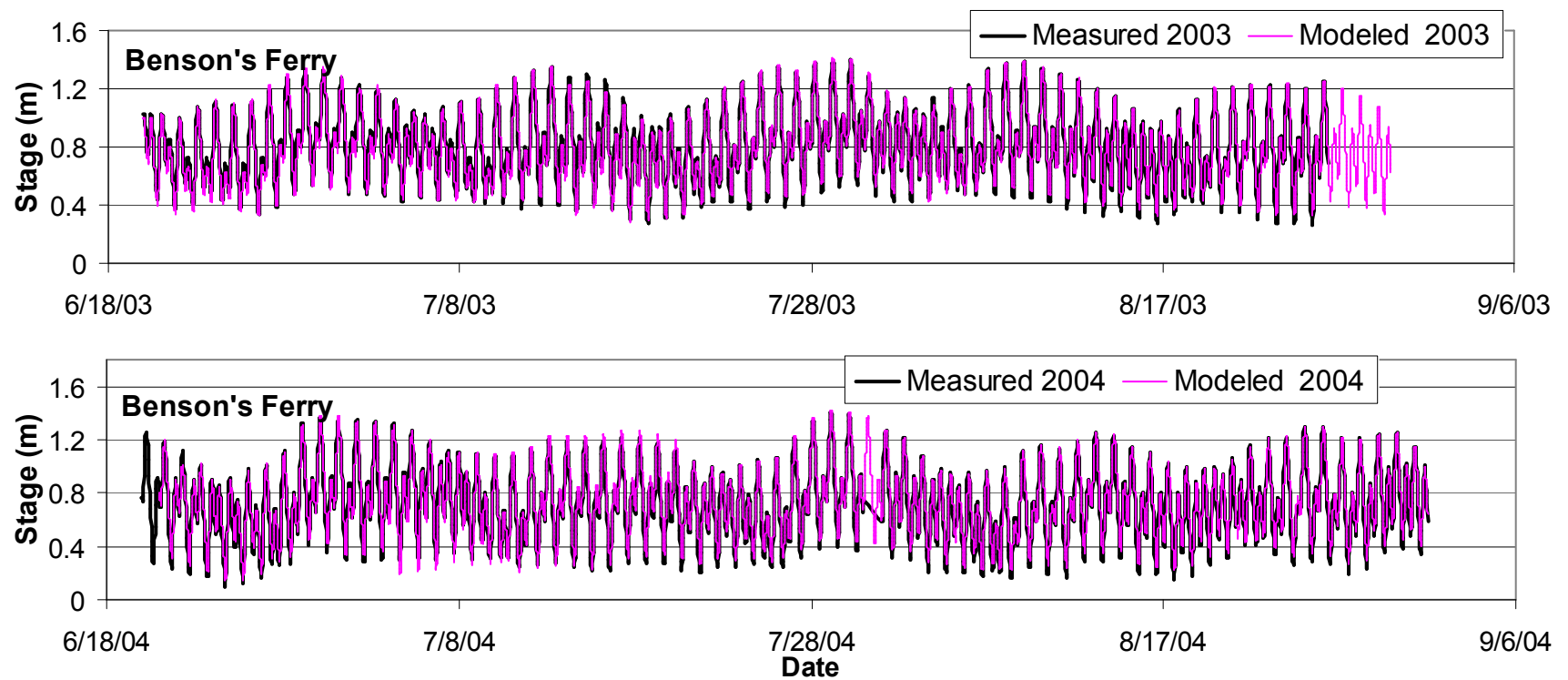


**Figure 10:** Comparison of measured and modeled water stage at New Hope in 2003 and 2004.

The model can also handle high flow events well. A comparison of model results with the measured data at New Hope during the 2000 storm event, which had 325cms flowing along the Cosumnes River at Michigan Bar are presented in Figure 11. The results in Figure 12 demonstrate how well the model simulated stage in the 1986 flood at New Hope. This event produced 1,200cms flowing along the Cosumnes River at Michigan Bar and several levees in the north delta failed, include the levees around McCormack-Williamson Tract.

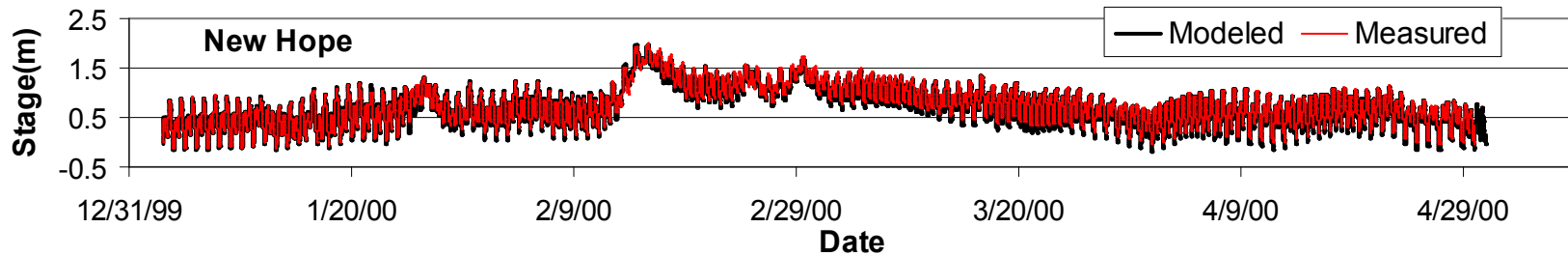


**Figure 11:** Comparison of measured and modeled water stage at Benson's Ferry in 2000.

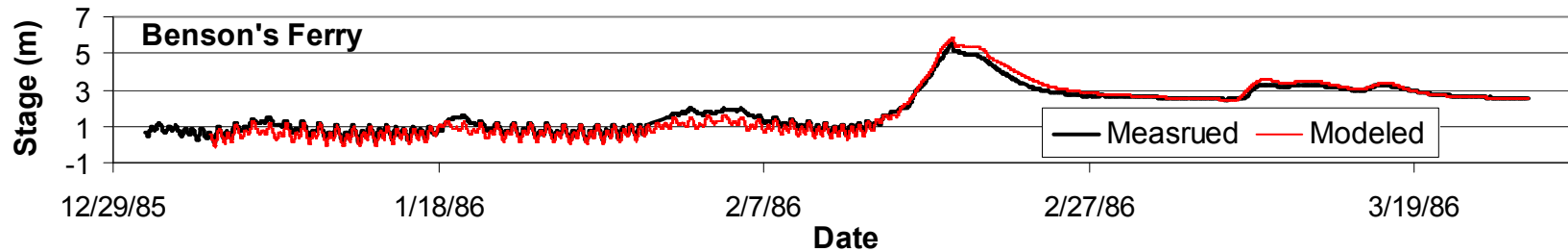


**Figure 12:** Comparison of measured and modeled water stage at Benson's Ferry in 1986.

### *Electrical Conductivity Model Calibration*

Only the summer months of 2004 had sufficient electrical conductivity data to calibrate the model. The two transport mechanisms are flow and dispersion. Since the hydrodynamic calibration (Blake, 2001 and Hammersmark, 2002) provided the necessary flow calibration, determining a dispersion coefficient was the main purpose for creating the conductivity model. Usually the values for dispersion coefficients range from 5-20m<sup>2</sup>/s for rivers (DHI, 2004). It was determined that a dispersion coefficient of 10 m<sup>2</sup>/s should be assigned to most of the region except for the lower reaches that border the San Joaquin River. They were given a higher value of 20 m<sup>2</sup>/s to account for the larger tidal exchange rate in those reaches. The calibrated dispersion coefficient values were used in the water temperature model well. The results are plotted below in Figure 13.

At both internal points the model results follow the trends of the actual data closely. At New Hope the modeled data are in phase with some of the diurnal fluxes that are present in the area, although the magnitude, particularly in June, is underestimated. However there is a dip from 8/9 to 8/21 at South Staten in the measured data, which is not represented in the modeled results. The deviation could be due to the localized effects that were not captured in the boundary conditions of the model. All along the South Fork Mokelumne there is localized pumping in the summer time, which could not be quantified and is not accounted for in the model. The local pumping and return could easily account for the dip.

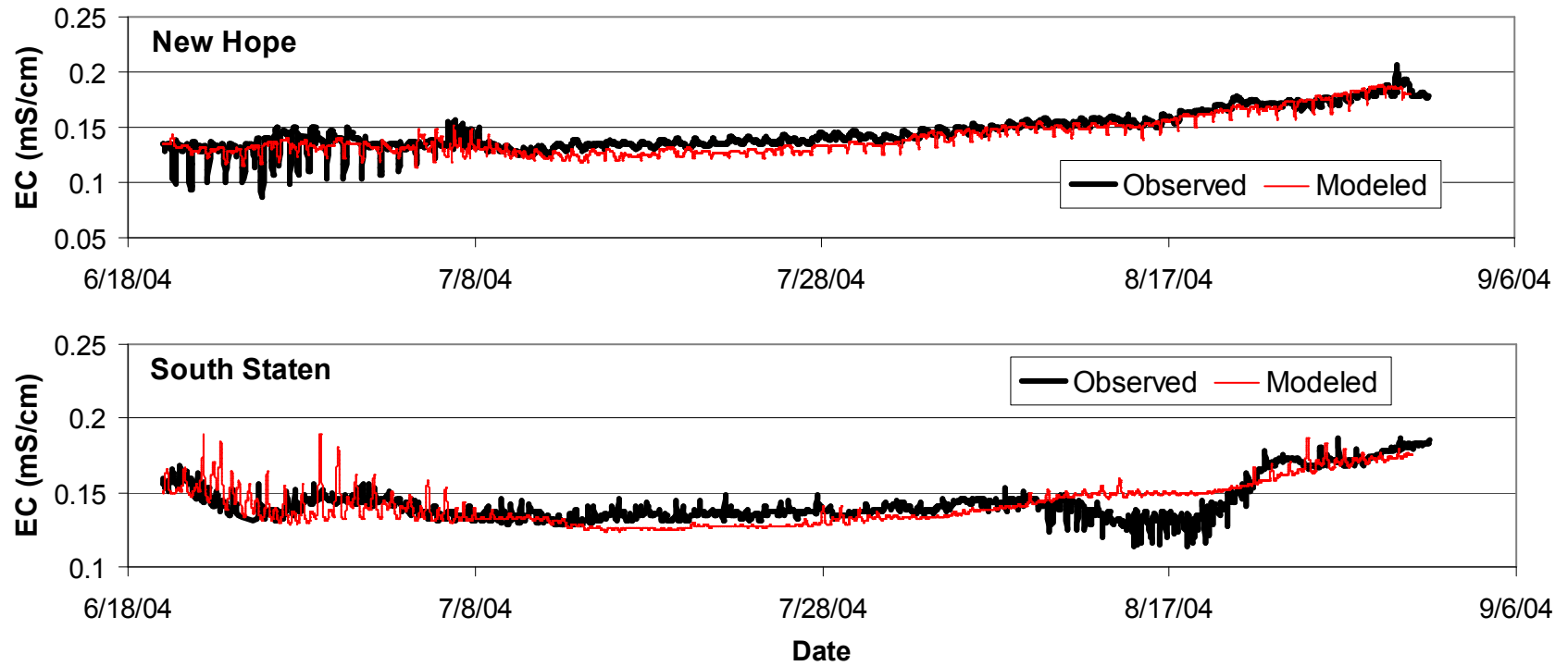


**Figure 13:** 2004 Observed and modeled electrical conductivity data at New Hope and South Staten.

### *Water Temperature Model Calibration*

Two input variables can be controlled to calibrate the water temperature model: maximum absorbed solar radiation and emitted heat radiation. Both of these two variables can be estimated from the measured meteorological data. However, this only provides approximate values because shading in different reaches must be considered. Thus, for this model an estimation was made taking into account both the meteorological data and an estimation for shading. For the years, 2003 and 2004, different values of maximum absorbed solar radiation and emitted heat radiation were used as seen in Tables 4 and 5.

	<b>Maximum Absorbed Solar Radiation (kJ/m<sup>2</sup>/hr)</b>	<b>Emitted Heat Radiation (kJ/m<sup>2</sup>/hr)</b>
<b>Cosumnes</b>	1575	400
<b>Mokelumne</b>	1575	400
<b>Middle Reaches</b>	1700	500
<b>Lower Reaches</b>	1800	600

**Table 4:** 2003 water temperature model variables (lower reaches refer to reaches below New Hope, while the middle reaches are between Benson's Ferry and New Hope).

	<b>Maximum Absorbed Solar Radiation (kJ/m<sup>2</sup>/hr)</b>	<b>Emitted Heat Radiation (kJ/m<sup>2</sup>/hr)</b>
<b>Cosumnes</b>	1400	450
<b>Mokelumne</b>	1400	450
<b>Middle Reaches</b>	1500	550
<b>Lower Reaches</b>	1600	650

**Table 5:** 2004 water temperature model variables (lower reaches refer to reaches below New Hope, while the middle reaches are between Benson's Ferry and New Hope).

Since ambient conditions vary from year to year it is to be expected that absorbed solar radiation and emitted heat radiation parameters should also vary. In 2004, the daily-average air temperature was consistently higher by about 15% when compared to the 2003 daily-average air temperature, creating different radiation coefficients. The daily average air temperature are plotted for both years in Figure 14.

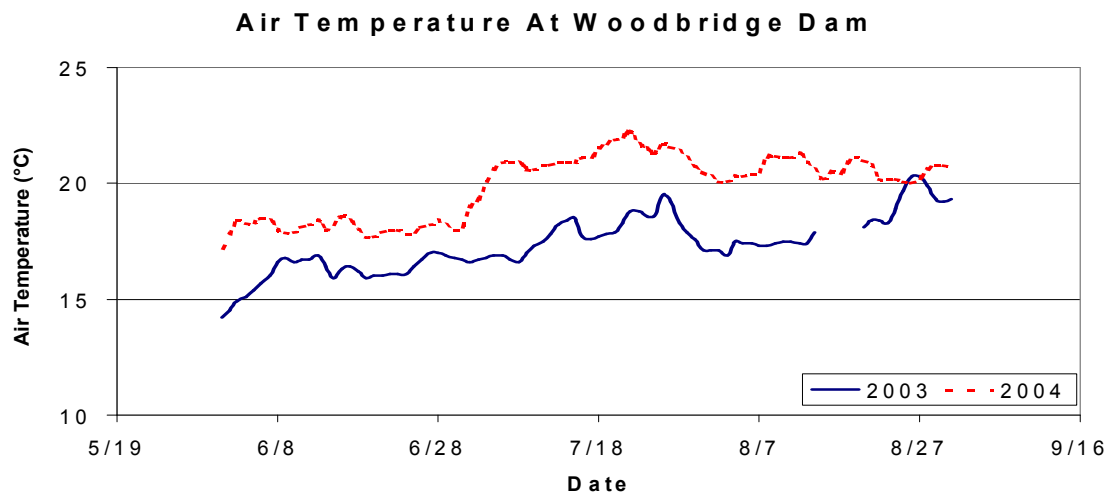


**Figure 14:** Daily averaged air temperature at Woodbridge Dam for summer of 2003 and 2004. Data were measured by East Bay Municipal Utility District.

It is also necessary to consider the ways in which the maximum absorbed solar radiation and emitted heat radiation changed spatially over time. Riparian vegetation creates a great deal of shade along much of the Cosumnes and Mokelumne Rivers above Benson's Ferry, which lowers both the maximum absorbed solar radiation and emitted heat radiation. By contrast the lower reaches below New Hope have the highest values due to the lack of riparian vegetation along the banks which leaves the river exposed, see Figure 15 and 16.



**Figure 15:** Mokelumne River just downstream of Benson's Ferry, looking upstream.



**Figure 16:** South Fork Mokelumne River near Sycamore Slough.

By using the above values for maximum absorbed solar radiation and emitted heat radiation in the model simulations, the calibrated results for 2003 and 2004 were produced and are plotted in Figure 17 and 18.

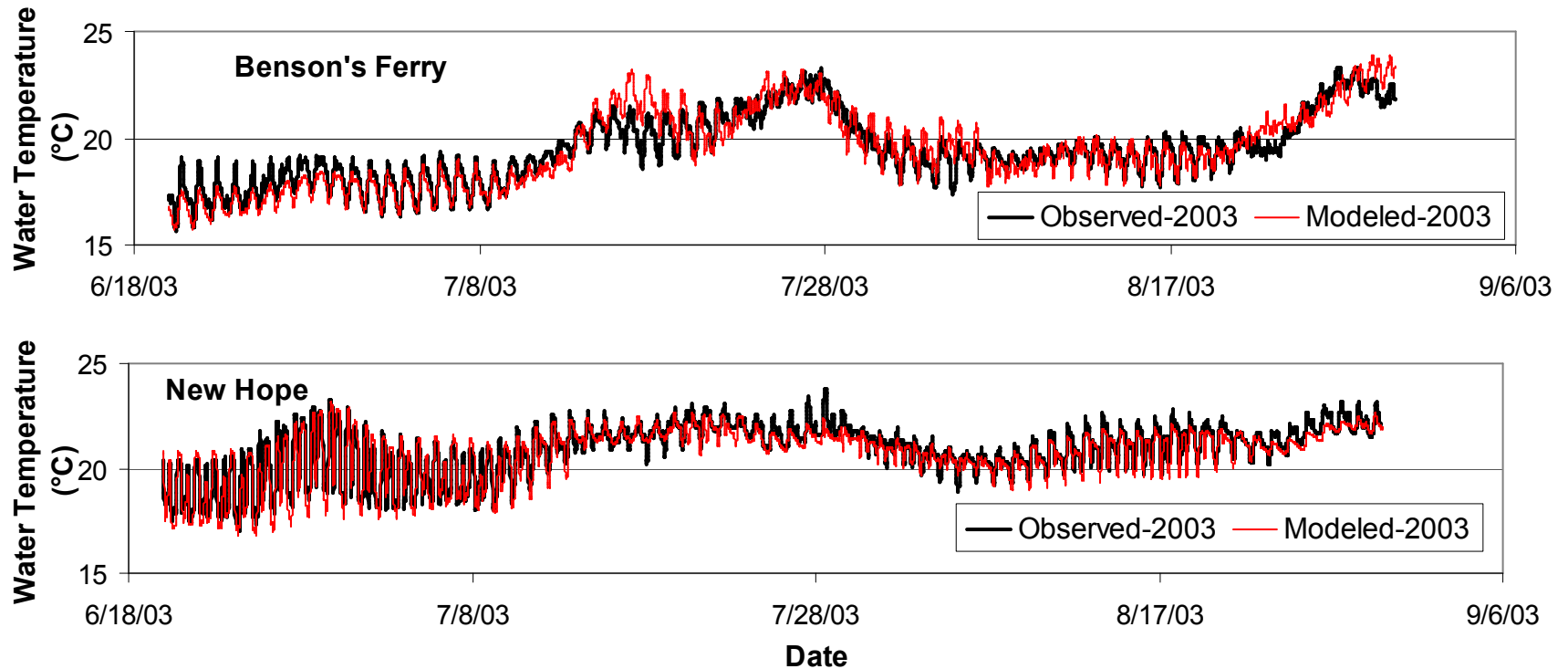


**Figure 17:** Comparison of observed and modeled water temperature data for 2003 at both Benson's Ferry and New Hope.

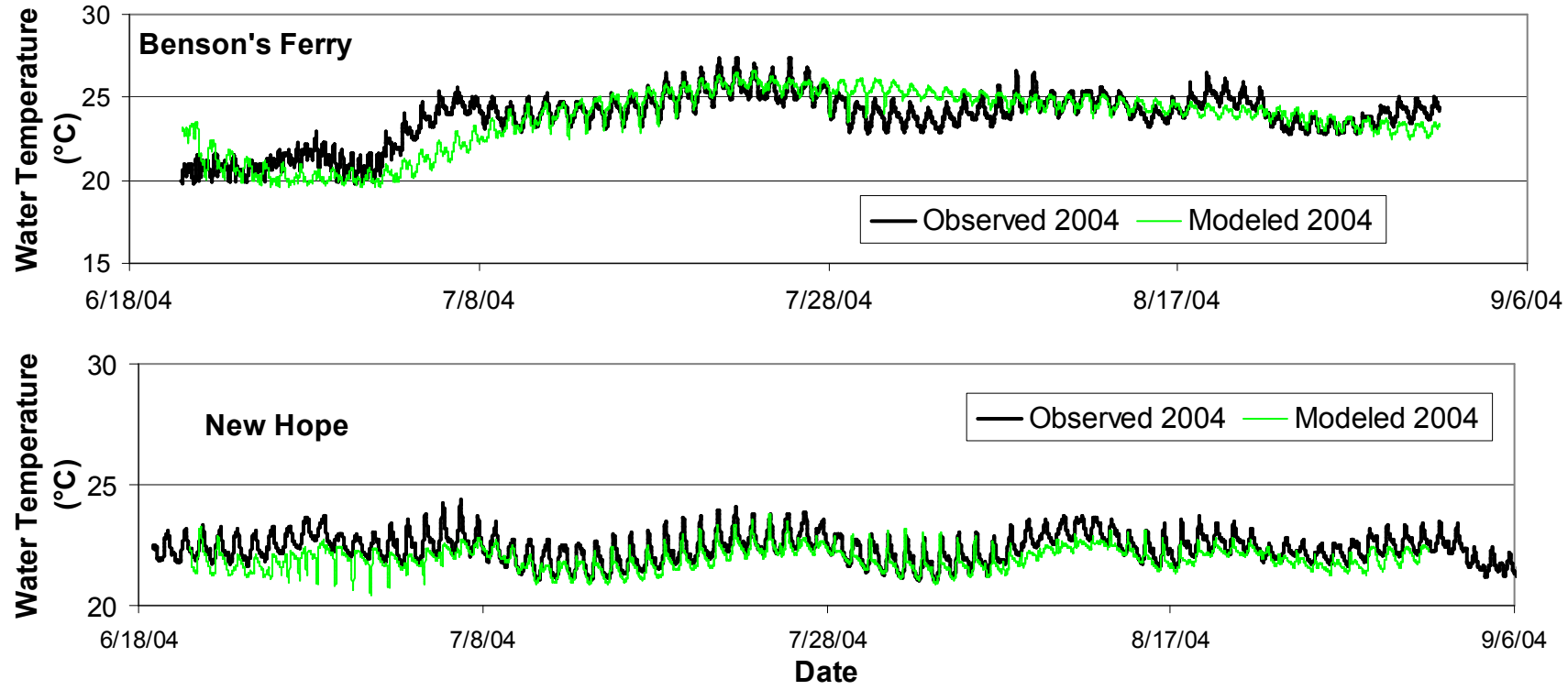


**Figure 18:** Comparison of observed and modeled water temperature data for 2004 at both Benson's Ferry and New Hope.

In these calibrated runs, it is apparent that the modeled data match the diurnal flux and does represent the general trend of what occurs in the system. However, there are some points in time where the amplitude of the modeled data does not correspond to the measured data. The deviation is partly due to the fact that the MIKE 11 water temperature module does not allow temporal variations in the maximum absorbed solar radiation and emitted heat radiation. Use of fixed values prevents the capture of the local effects of the system that affect the output. It also does not allow for short-term variations in the two variables.

Notice that in 2004 the Benson's Ferry predictions do not match the observed data as well as they did in 2003. The difference could be attributed to the fact that the flow along the Mokelumne is about five times higher in 2003 than 2004, see Figure 19, therefore making it very difficult for the model to capture the local effect of water temperature at Benson's Ferry by the Mokelumne flow, since the water quality model is very dependent on flow rates.

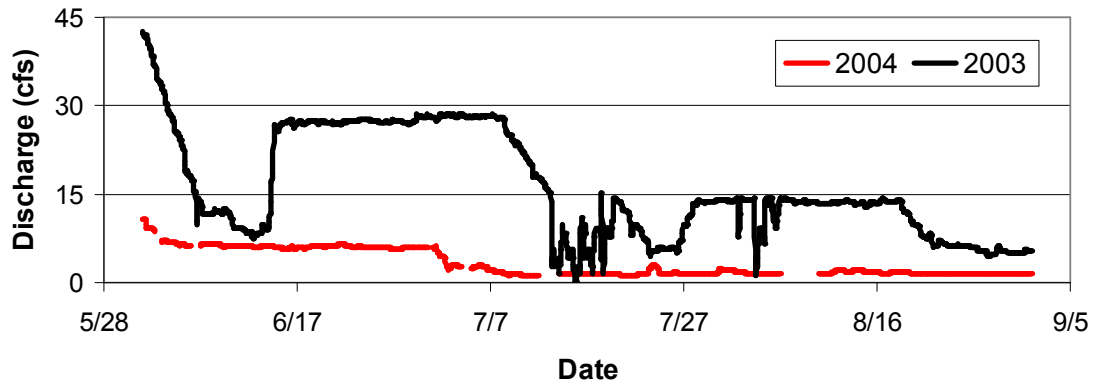


**Figure 19:** Discharge of the Mokelumne River for measured at Woodbridge Dam during the summer months of 2003 and 2004.

## SENSITIVITY ANALYSIS

A sensitivity analysis was performed on both the water temperature and electrical conductivity model. The sensitivity analysis was undertaken to determine the effect of specific changes in critical variables that dictate the behavior of the system.

### *Electrical Conductivity Model Sensitivity Analysis*

Since the two main mechanisms of transport are advection and dispersion in this model, the flow and the dispersion coefficient were varied to determine their relative contributions to the system. The discharge was increased by 20% on both the Mokelumne and Sacramento Rivers. These were the two major sources of input water to the area during the modeled period. The dispersion coefficients were systematically doubled along individual reaches such as the Sacramento River, Mokelumne River, lower reaches, middle reaches and then for all the reaches.

The sensitivity to changes in flow was checked at three internal points New Hope, Benson's Ferry, and South Staten. At these three locations the results varied from the calibrated results, especially when the flows along both the Sacramento and Mokelumne Rivers where changed. The average percent change and the maximum percent change each flow increase had on the particular location is given in Table 6. These values illustrate the average and maximum change the increased flow has on the three internal points. The percent changes were calculated by taking the absolute value of the difference between the value predicted in the sensitivity trial and the calibrated value, then dividing by the calibrated value. The maximum and the average percent changes over the entire time series were then calculated.

	<b>+20% Sacramento River Flow</b>		<b>+20% Mokelumne River Flow</b>	
	Average Percent Difference	Maximum Percent Difference	Average Percent Difference	Maximum Percent Difference
<b>New Hope</b>	1%	9%	0%	4%
<b>South Staten</b>	2%	14%	0%	1%
<b>Benson's Ferry</b>	0%	2%	1%	4%

**Table 6:** Average and maximum percent difference between calibrated model electrical conductivity results and increase flow model results. Appendix E has all graphical plots of this sensitivity analysis.

It is evident that little change occurred in the electrical conductivity readings at Benson's Ferry when the Sacramento River flow was increased. At New Hope and South Staten there were not great changes when the Mokelumne discharge was increased. The lack of significant response is due to the fact that only a small amount of the water releases reach these areas.

However, a change in the results occurred at Benson's Ferry when the Mokelumne flow was increased. It is apparent from the results shown in Table 6 and Figure 20 that the increase in flow has diluted the spikes in the readings.

At both New Hope and South Staten dilution of EC also occurs when the Sacramento River flow was increased. The dilution of the spike can be seen in figure 21 and 22 below, which dampens the effects of the tidal influence.

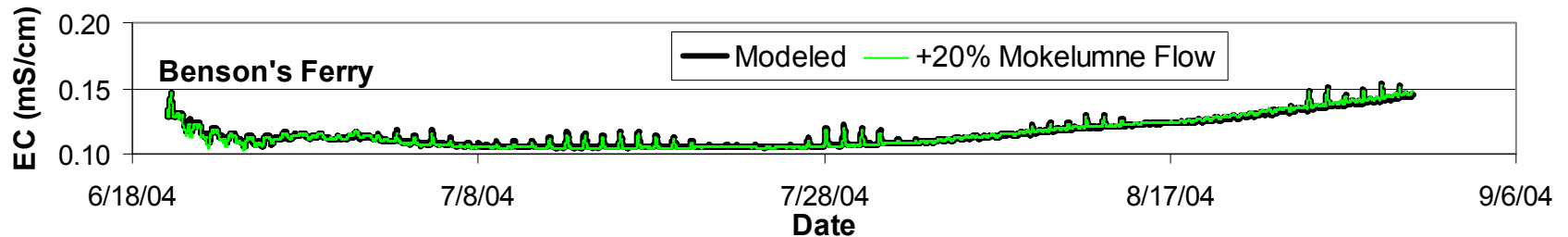


**Figure 20:** Calibrated 2004 electrical conductivity run plotted with the 2004 electrical conductivity run with a 20% increase of Mokelumne flow at Benson's Ferry.

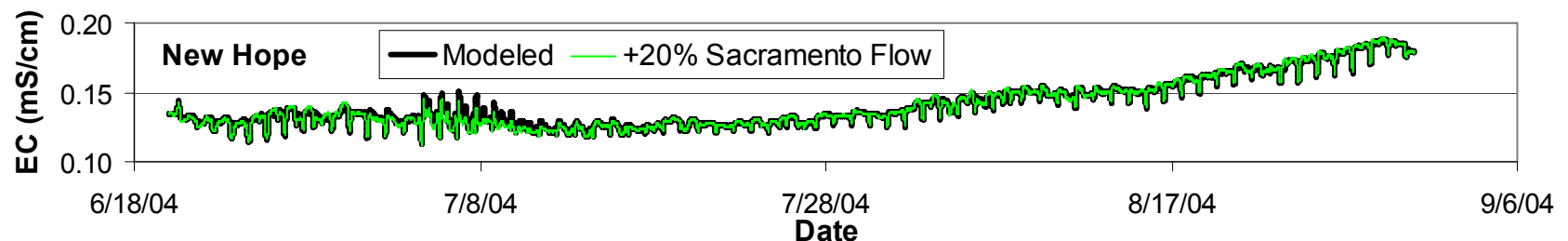


**Figure 21:** Calibrated 2004 electrical conductivity run plotted with 2004 electrical conductivity run with a 20% increase in Sacramento flow at New Hope.

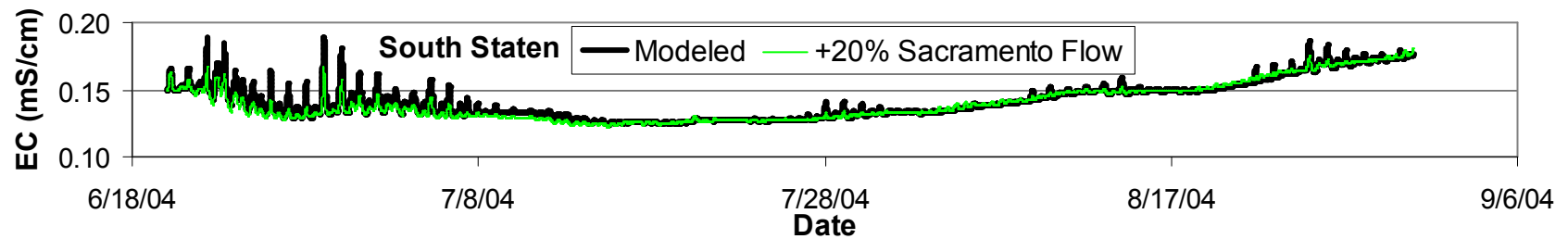


**Figure 22:** Calibrated 2004 electrical conductivity run plotted with 2004 electrical conductivity run with a 20% increase in Sacramento flow at South Staten.

The dispersion coefficient was doubled for all the reaches, and then individual reaches were selected where only the dispersion values in those reaches were doubled. The reaches considered were the Mokelumne River, Sacramento River, the middle reaches (between Benson's Ferry and New Hope), and the lower reaches (below New Hope). The calculated average and maximum percent differences are presented in Table 7. Only the two locations used to calibrate the electrical conductivity model were examined.

**2004 (Doubling the calibrated dispersion coefficient)**

	New Hope	South Staten		
	Average Percent Difference	Maximum Percent Difference	Average Percent Difference	Maximum Percent Difference
<b>All Reaches</b>	0%	3%	1%	11%
<b>Mokelumne</b>	0%	0%	0%	0%
<b>Sacramento</b>	0%	0%	0%	0%
<b>Middle</b>	0%	3%	0%	0%
<b>Lower</b>	0%	2%	1%	11%

**Table 7:** The average and maximum percent difference found in the varied dispersion coefficient runs with the calibrated 2004 runs for electrical conductivity. Appendix D has all the graphical plots of this sensitivity analysis.

At New Hope no changes occurred when the dispersion values of the Sacramento and Mokelumne Rivers were double. However, a slight change in the maximum percent difference occurs when all the reaches values are doubled. The results mean that there was no significant overall change, while slight changes in individual values were present. The same type of change occurred when the middle and lower reaches dispersion coefficient values were doubled. The results are also illustrated in Figure 23 which has the plot of the base case along with the model run in which all the dispersion coefficients

were doubled. One can see that there is not a great change in the overall levels, but there are isolated changes in the minimum values.

Looking at the South Staten responses to the coefficient changes, none were created when the Mokelumne River, Sacramento River, and Middle reaches coefficients were increased. However, changes in EC levels occurred when the coefficients of all the reaches and the lower reaches were doubled. There is a slight overall average change, but also a significant change in the maximum values as well. The results can be seen in Figure 24, below, which plots the calibrated results with the sensitivity run where all reaches dispersion coefficient values were doubled.

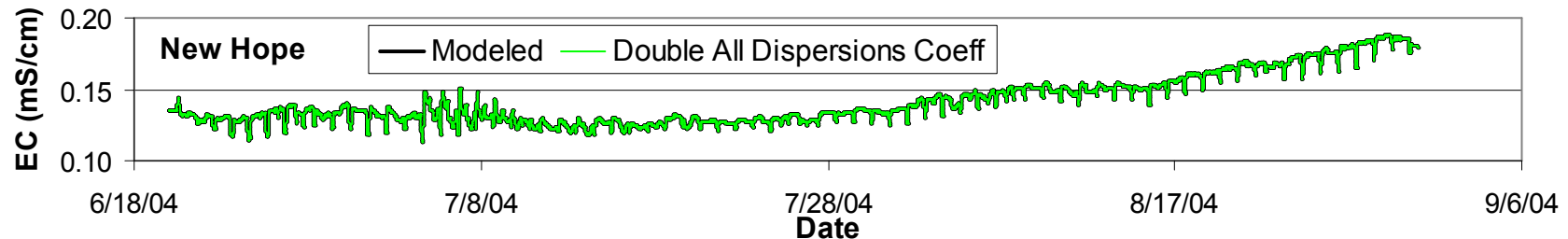


**Figure 23:** Calibrated 2004 electrical conductivity run plotted with 2004 electrical conductivity run at New Hope with doubled dispersion coefficient values in all reaches.

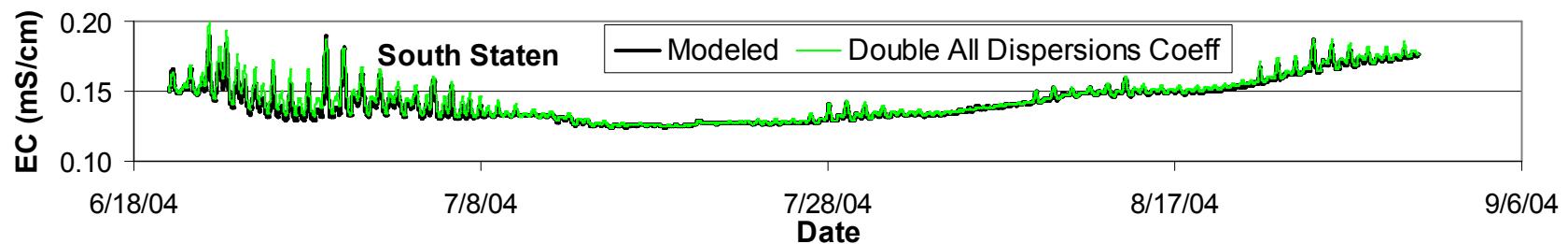


**Figure 24:** Calibrated 2004 electrical conductivity run plotted with 2004 electrical conductivity run at South Staten with doubled dispersion coefficient values in all reaches.

### *Water Temperature Model Sensitivity Analysis*

Three input parameters, flow rate, the maximum absorbed solar radiation, and the emitted heat radiation, were varied to determine the effects they had on the water temperature predictions. The sensitivity analyses were performed on both the 2003 and 2004 water temperature simulations and two internal points were examined, Benson's Ferry and New Hope.

The maximum absorbed solar radiation and the emitted heat radiation, which were used to calibrate the heat balance, were both increased by 20% to determine how sensitive the model is to these changes. The parameters were varied spatially to examine how a change at a particular location affects Benson's Ferry and New Hope water temperatures. Runs were performed that changed the two variables along the Mokelumne, Sacramento, the Middle reaches and the lower reaches. In another run, all the reaches in the model were increased by 20%.

In all the sensitivity runs, for both 2003 and 2004, when the maximum solar radiation was increased the water temperature increased as well. By increasing this value more radiation was allowed into the water; therefore increasing the water temperature. Increasing the emitted heat radiation allows more heat to escape the system and in turn lowers the water temperature.

In the 2003 sensitivity runs it was apparent that Benson's Ferry was much more responsive to the effects of the increase in the variables than New Hope, Table 8. When the maximum absorbed solar radiation was increased by 20% for all the reaches, Benson's Ferry had a higher average and maximum percent difference than New Hope.

**2003 (20% change in Maximum Absorbed Solar Radiation)**

	<b>Benson's Ferry</b>	<b>New Hope</b>
	<b>Average Percent Difference</b>	<b>Maximum Percent Difference</b>
<b>All Reaches</b>	7%	16%
<b>Middle Reaches</b>	4%	12%
<b>Lower Reaches</b>	0%	0%
<b>Mokelumne</b>	1%	3%
<b>Sacramento</b>	0%	0%

**Table 8:** Average and maximum percent difference of 2003 runs where maximum absorbed solar radiation was changed by 20%, compared to the calibrated 2003 runs. Appendix B and C have all the graphical plots of this sensitivity analysis.

When the values in the Middle reaches were varied, a significant change occurred on average in the water temperature, yet when varying the other reaches individually, none of them produced a similar change. The only other simulation that produced a change was seen at Benson's Ferry from varying the parameters on Mokelumne River.

The sensitivity analysis performed on the 2004 water temperature runs produced results similar to those in 2003, Table 9. The 2003 sensitivity runs produced a lower percentage difference with both the average and maximum values. However this is due to the different calibration parameters used for the two different years. A similar trend is observed when only the Middle reaches were varied. When the Mokelumne River's parameters were increased a corresponding change in water temperature occurred at Benson's Ferry.

### 2004 (20% change in Maximum Absorbed Solar Radiation)

#### Benson's Ferry

#### New Hope

	Average Percent Difference	Maximum Percent Difference	Average Percent Difference	Maximum Percent Difference
<b>All Reaches</b>	25%	40%	2%	17%
<b>Middle Reaches</b>	18%	29%	1%	12%
<b>Lower Reaches</b>	0%	0%	0%	1%
<b>Mokelumne</b>	5%	7%	0%	3%
<b>Sacramento</b>	0%	0%	0%	0%

**Table 9:** Average and maximum percent difference of 2004 runs where maximum absorbed solar radiation was changed by 20% compared to the calibrated 2004 runs. Appendix B and C have all the graphical plots of this sensitivity analysis.

The changes that occur when the emitted heat radiation is increased by 20% show similar trends to when the maximum absorbed solar radiation is changed. In 2003 Benson's Ferry water temperature is more sensitive to the changes in this parameter than New Hope, Table 10. The only reaches that produce a significant change are the Middle reaches while the others make almost negligible changes to the water temperature.

### 2003 (20% change in Emitted Heat Radiation)

#### Benson's Ferry

#### New Hope

	Average Percent Difference	Maximum Percent Difference	Average Percent Difference	Maximum Percent Difference
<b>All Reaches</b>	5%	13%	1%	7%
<b>Middle Reaches</b>	4%	10%	1%	6%
<b>Lower Reaches</b>	0%	0%	0%	0%
<b>Mokelumne</b>	1%	3%	0%	1%
<b>Sacramento</b>	0%	0%	0%	0%

**Table 10:** Average and maximum percent difference of 2003 runs where emitted heat radiation was changed by 20% compared to the calibrated 2003 runs. Appendix B and C have all the graphical plots of this sensitivity analysis.

As expected, 2004 water temperature runs produced similar trends to those of 2003, Table 11. The middle reach changes seem to have a greater effect on the

sensitivity at Benson's Ferry and New Hope with Benson's Ferry more sensitive to these changes than New Hope. The Mokelumne River produced slight effects on the water temperature at Benson's Ferry while the rest of the reaches showed minimal effects. Even the percent changes are higher in 2004 when compared to 2003 similar to the sensitivity run on the maximum absorbed solar radiation.

#### 2004 (20% change in Emitted Heat Radiation)

	<u>Benson's Ferry</u>	<u>New Hope</u>		
	<b>Average Percent Difference</b>	<b>Maximum Percent Difference</b>	<b>Average Percent Difference</b>	<b>Maximum Percent Difference</b>
<b>All Reaches</b>	22%	35%	2%	15%
<b>Middle Reaches</b>	16%	22%	1%	0%
<b>Lower Reaches</b>	0%	0%	0%	0%
<b>Mokelumne</b>	5%	7%	0%	3%
<b>Sacramento</b>	0%	0%	0%	0%

**Table 11:** Average and maximum percent difference of 2004 runs where emitted heat radiation was changed by 20% compared to the calibrated 2004 runs. Appendix B and C have all the graphical plots of this sensitivity analysis.

The sensitivity of the water temperature model to flow changes was checked at Benson's Ferry and New Hope. As in the simulations of electrical conductivity to flow sensitivity, the flow of the Sacramento and Mokelumne Rivers was increased by 20%. In Table 12 below, the average and maximum percent difference of the flow alterations for the 2003 runs are presented. In the 2003 runs it was apparent that increasing the Mokelumne flow had a greater impact on the average water temperature, when compared to increasing Sacramento River flow.

2003 (20% Increase in Flow)				
	Sacramento River	Mokelumne River		
	Average Percent Difference	Maximum Percent Difference	Average Percent Difference	Maximum Percent Difference
<b>Benson's Ferry</b>	0%	1%	1%	5%
<b>New Hope</b>	0%	3%	1%	9%

**Table 12:** Average and maximum percent difference between calibrated model water temperature results and increase flow model results for 2003. Appendix E has all the graphical plots of this sensitivity analysis.

The calibrated model along and the model run where the flow of the Mokelumne is increased by 20% at Benson's Ferry is presented in Figure 25. It is important to notice that increasing the flow on the Mokelumne decreases the daily maximum water temperature at Benson's Ferry. This trend is also propagated downstream to New Hope as well, Figure 26. The daily maximum values stay the same the same but the daily minimum values decrease.

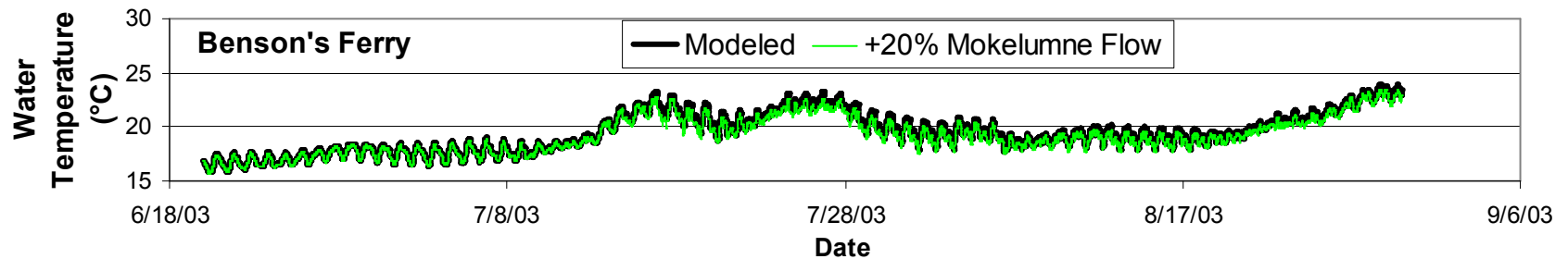


**Figure 25:** Calibrated 2003 water temperature run plotted with 2003 water temperature run with a 20% increase of Mokelumne flow at Benson's Ferry.

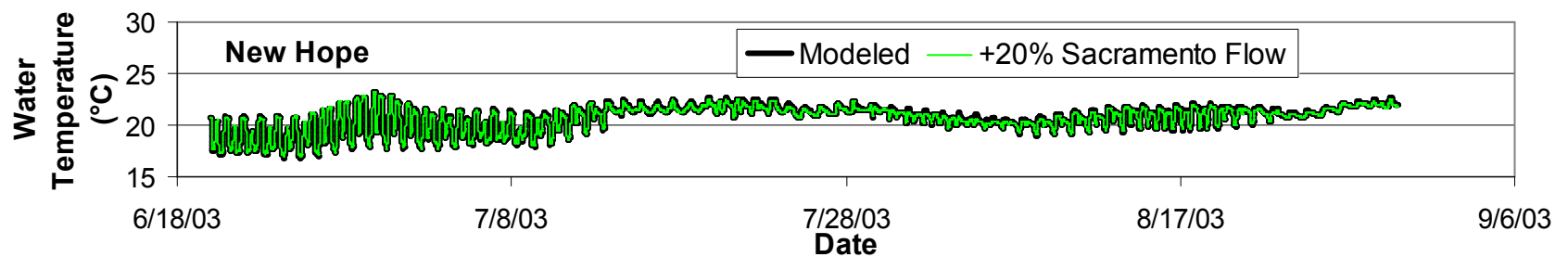


**Figure 26:** Calibrated 2003 water temperature run plotted with 2003 water temperature run with a 20% increase of Mokelumne flow at New Hope.

The results from the 2004 flow sensitivity runs, Table 13, show the percent changes in water temperature produced by the varying flows. As in the 2003 sensitivity runs, increasing the Sacramento River flow did not make a substantial difference at Benson's Ferry and New Hope.

	<b>2004 (20% Increase in Flow)</b>			
	<b>Sacramento River</b>		<b>Mokelumne River</b>	
	<b>Average Percent Difference</b>	<b>Maximum Percent Difference</b>	<b>Average Percent Difference</b>	<b>Maximum Percent Difference</b>
<b>Benson's Ferry</b>	0%	1%	2%	5%
<b>New Hope</b>	0%	2%	0%	2%

**Table 13:** Average and maximum percent difference between calibrated water temperature model with and increase flow model results for 2004 at Benson's Ferry and New Hope. Appendix E has all the graphical plots of this sensitivity analysis.

Increasing the Mokelumne River flow did decrease the water temperature a significant amount at Benson's Ferry. The daily maximum values are decreased just like the 2003 sensitivity runs, Figure 27.

However at New Hope a decrease in water temperature was not observed, as was seen in 2003, Figure 28. The lack of change was due to the fact that the Mokelumne release water was very similar to the water temperature at New Hope, therefore not creating a huge temperature difference.

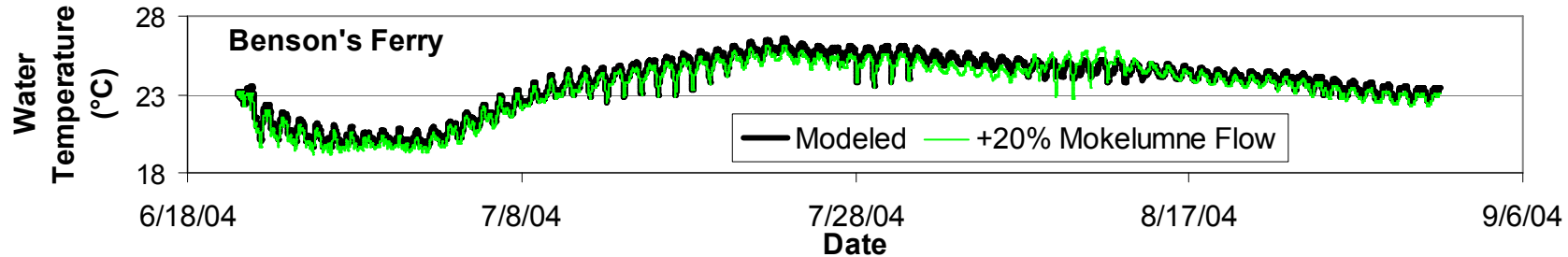


**Figure 27:** Calibrated 2004 water temperature run plotted with 2004 water temperature run with a 20% increase of Mokelumne flow at Benson's Ferry.

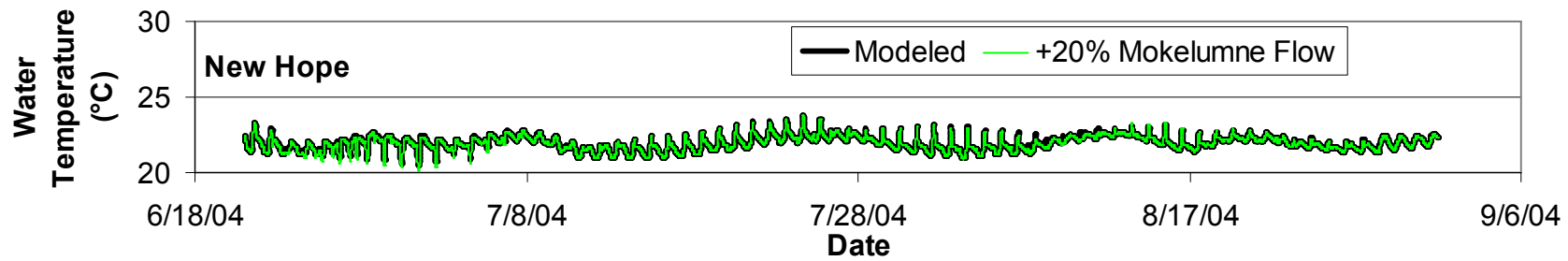


**Figure 28:** Calibrated 2004 water temperature run plotted with 2004 water temperature run with a 20% increase of Mokelumne flow at New Hope.

## SCENARIOS

Several management scenarios were implemented once the model was calibrated and verified to examine their effect on water temperature and electrical conductivity. The scenarios were developed based upon input from The Nature Conservancy, the California Department of Water Resources (DWR), and an expert panel convened by DWR. All of the simulations were performed for summer months periods when low flow conditions were present. The low flow case was modeled because typically this is the time when water quality parameters are the most susceptible to change.

The first scenario, shown in Figure 29, has the northeast levee of McCormack-Williamson Tract lowered to +2.6m NGVD 29 (+8.5 ft) and the southwest levee degraded to -0.76m NGVD 29 (-2.5ft). By degrading the southwest levee, the bottom of the McCormack-Williamson Tract was open to tidal activity, creating a wetland for fish, birds and other species. By lowering the east levee, which was originally +5.64m NGVD 29 (+18.5 ft), flood events will periodically overtop the levee, bringing water and sediment to the entire tract. In addition, a section of the levee that borders the Mokelumne River was degraded down to 0 ft NGVD 29 over a 30.5m (100 ft) length and then on either side of that was degraded to +1.07m NGVD 29 (+3.5 ft) for 30.5m (100 ft), creating a 91.4m wide (300ft) notch. From that notch an excavated secondary channel was created that is 457.2m (1500ft) long and with an invert elevation of 0m NGVD 29. The notch will let water coming from Benson's Ferry enter the upper end of the tract and drain out the bottom.

The second scenario, shown in Figure 30, had the east levee of the McCormack-Williamson Tract lowered to +2.6m NGVD 29 (+8.5ft), which is similar to the first

scenario described above. However, the southwest levee was lowered to +1.68m NGVD 29 (+5.5ft) which is higher than in the first scenario. Unlike the first scenario the second does not allow tidal water in from the southwest side and water in from the notch on the Mokelumne levee side of the tract. This option also allows for more control of the inundation in the island because it does not have tidal water coming into the island. The east levee should overtop in 2-year recurrence interval events and the water level of the island could be controlled by pumping the island, unlike in scenario one. The nekton gates were not included in the model due to the fact that they will only be in use during higher flow events.

The third scenario, shown in Figure 31, is almost identical to the second except that there is an additional cross levee about 1300 meters north from the southwest levee. The cross levee is +1.68m NGVD 29 (+5.5ft) and separates the tract, possibly allowing water in one section and not in the other, creating a subsidence reversal scenario in the bottom portion of the island. The siphons were not included in the model due to the fact that they will only be in use during higher flow events.

The fourth scenario examines changes in the operation of the Delta Cross Channel (DCC). It closes the DCC during low flow periods instead of its normal operation where it is open during the summer time.

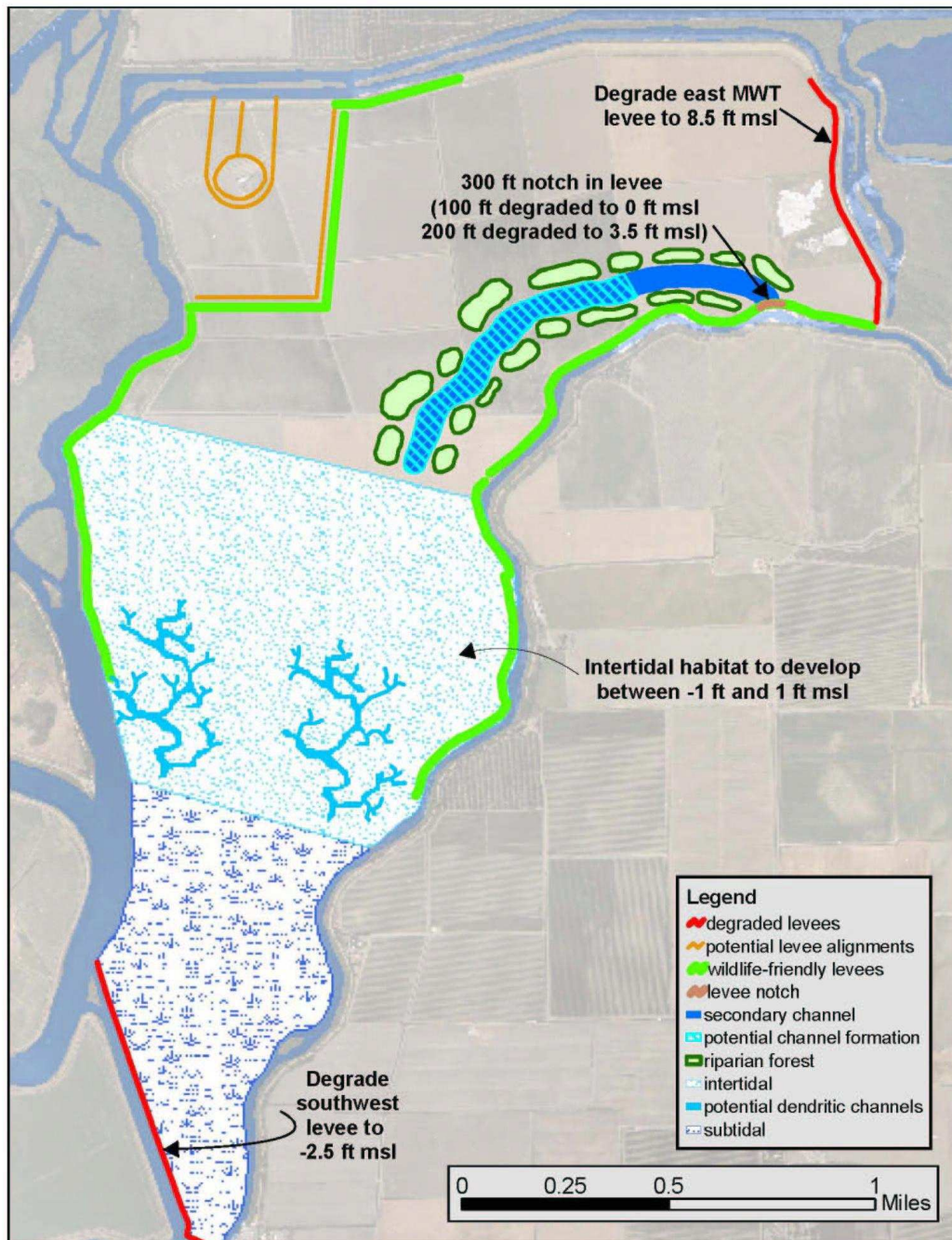


**Figure 29:** Scenario one: minimum control and maximum fluvial flow

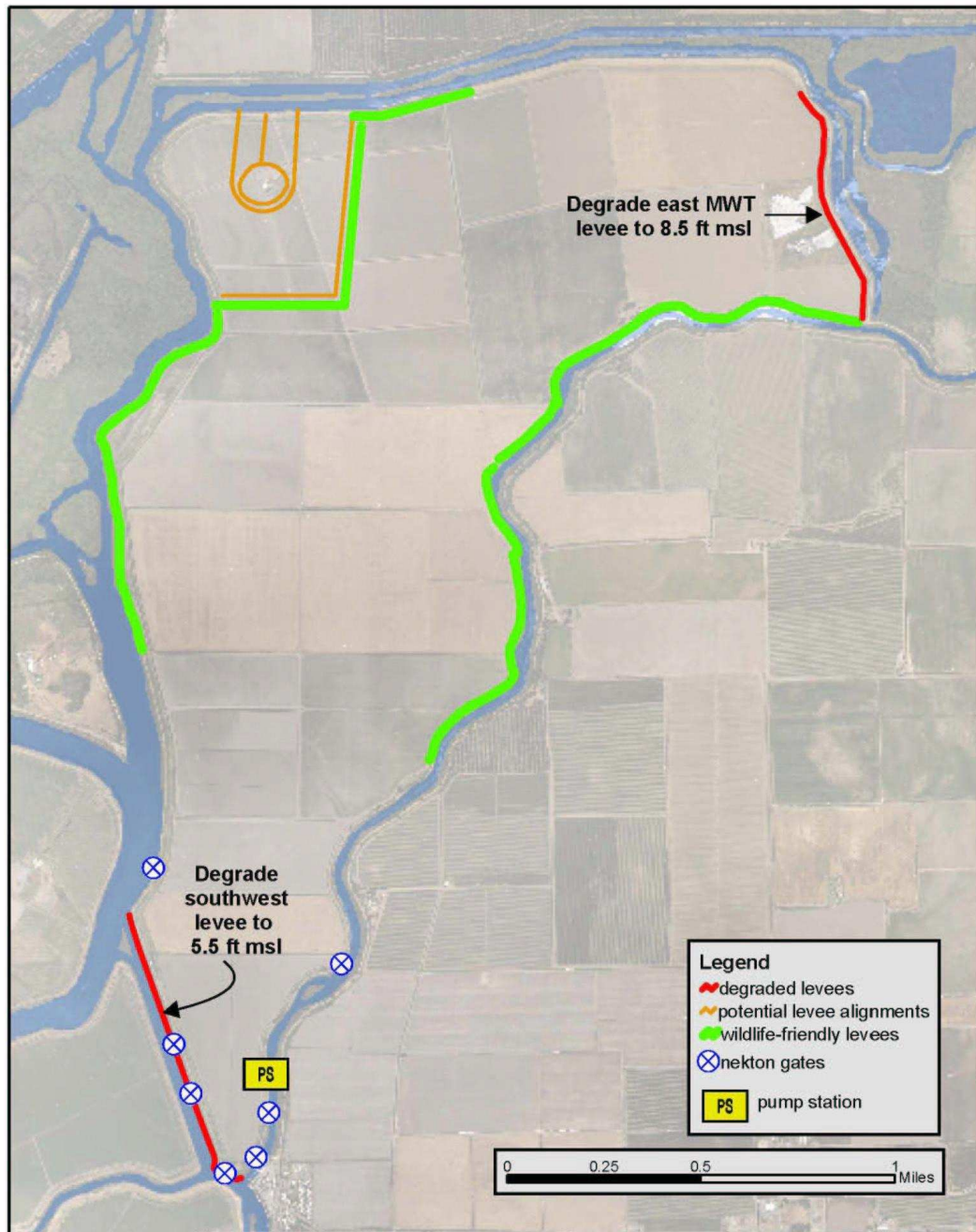


**Figure 30:** Scenario two: maximum control of water in and out of tract.

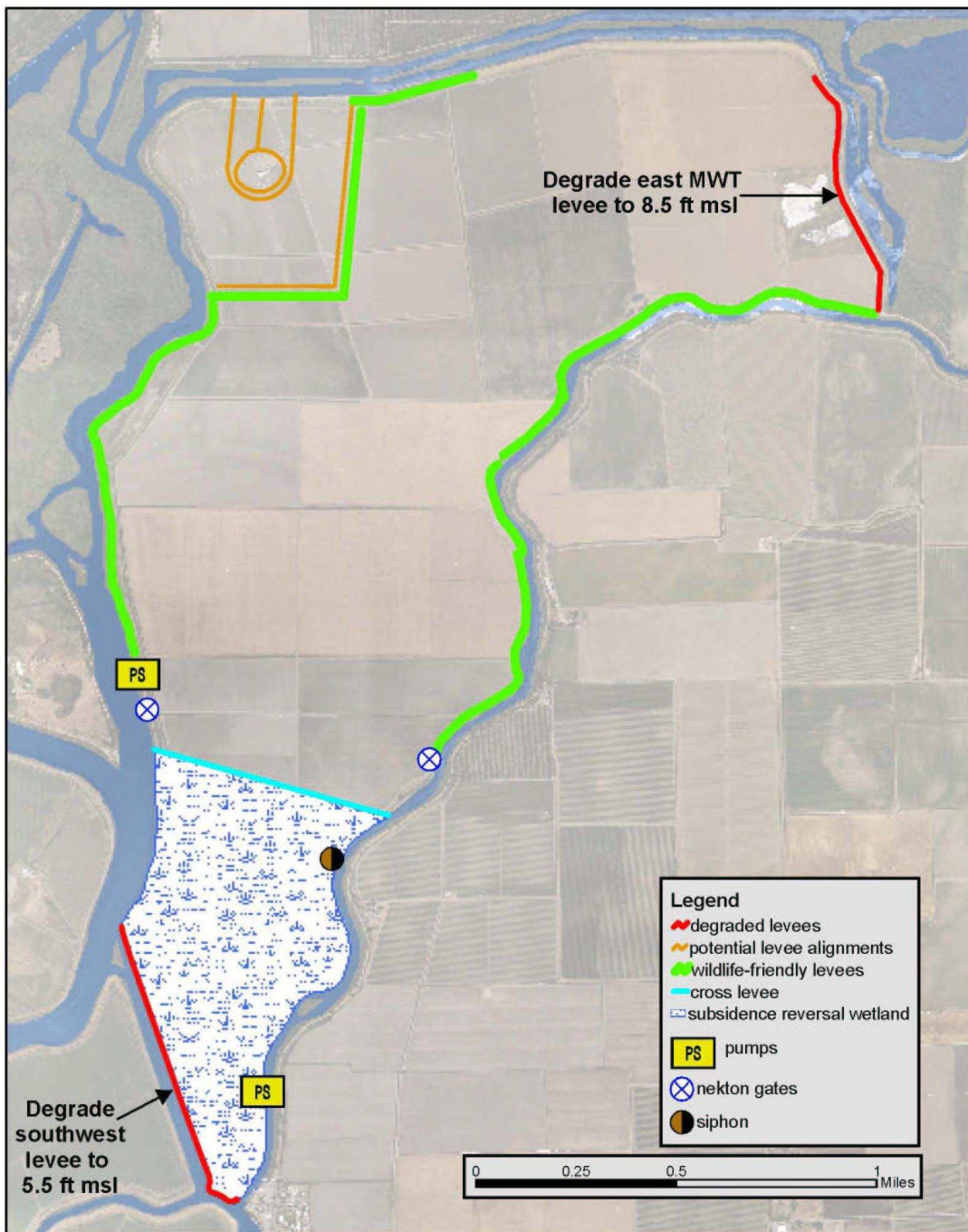


**Figure 31:** Scenario three: a hybrid of subsidence reversal and season floodplain.

## SCENARIO RESULTS

The management scenarios were input into the model definition and simulated with the calibrated parameters for both the water temperature and electrical conductivity models. Scenarios 2 and 3 did not alter water temperature or electrical conductivity levels. Since the water levels did not get high enough at either the southwest or northeast side of McCormack-Williamson Tract to over top those degraded levees during low flow periods, no water quality changes would be expected. In 2004 the water level at the southwest side of McCormack-Williamson Tract reached a maximum level of +1.5m NGVD 29 (+4.9 ft), still nearly 25cm below the lowered levee; the northeast side reached a maximum water level of +1.4m NGVD 29 (+4.6ft), which is about 1.2m (4 ft) below the lowered levee. Similar water levels occurred in 2003 still creating no opportunity for water to enter the tract. Since it does not alter the original flow it never alters water quality parameters.

Scenario 1 created no significant changes upstream at Benson's Ferry for water temperature in both 2003 and 2004. Both years only created an average 1% change when compared to the calibrated runs. Downstream of McCormack-Williamson Tract in 2003, the water temperature was altered, producing an average 4% difference. A greater diurnal flux in water temperature was created and also the minimums and maximums values were increased overall. This is attributed to the fact that by opening up McCormack-Williamson Tract the water has to travel through that area which is very shallow, wetland habitat which will heat up the water. The warmer water travels back into the system and heads toward downstream areas, Figure 32.

A similar trend was seen during the 2004 simulations. A greater diurnal variation was produced, although in this case the overall temperature did not increase as much as the simulations for 2003, Figure 33. The 2004 simulation predicted a 2% difference from the calibrated base case.

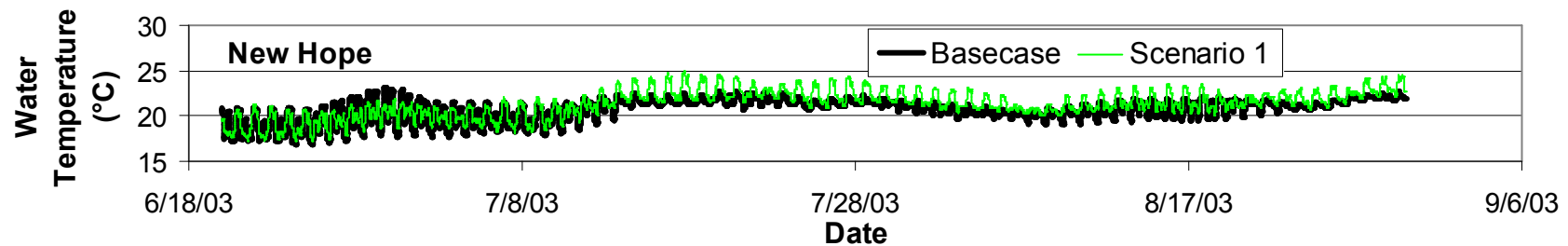


**Figure 32:** Comparison of calibrated base case plotted with the application of scenario 1 to 2003 at New Hope.

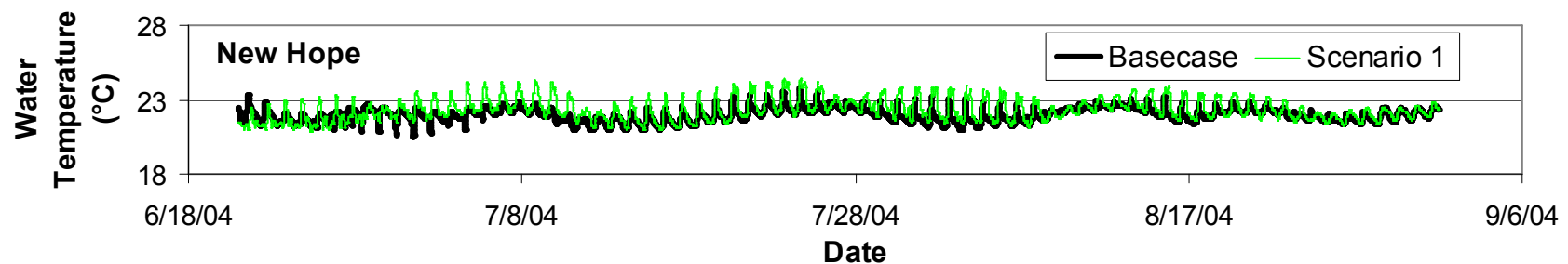


**Figure 33:** Comparison of calibrated base case plotted with the application of scenario 1 to 2004 at New Hope.

In examining changes to the electrical conductivity, there was a slight increase upstream of MWT at Benson's Ferry, Figure 34. The results show an approximate 3% difference when compared to the calibrated run. The change is due to the fact that MWT is acting as a holding basin for water and not allowing it to travel upstream to flush out the salinity which would increase the electrical conductivity levels.

Downstream of the altered tract along the South Fork Mokelumne River at the location referred to as South Staten, the EC levels increase just similar to Benson's Ferry. The increase occurs due to the same reason, Figure 35, McCormack-Williamson Tract is holding water that would have otherwise flushed salinity out the system. At the South Staten location, ecological option 1 created a 4% difference from the calibrated base case.

At New Hope an interesting result was produced where the electrical conductivity levels had less fluctuation but the average levels were similar, Figure 36. This damping effect could be contributed to the fact that New Hope is very close to the degraded levee. Having this degraded levee creates a new route for the tidal water to enter therefore creating more tidal exchange in that area allowing the electrical conductivity levels to be muted near the degraded levee. This scenario created a 2% average difference at New Hope.

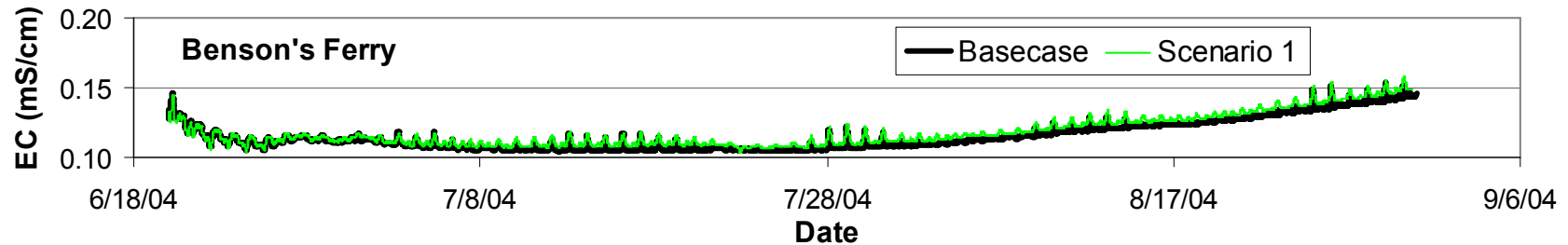


**Figure 34:** Comparison of calibrated base case plotted with scenario 1 for 2004 electrical conductivity at Benson's Ferry.

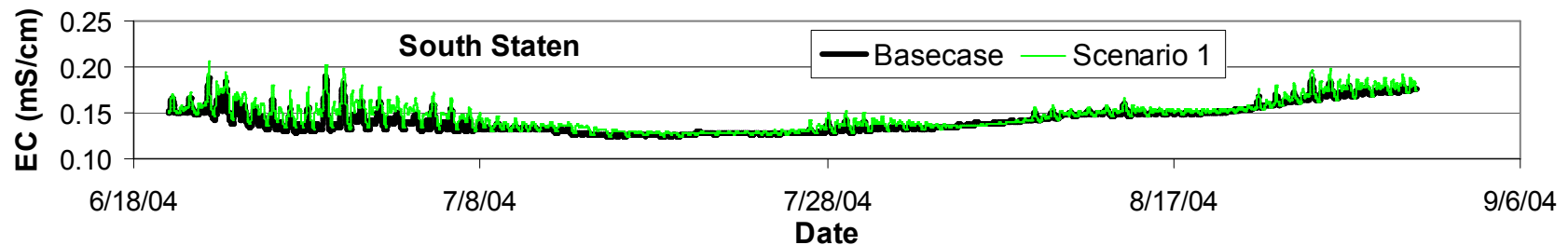


**Figure 35:** Comparison of calibrated base case plotted with scenario 1 for 2004 electrical conductivity at South Staten.

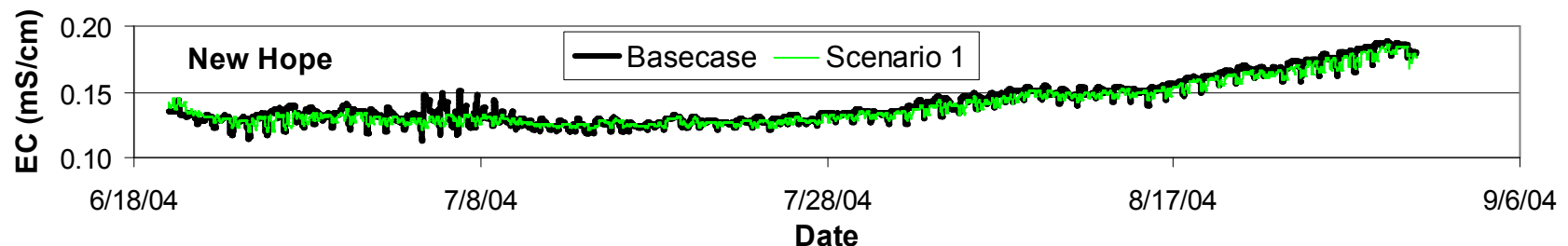


**Figure 36:** Comparison of calibrated base case plotted with scenario 1 for 2004 electrical conductivity at New Hope.

Changing the Delta Cross Channel operations created no significant change upstream of McCormack-Williamson Tract, at Benson's Ferry, on water temperature during either 2003 and 2004. Only a 1% average difference was predicted in the 2004 runs while there was no difference in the 2003 simulation. Downstream at New Hope, the water temperature changed in both 2003 and 2004 but in different manners. In 2004 the Sacramento River water was cooler than the water at New Hope so by closing the DCC cooler water was blocked from entering the system therefore increasing the overall temperature, Figure 37. The blockage of cooler water created a 5% average water temperature increase compared to when the DCC was open.

The 2003 run predicted a different result, although it also produced a 5% difference from the calibrated run. There was an initial drop in water temperature which is due to the fact that in 2003 the Sacramento River water was warmer than the New Hope water. In closing the Delta Cross Channel the warmer Sacramento water was prevented from ever reaching this location. However, the water temperature then rose due to an increase in air temperature, then the simulations of the two years seem to follow a similar pattern, Figure 38.

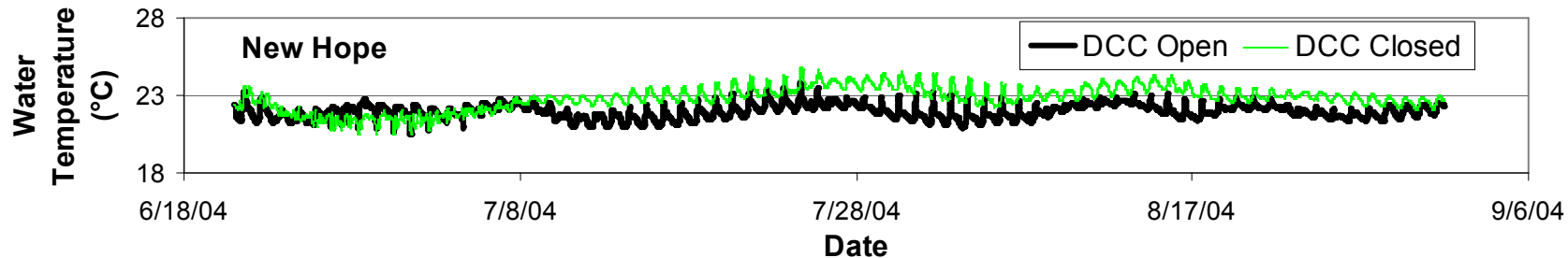


**Figure 37:** Comparison of water temperatures at New Hope when DCC is open (calibrated base case) to when DCC is closed in 2004.

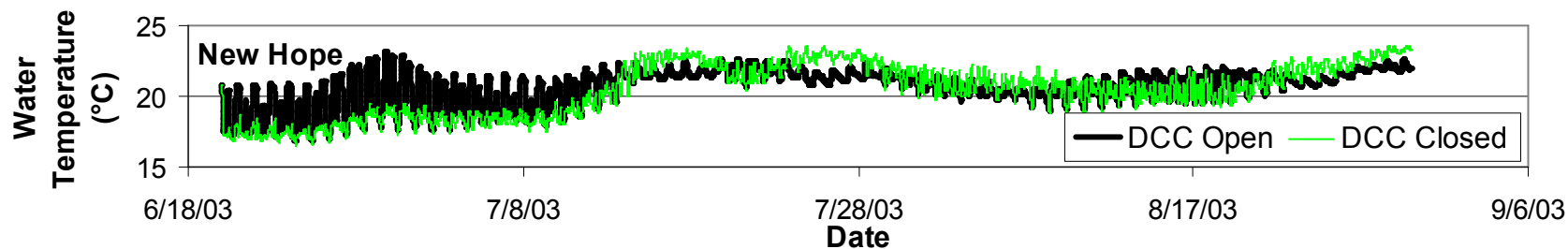


**Figure 38:** Comparison of at New Hope when DCC is open (calibrated base case) to when DCC is closed in 2003.

Looking at the effects of the Delta Cross Channel closure on electrical conductivity there is no significant change at Benson's Ferry. Only an increase in the maximum values occurs producing a 1% average change, Figure 39.

The spikes occurred because the lower electrical conductivity of the Sacramento River water did not reach Benson's Ferry to mitigate the spikes coming down the Mokelumne River. While there is not a vast amount of water flow from the Sacramento River, it is significant enough to make the above slight changes in those peaks. Inspecting the downstream changes, both New Hope and South Staten's electrical conductivity levels were increased, Figures 40 and 41, without the inflow of the lower electrical conductivity Sacramento River water.

At New Hope a 9% average increase in electrical conductivity was simulated while at South Staten a 15% average increase was predicted. The change is due to the fact that, with the Delta Cross Channel closed, Sacramento River water is prevented from entering and therefore cannot flush and mix the higher electrical conductivity water from the delta. It is also interesting to notice that the electrical conductivity levels are somewhat more constant when the Sacramento River is closed off from the north delta area. Without the tidally influenced periodic inflow from the lower electrical conductivity Sacramento River water there is only one flow source for salinity, the Mokelumne River.

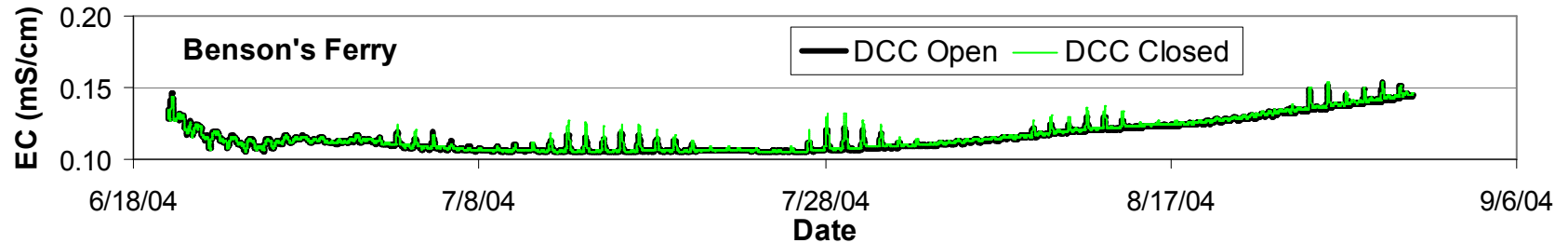


**Figure 39:** Scenario four at Benson's Ferry where the Delta Cross Channel (DCC) is closed with the calibrated base case that has the DCC open.

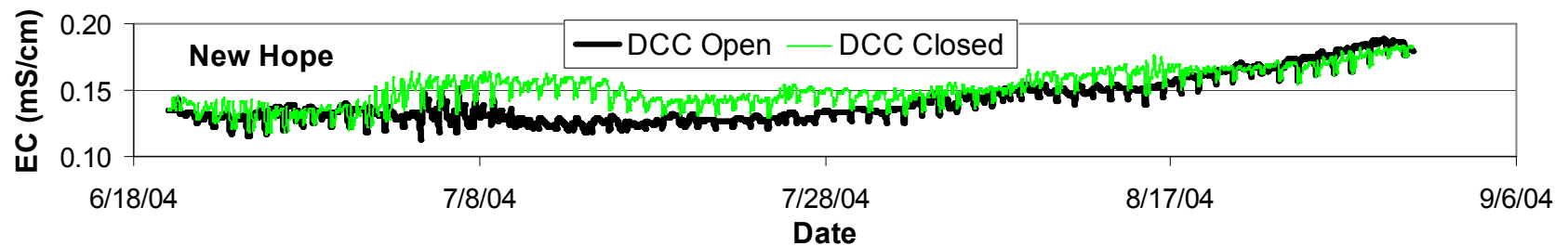


**Figure 40:** Scenario four at New Hope where the Delta Cross Channel (DCC) is closed with the calibrated base case that has the DCC open.

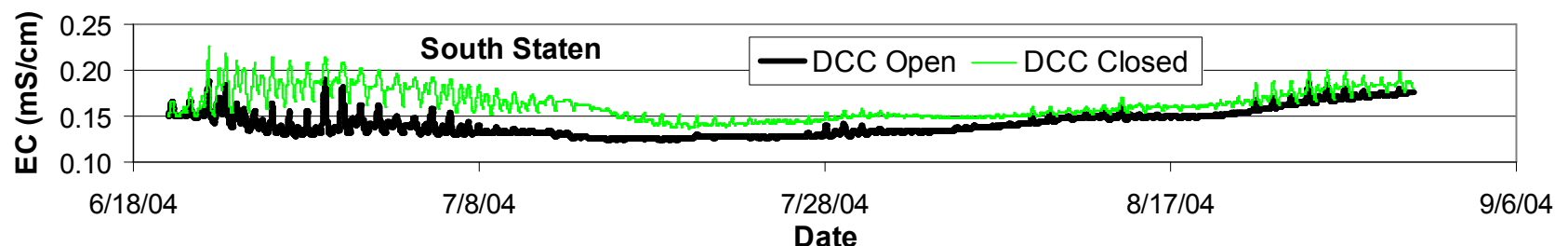


**Figure 41:** Scenario four at South Staten where the Delta Cross Channel (DCC) is closed with the calibrated base case that has the DCC open.

## DISCUSSION AND CONCLUSION

The development and application of the North Delta water quality model to investigate changes in water temperature and electrical conductivity when various McCormack Williamson management scenarios were implemented provided insight to the complex water quality dynamics of the system. Both the water temperature and electrical conductivity model results prove that the model can simulate the two parameters, in the low flow events of the summer. However, it is important to realize that the main use of this model is not meant to be predictive instead it is intended to be used to show trends and provide a tool to evaluate differences in various management scenarios.

The only management scenarios that yielded any type of change in water temperature and electrical conductivity were the ones that altered the original state of the flow; those were scenarios one and four. In scenario four the Delta Cross Channel was closed and changes to both the water temperature and electrical conductivity downstream of the gate occurred. Changes were observed upstream of the cross channel gates but they were not as significant as the changes downstream.

Scenario one, which degraded levees on McCormack-Williamson Tract so low flow events could enter the tract, produced slight changes in water quality both about 3km upstream and downstream. However, the greatest change was seen at New Hope which is very close to the lower degraded levee. This means that changes in water quality during a low flow event can be seen in a localized area around the altered tract, while there are slight changes upstream and downstream.

An important outcome from this study is the vast database that was complied for the North Delta. Continuous water quality data are quite scarce. There were some electrical conductivity data but very little water temperature data. It was discovered that the maximum summer water temperature at Benson's Ferry for 2003 was 23.3°C with a minimum of 15.7°C. In 2004 the maximum was 27.3°C with a minimum of 17.7°C. At New Hope in 2003 the maximum water temperature was 23.8°C with a minimum of 17.0°C. In 2004 the maximum was 24.4°C with a minimum of 20.5°C. This illustrates that Benson's Ferry has more change in minimum and maximum temperatures meaning that New Hope is closer to an equilibrium temperature. Part of this is due to the fact that New Hope has a stronger tidal influence than Benson's Ferry. To find water measured quality data at other boundary points refer to Appendix H. This data set could also be used by others to investigate other water quality issues, such as algae growth and nutrient cycles in the North Delta.

The current model study produced results that are similar to measured data; however this does not mean that more improvements could not be made in the water quality model solution scheme. In modeling electrical conductivity the advection-dispersion equation was used, the best available solution scheme today. However, in the water temperature model the user is not allowed to change the solar radiation variable temporally. A constant solar radiation value confines the user into using only a typical value instead of a value that changes over time which is more realistic. The constant input value does not allow the model to capture events that do not follow the average. In addition there is no shading term in the MIKE 11 model which makes it very difficult to get accurate solar radiation values where shading varies spatially or seasonally.

## REFERENCES

- Ahearn, D.S., Sheibley, R.W., Dahlgren, R.A., and Keller, K.E. 2004. Temporal Dynamics of Stream Water Chemistry in the last free-flowing River Draining the Western Sierra Nevada, California. *Journal of Hydrology*, vol. 295, p 47-63.
- Beschta, R.L. and Taylor, R.L., 1988. Stream Temperature Increase and Land-Use in a Forested Oregon Watershed. *Water Resources Bulletin*, vol. 24, no. 1, p. 19-25.
- Blake, S.H., 2001 An unsteady hydraulic surface water model of the Lower Cosumnes River, California, for the investigation of floodplain dynamics. Masters Thesis. University of California, Davis, California.
- Brown, K.J. and Pasternack, G.B., 2004. The Geomorphic Dynamics and Environmental History of an Upper Deltaic Floodplain Tract in the Sacramento-San Joaquin Delta, California, USA. *Earth Surface Processes and Landforms*, vol. 29, p. 1235-1258.
- CALFED Day/ Delta Program, 2000. Ecosystem restoration plan, strategic plan for deltaic floodplain tract in the Sacramento-San Joaquin Delta, California, USA.
- California Department of Water Resources, 1992. North delta study, AutoCAD drawings of study region.
- California Department of Water Resources, 2002. McCormack-Williamson Tract survey, SR02-05. surveyed January 2002.
- Campbell, J.E., Briggs, D.A., Denton, R.A., and Gartrell, G. 2002. Water Quality Operation with a Blending Reservoir and Variable Sources. *Journal of Water Resources Planning and Management*, vol. 128, no 4, p. 288-302.
- Hammersmark, C. T., 2002. Hydrodynamic Modeling and GIS Analysis for the Habitat Potential and Flood Control Benefits of the Restoration of a Leveed Delta Island. Masters Thesis. University of California, Davis, California.
- National Oceanic and Atmospheric Association-Ocean Service, 2002. Tidal characteristic data for New Hope Bridge, Mokelumne River, CA. Provided by NOAA Ocean Service, Silver Spring, Maryland on October 3, 2002.
- Oltmann, R.N. and Simpson, M.R., 1999. Measurement of Tidal Flows in the Sacramento-San Joaquin Delta, California. U.S. Geological Survey publication.
- Orlob, G.T., 1992. Water-Quality Modeling for Decision Making. *Journal of Water Resources Planning and Management*, vol. 118, no. 3, p. 295-307.

Rojstaczer, S.A., Hamon, R.E., Deveral, S.J, and Massey, C.A, 1991. Evaluation of selected data to assess the causes of subsidence in the Sacramento-San Joaquin Delta, California. United State Geological Survey Open-File Report 91-193.

State of California Reclamation Board, 1941. Meeting minutes re: application no. 855, dated August 20, 1941.

Simenstad, C., Toft, J., Higgns, H., Cordell, J., and Orr, M., 2000. Sacramento/San Joaquin Delta breached levee wetland study (BREACH), Preliminary Report.

Thomann, R.V., O'Connor, D.J., and DiToro, D.M., 1970. Modeling of the Nitrogen and Algal Cycles in Estuaries. Water Pollution Research. vol. 70, p 14.

U.S. Army Corps of Engineers, Sacramento District, 1988. Downstream flood impacts for the proposed Lambert Road outlet facility, office report.

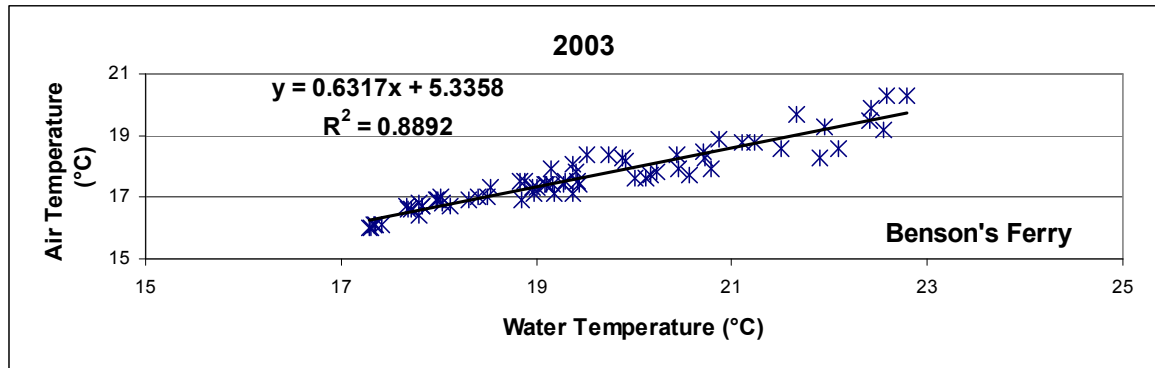
U.S. Geological Survey, 1911. Topographical map of the Sacramento Valley, California. U.S. Geological Survey Atlas Sheets.

Whitehead, P.G., 1980. Water Quality Modeling for Design. The influence of man on the hydrological regime with special reference to representative and experimental basins. No. 130, p. 465-475.

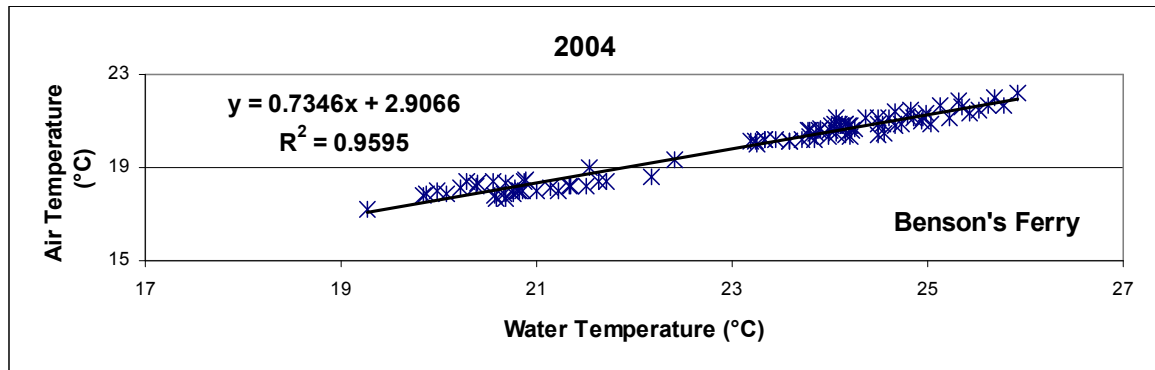
Wong, H.F.N., 1990. A branched Mass Transport Model of the Sacramento San Joaquin Delta, California. Hydraulic Engineering. vol. 1990, p. 103-108.

## APPENDIX A

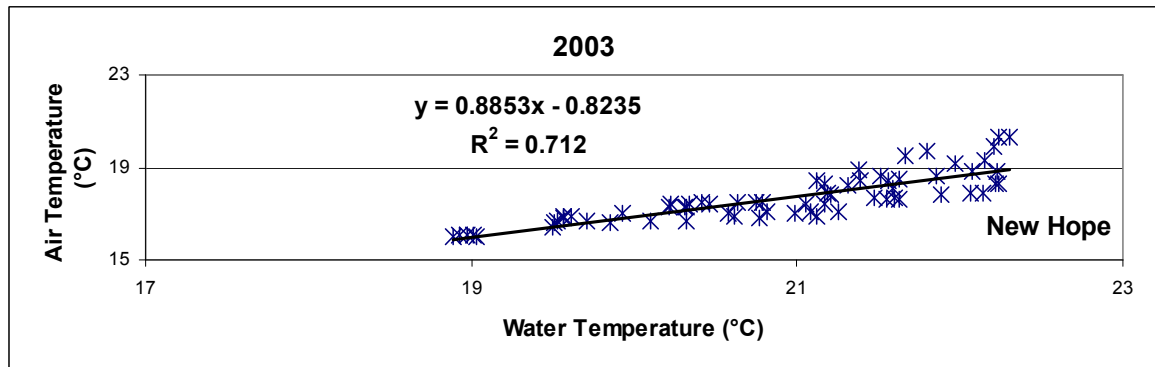
This appendix contains the data correlation plots mentioned in the data correlation section.



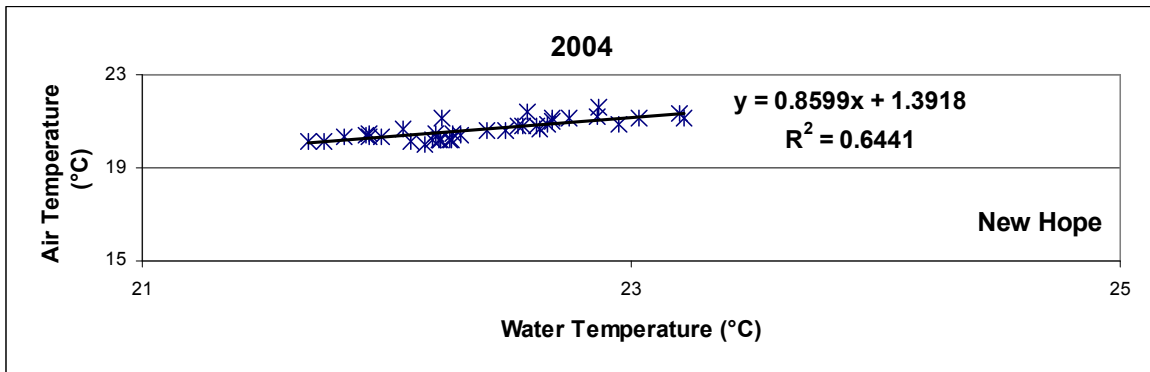
**Figure A-1:** Correlation plot at Benson's Ferry of water temperature with air temperature for the year of 2003.



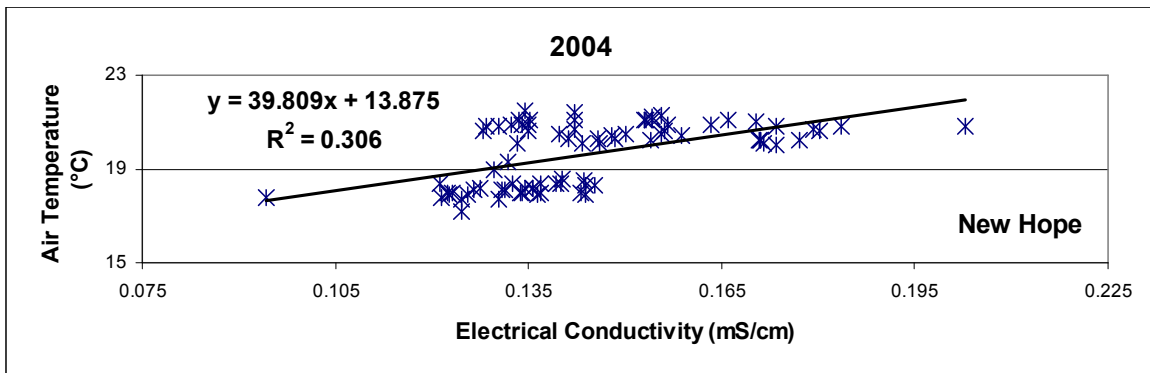
**Figure A-2:** Correlation plot at Benson's Ferry of water temperature with air temperature for the year of 2004.



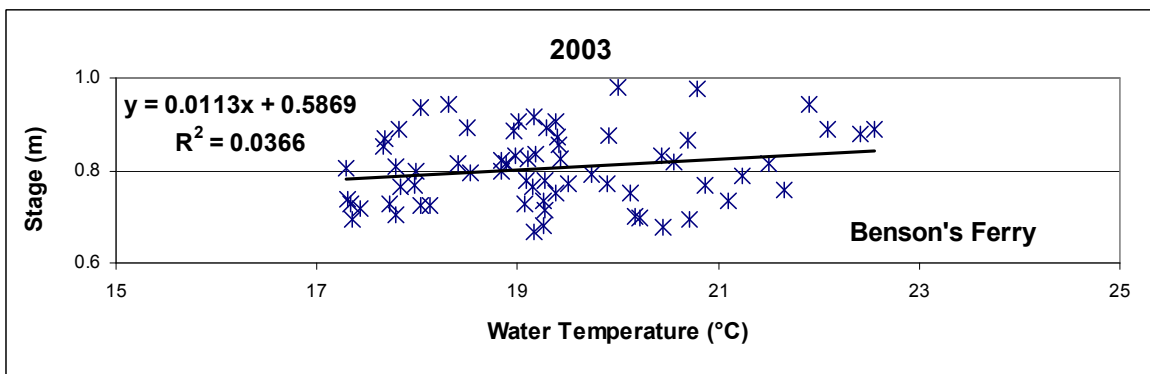
**Figure A-3:** Correlation plot at New Hope of water temperature with air temperature for the year of 2003.



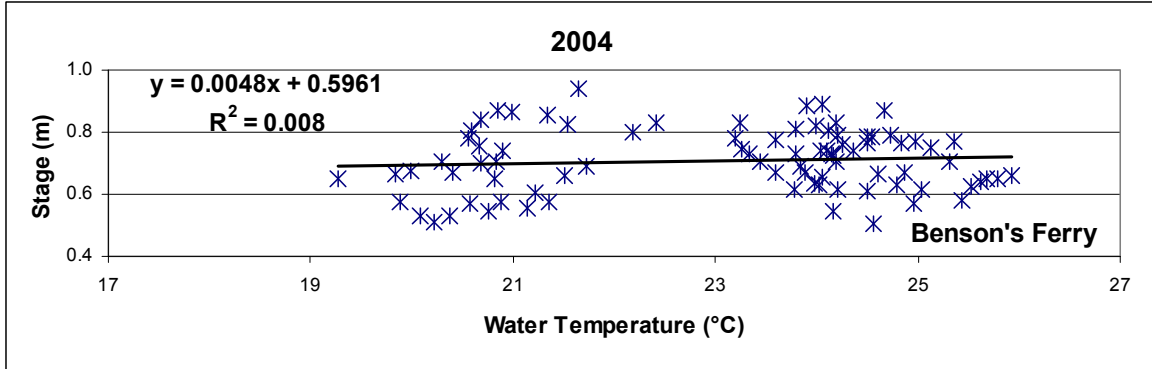
**Figure A-4:** Correlation plot at New Hope of water temperature with air temperature for the year of 2004.



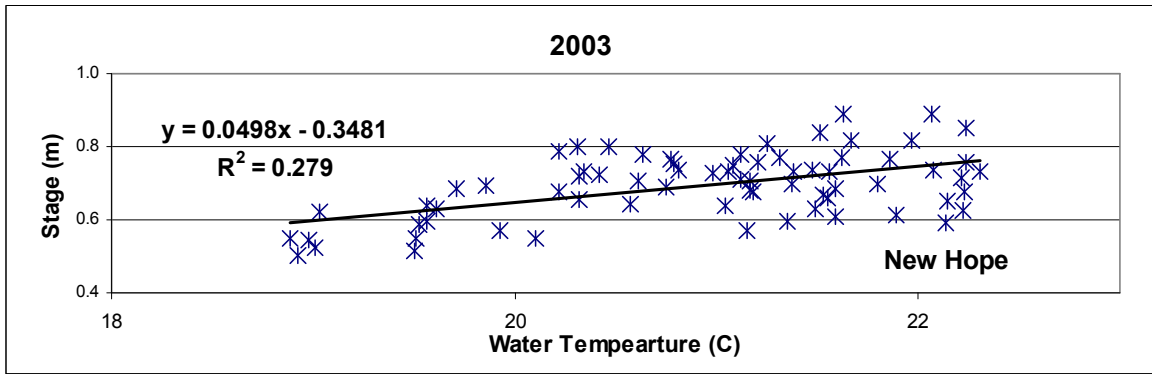
**Figure A-5:** Correlation plot at New Hope of electrical conductivity with air temperature for the year of 2004.



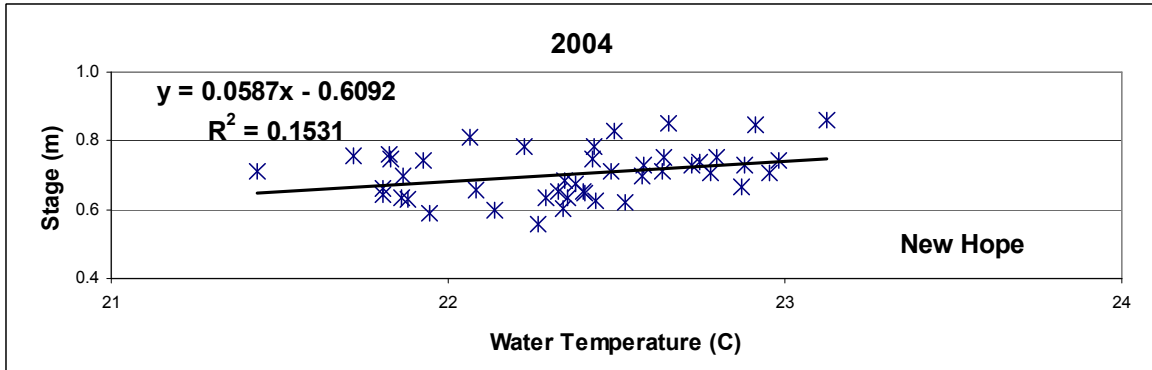
**Figure A-6:** Correlation plot at Benson's Ferry of water temperature with stage for the year of 2003.



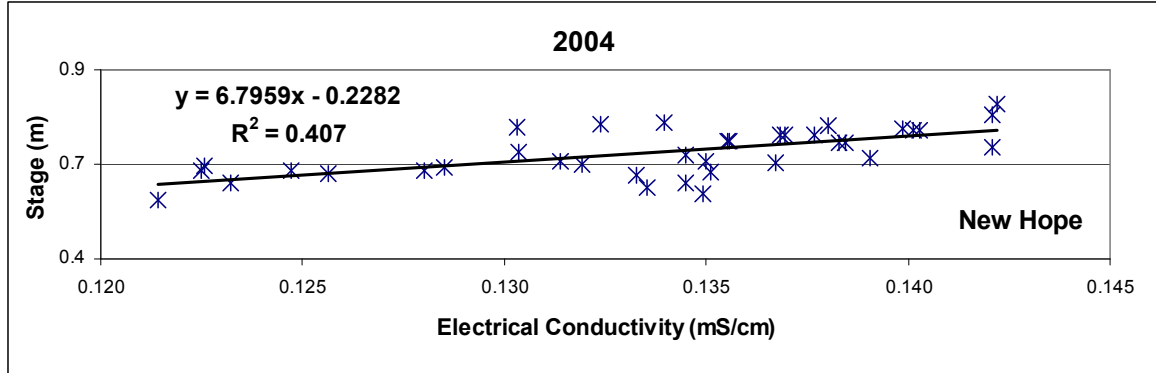
**Figure A-7:** Correlation plot at Benson's Ferry of water temperature with stage for the year of 2004.



**Figure A-8:** Correlation plot at New Hope of water temperature with stage for the year of 2003.



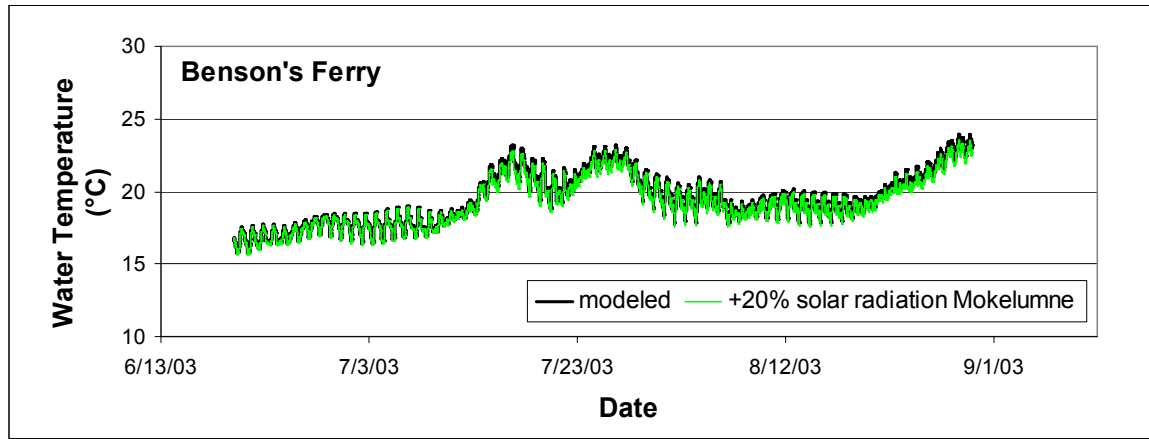
**Figure A-9:** Correlation plot at New Hope of water temperature with stage for the year of 2004.



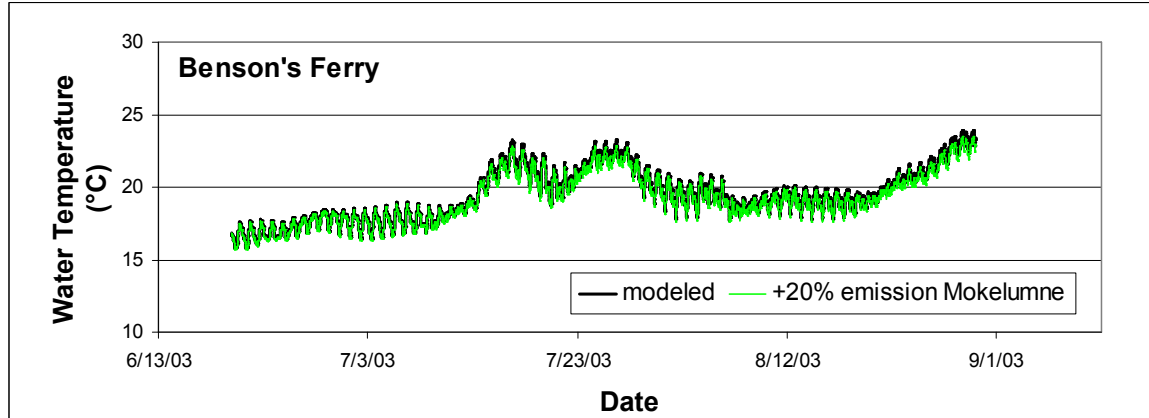
**Figure A-10:** Correlation plot at New Hope of electrical conductivity with stage for the year of 2004.

## APPENDIX B

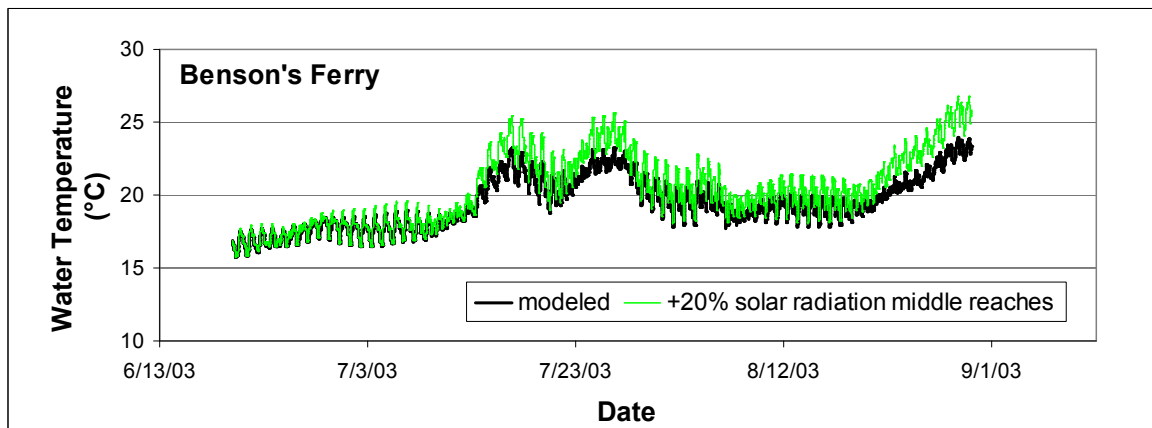
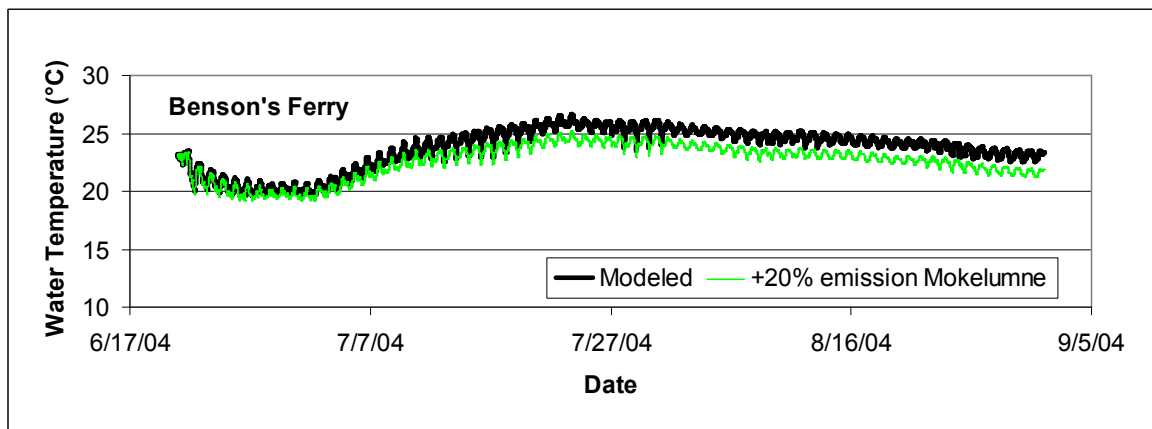
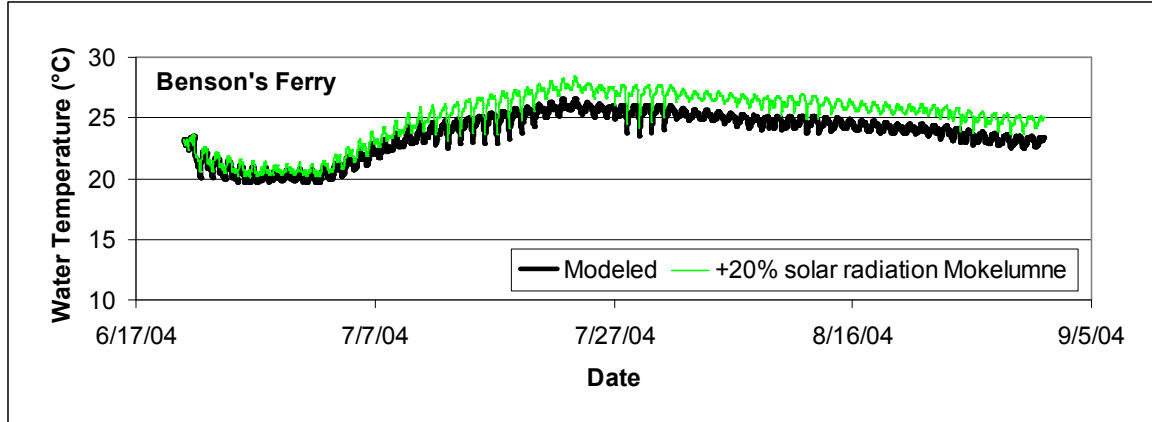
This appendix contains graphs which plot the results from the water temperature sensitivity analysis when the maximum solar radiation and the emission values were varied at Benson's Ferry.

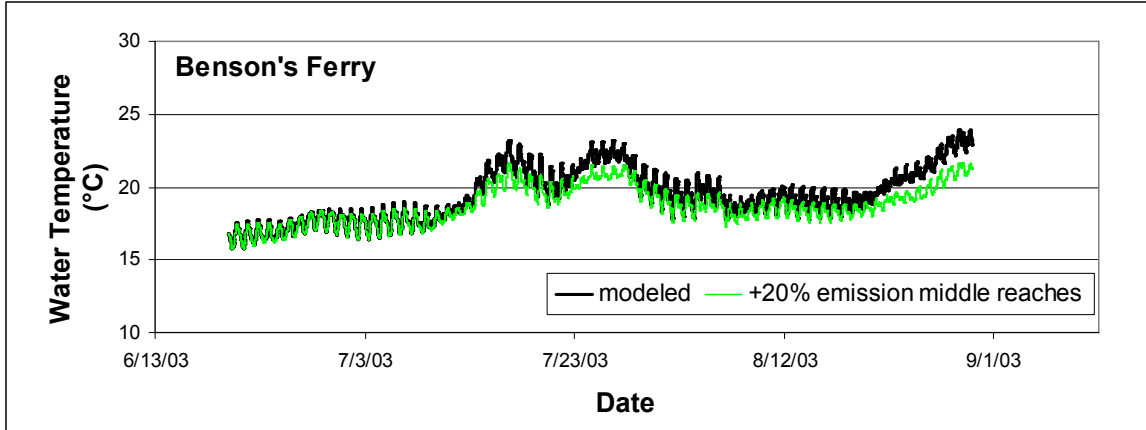


**Figure B-1:** Calibrated 2003 water temperature run plotted with 2003 water temperature run that has a 20% increase of the maximum solar radiation value along the Mokelumne at Benson's Ferry.

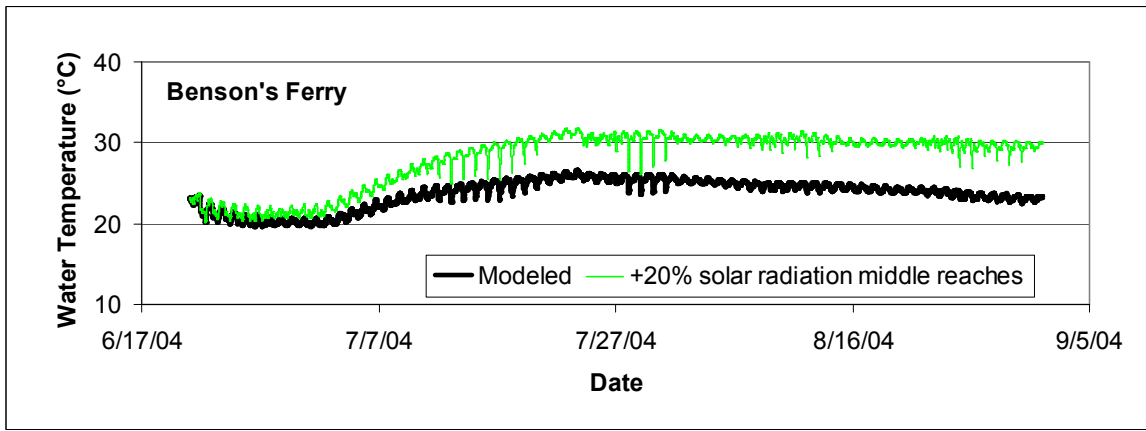


**Figure B-2:** Calibrated 2003 water temperature run plotted with 2003 water temperature run that has a 20% increase of the emission value along the Mokelumne at Benson's Ferry.

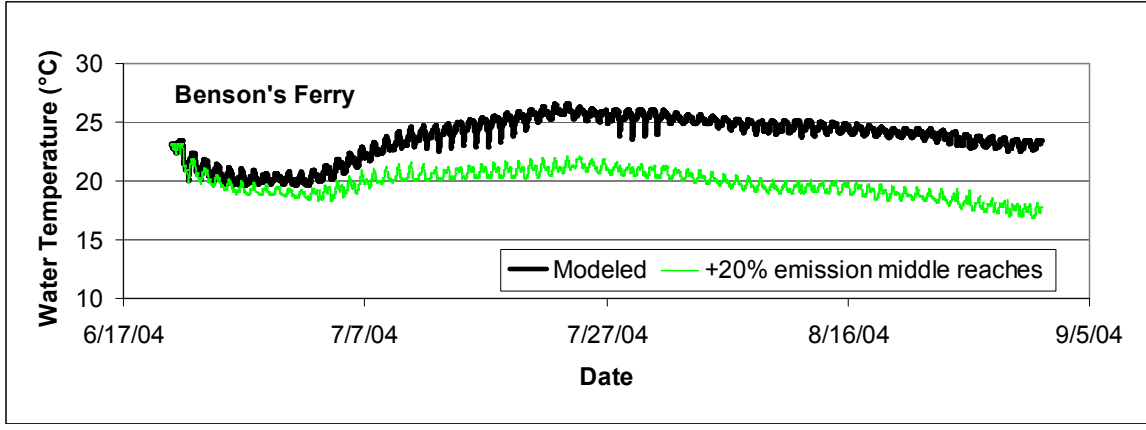




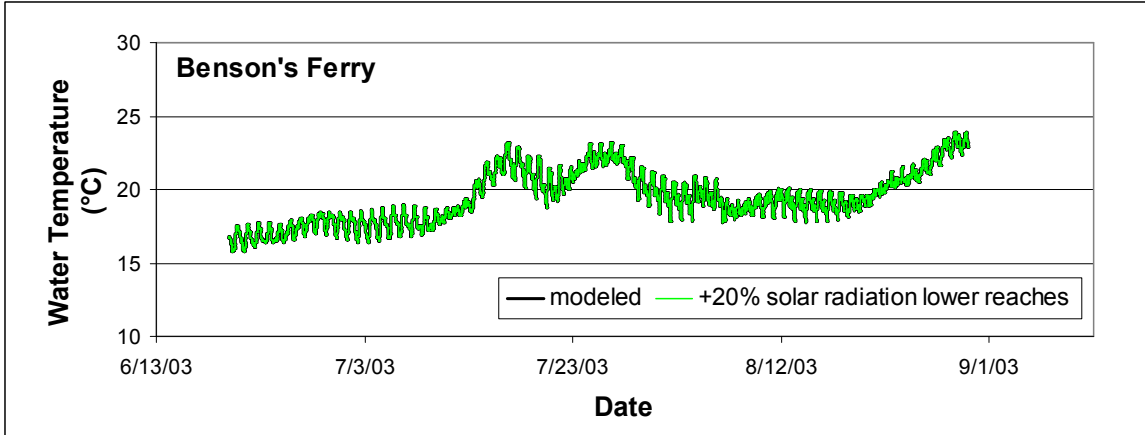
**Figure B-6:** Calibrated 2003 water temperature run plotted with 2003 water temperature run that has a 20% increase of the emission value along all the middle reaches at Benson's Ferry.



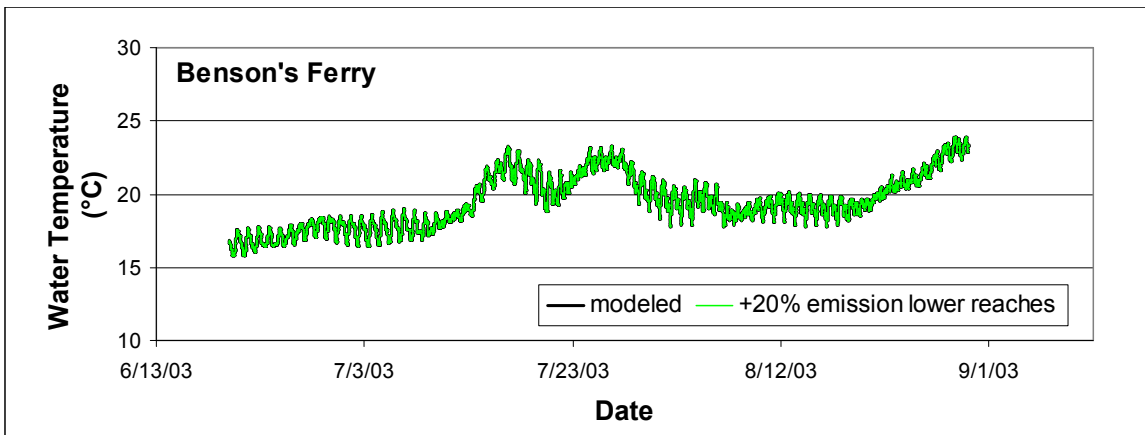
**Figure B-7:** Calibrated 2004 water temperature run plotted with 2004 water temperature run that has a 20% increase of the maximum solar radiation value along all the middle reaches at Benson's Ferry.



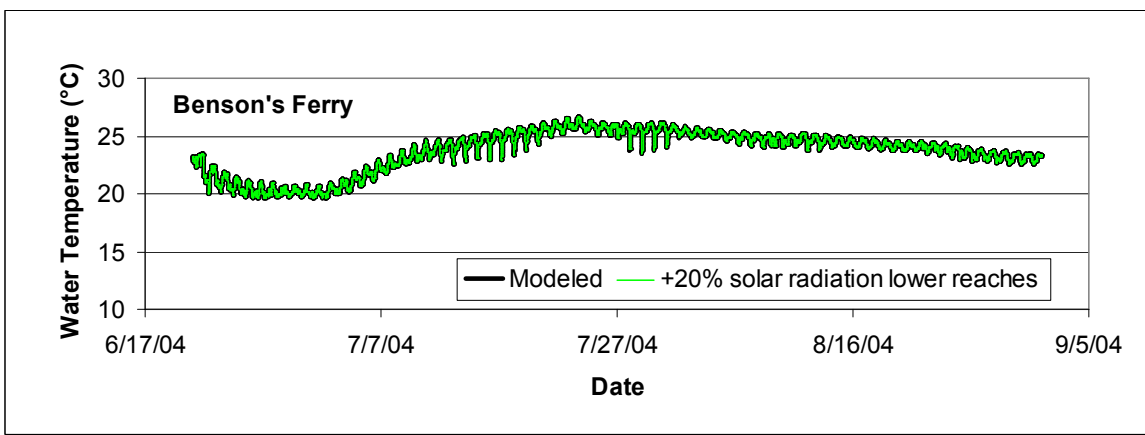
**Figure B-8:** Calibrated 2004 water temperature run plotted with 2004 water temperature run that has a 20% increase of the emission value along all the middle reaches at Benson's Ferry.



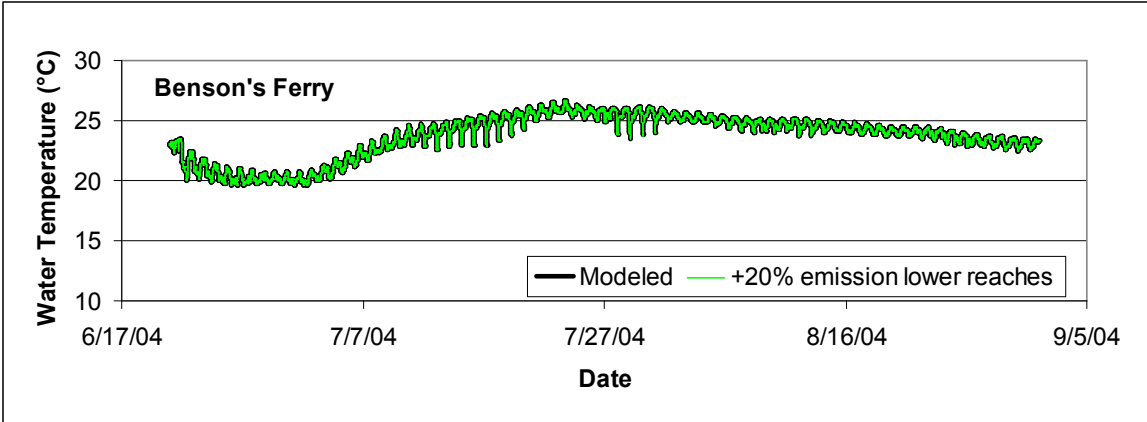
**Figure B-9:** Calibrated 2003 water temperature run plotted with 2003 water temperature run that has a 20% increase of the maximum solar radiation value along all the lower reaches at Benson's Ferry.



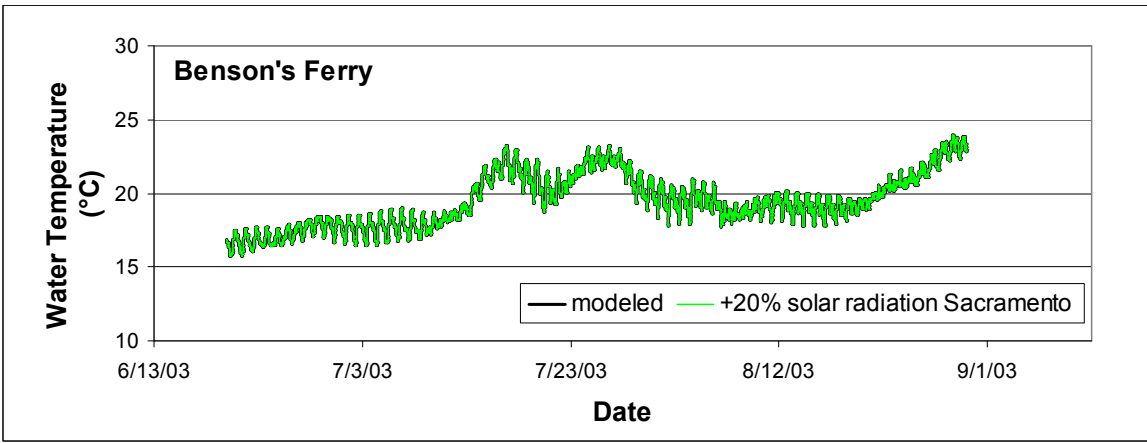
**Figure B-10:** Calibrated 2003 water temperature run plotted with 2003 water temperature run that has a 20% increase of the emission value along all the lower reaches at Benson's Ferry.



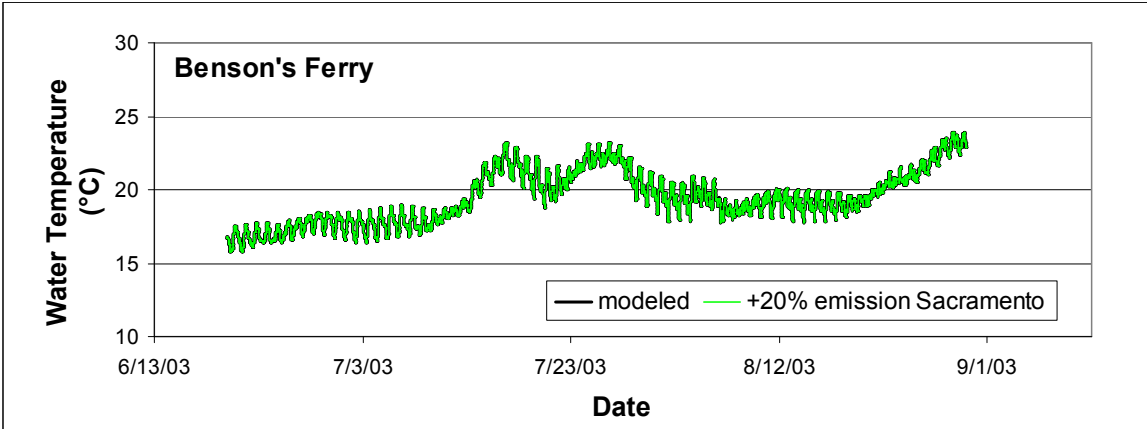
**Figure B-11:** Calibrated 2004 water temperature run plotted with 2004 water temperature run that has a 20% increase of the solar radiation value along all the lower reaches at Benson's Ferry.



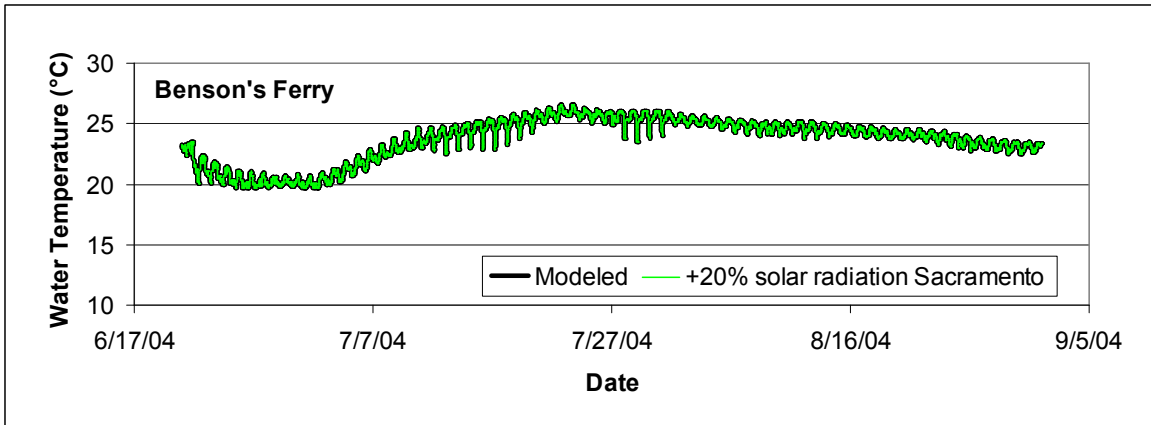
**Figure B-12:** Calibrated 2004 water temperature run plotted with 2004 water temperature run that has a 20% increase of the emission value along all the lower reaches at Benson's Ferry.



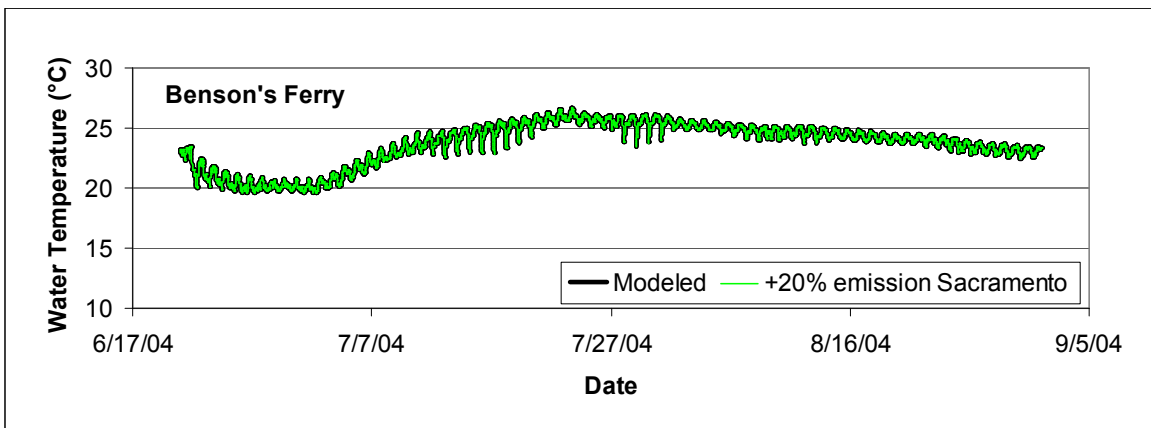
**Figure B-13:** Calibrated 2003 water temperature run plotted with 2003 water temperature run that has a 20% increase of the maximum solar radiation value along the Sacramento River at Benson's Ferry.



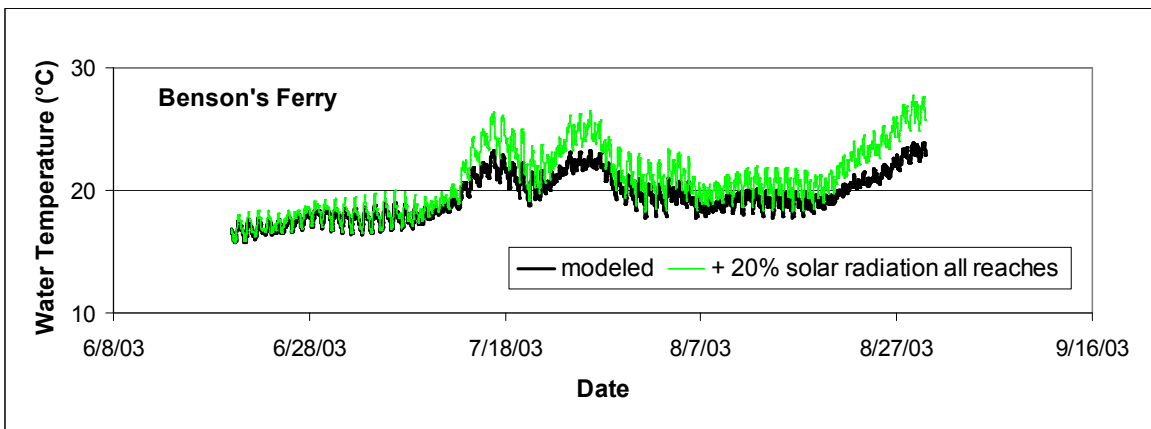
**Figure B-14:** Calibrated 2003 water temperature run plotted with 2003 water temperature run that has a 20% increase of the emission value along the Sacramento River at Benson's Ferry.



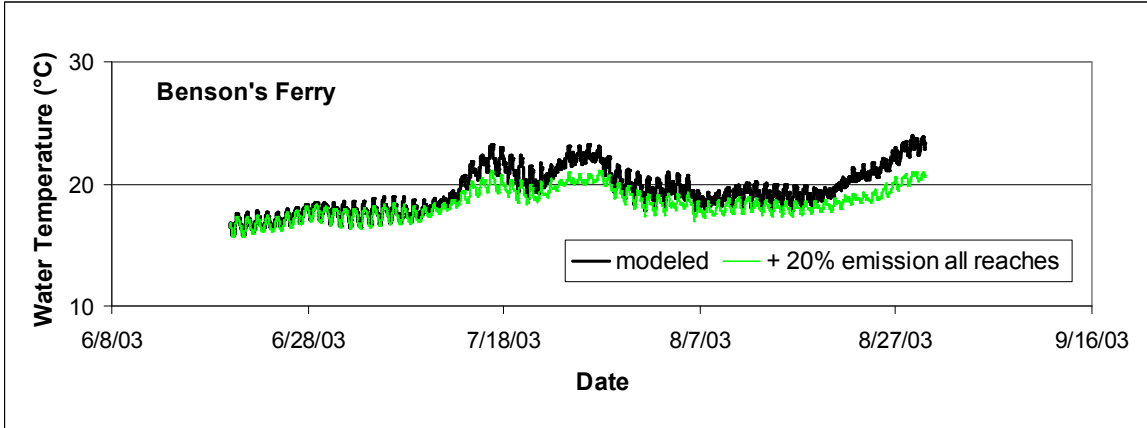
**Figure B-15:** Calibrated 2004 water temperature run plotted with 2004 water temperature run that has a 20% increase of the maximum solar radiation value along the Sacramento River at Benson's Ferry.



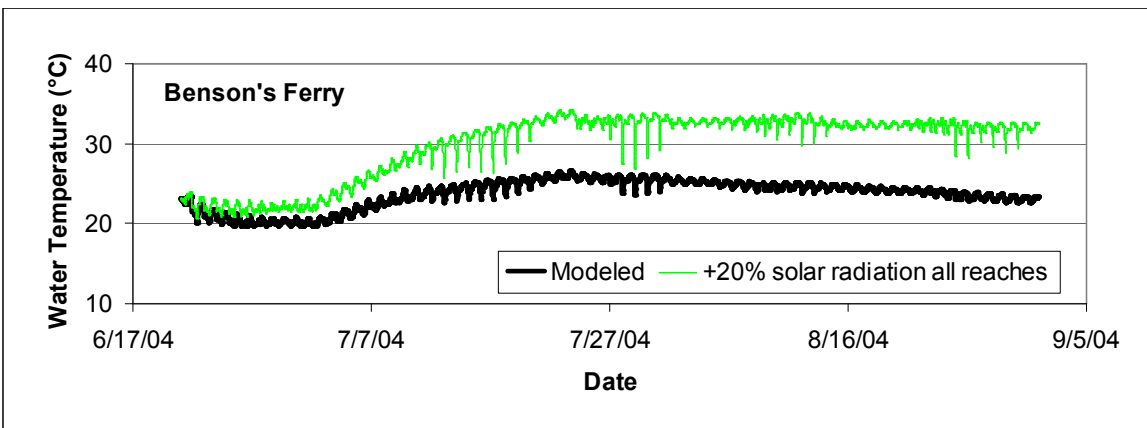
**Figure B-16:** Calibrated 2004 water temperature run plotted with 2004 water temperature run that has a 20% increase of the emission value along the Sacramento River at Benson's Ferry.



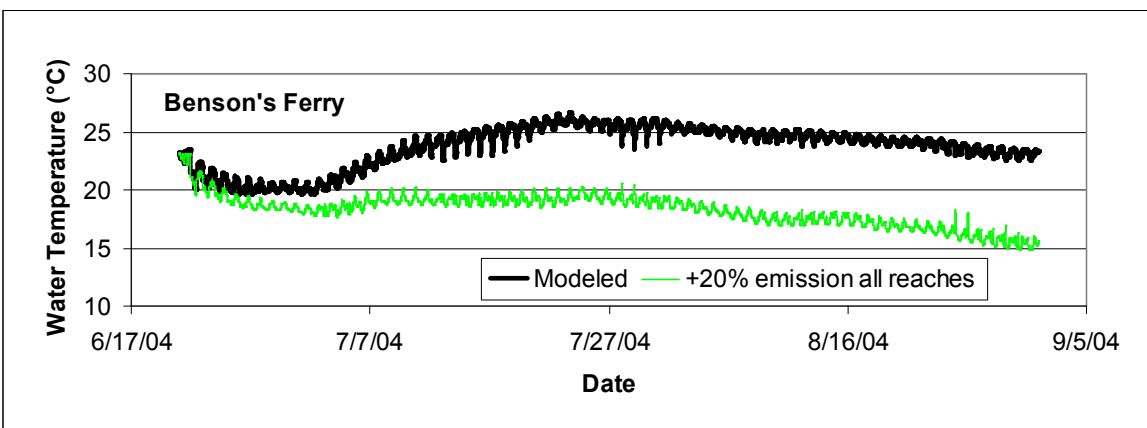
**Figure B-17:** Calibrated 2003 water temperature run plotted with 2003 water temperature run that has a 20% increase of the maximum solar radiation value along all reaches at Benson's Ferry.



**Figure B-18:** Calibrated 2003 water temperature run plotted with 2003 water temperature run that has a 20% increase of the emission value along all reaches at Benson's Ferry.



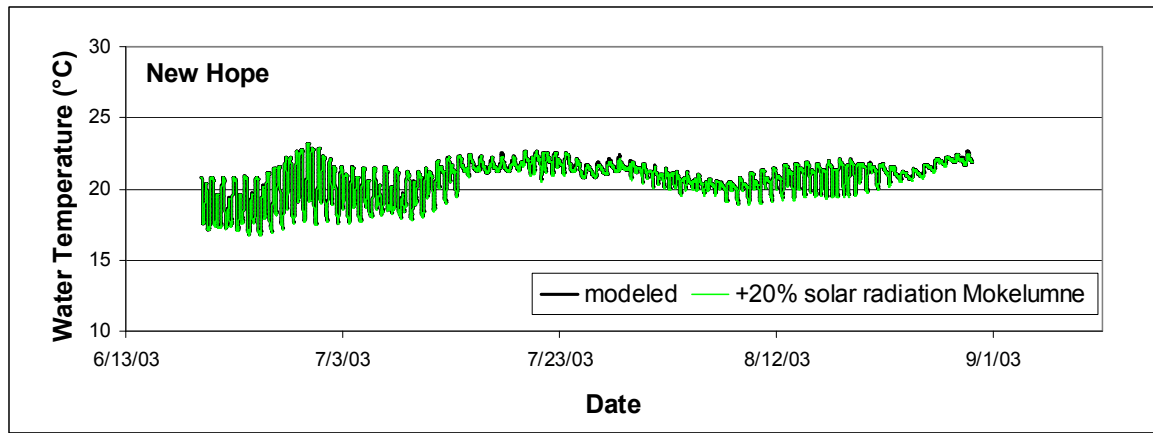
**Figure B-19:** Calibrated 2004 water temperature run plotted with 2004 water temperature run that has a 20% increase of the maximum solar radiation value along all reaches at Benson's Ferry.



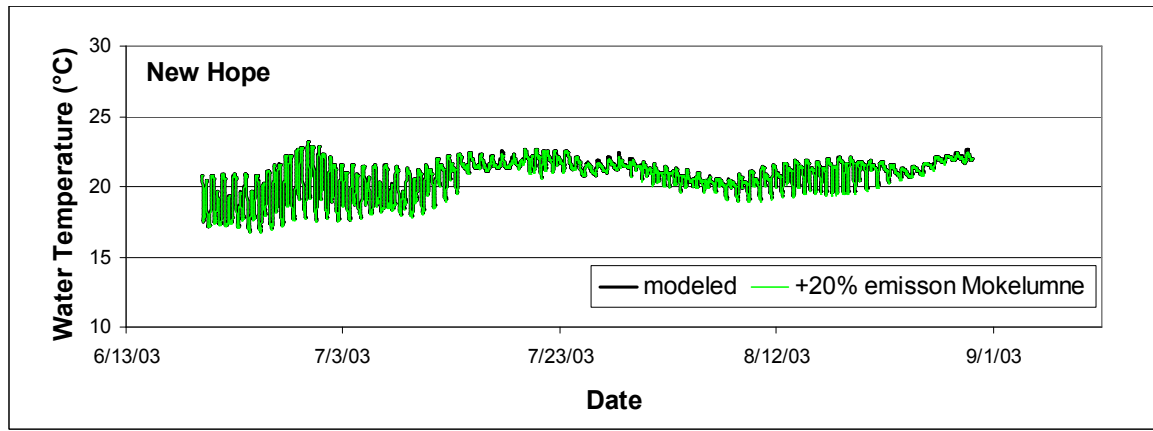
**Figure B-20:** Calibrated 2004 water temperature run plotted with 2004 water temperature run that has a 20% increase of the emission value along all reaches at Benson's Ferry.

## APPENDIX C

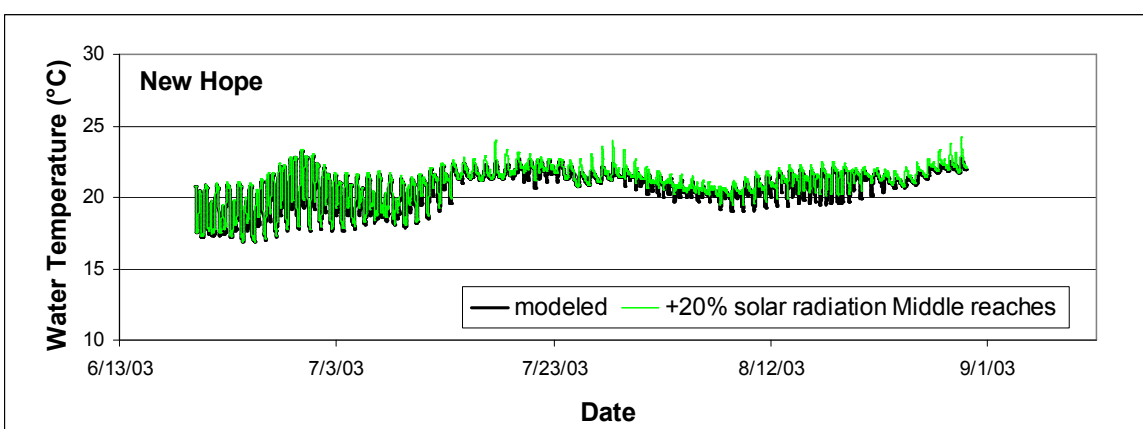
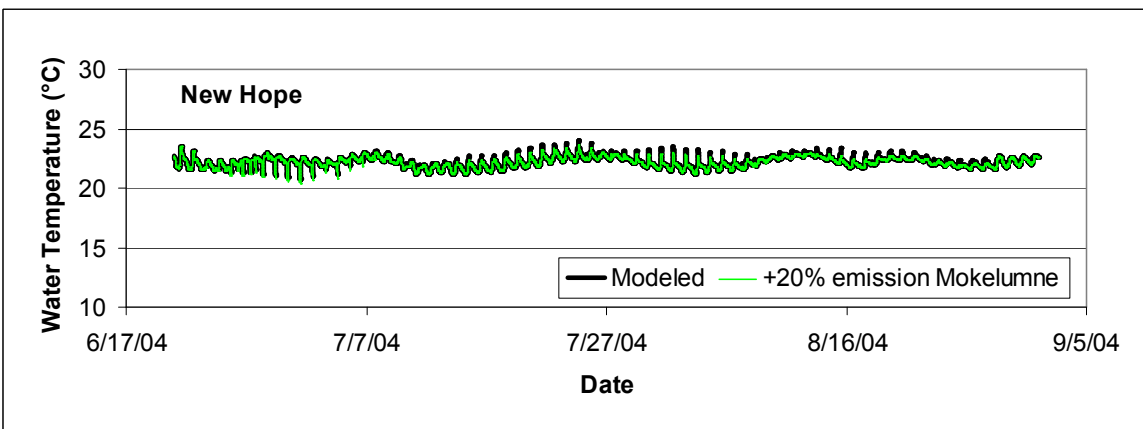
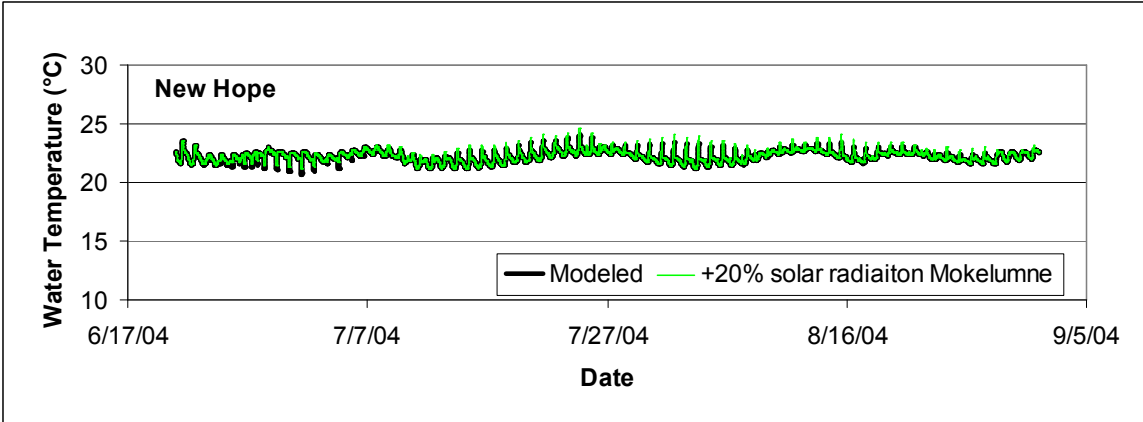
This appendix contains graphs which plot the results from the water temperature sensitivity analysis when the maximum solar radiation and the emission values were varied at New Hope.

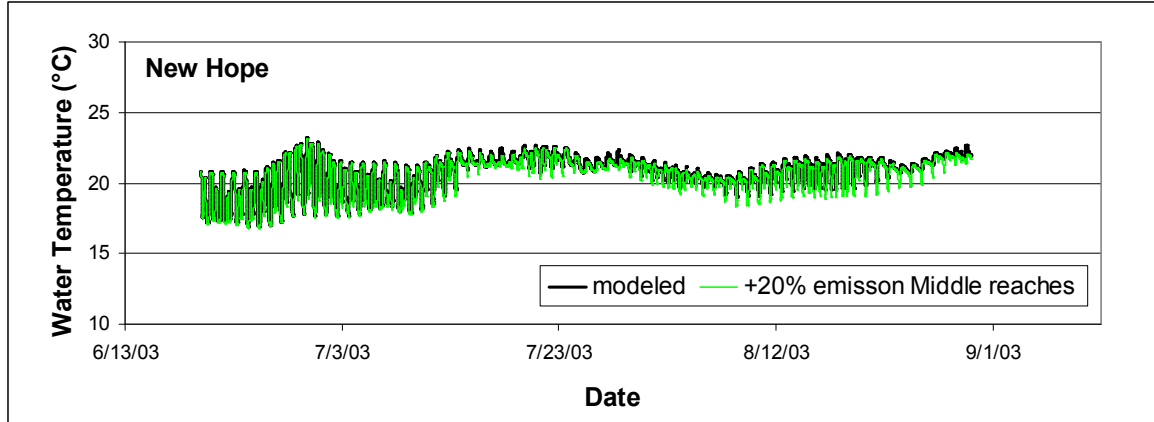


**Figure C-1:** Calibrated 2003 water temperature run plotted with 2003 water temperature run that has a 20% increase of the maximum solar radiation value along the Mokelumne at New Hope.

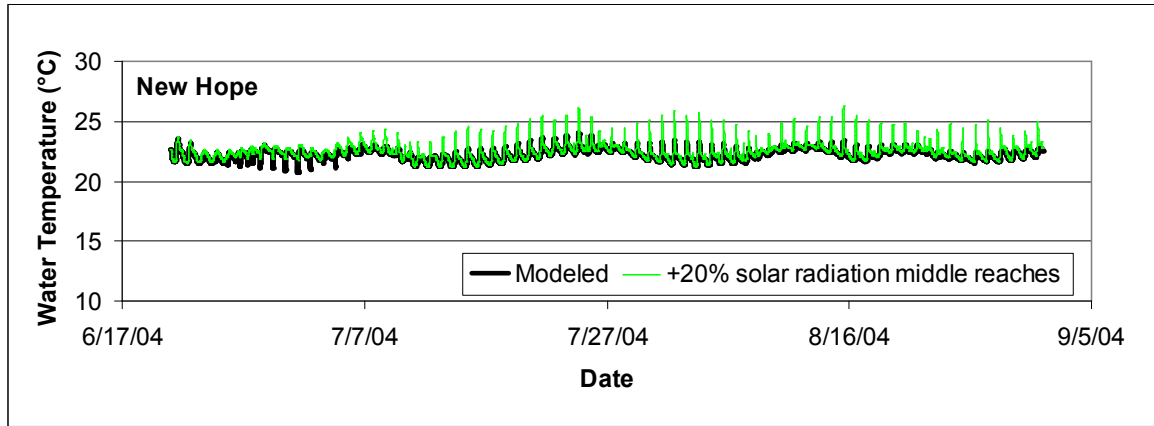


**Figure C-2:** Calibrated 2003 water temperature run plotted with 2003 water temperature run that has a 20% increase of emission value along the Mokelumne at New Hope.

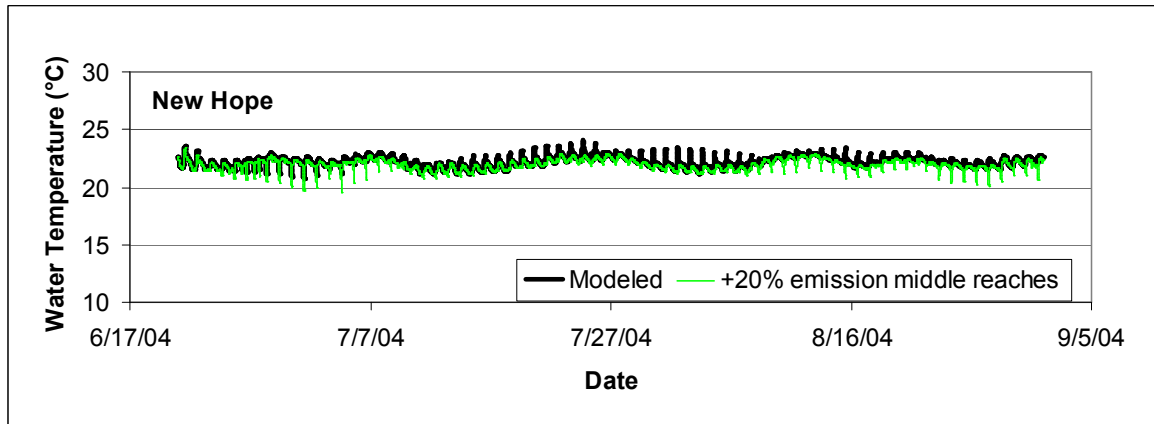




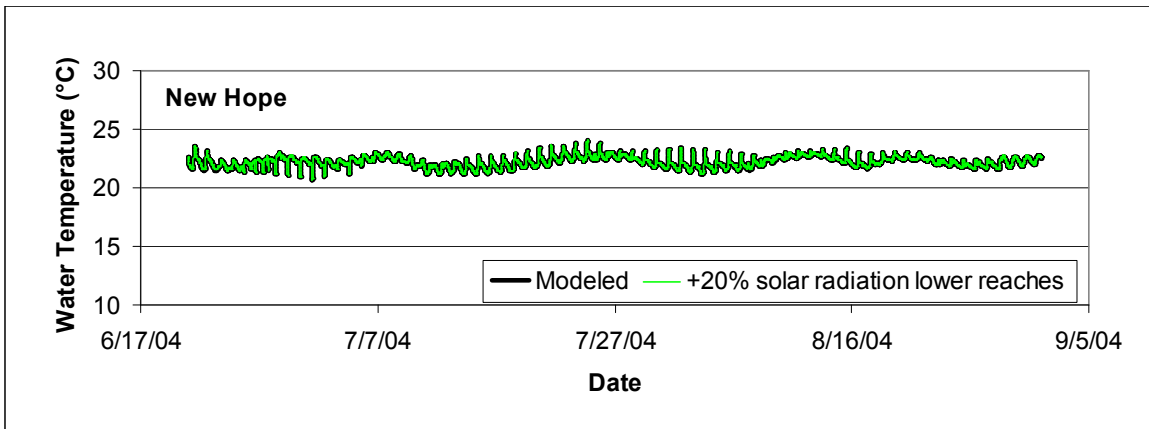
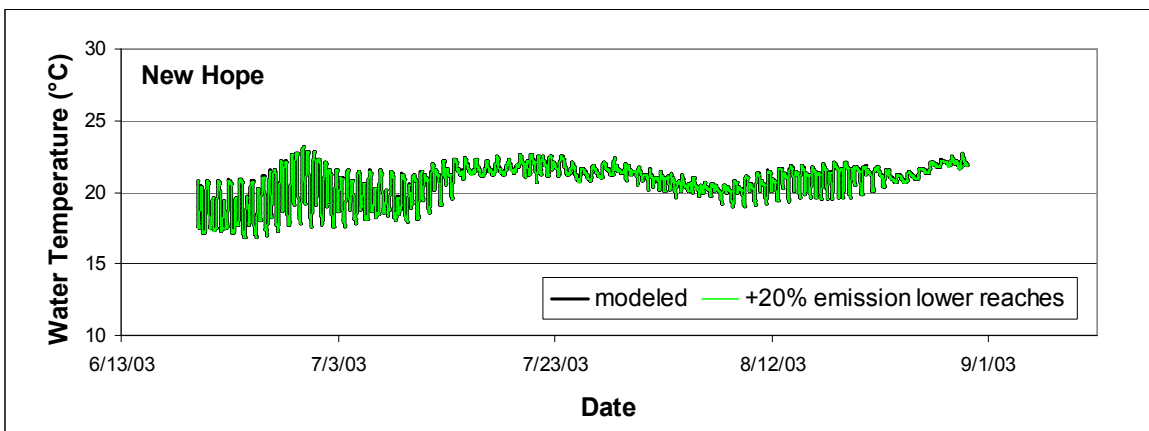
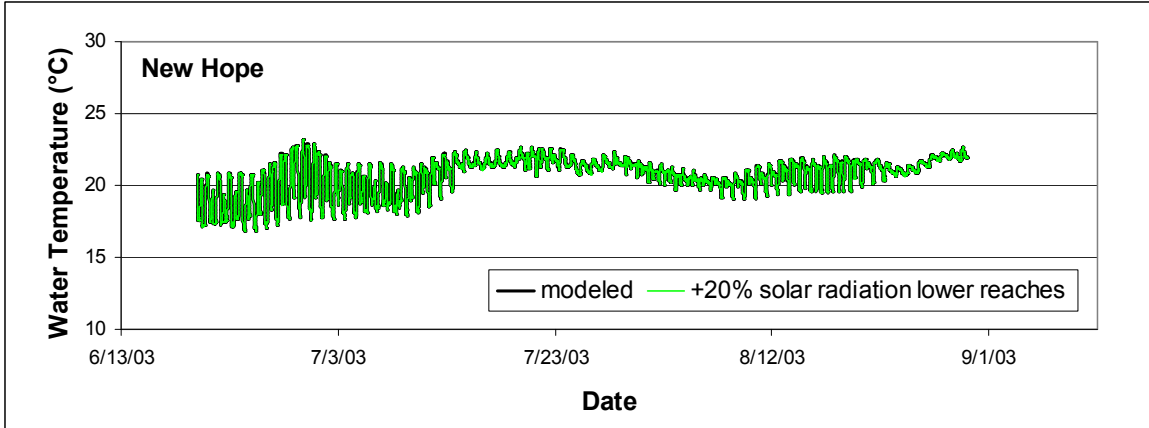
**Figure C-6:** Calibrated 2003 water temperature run plotted with 2003 water temperature run that has a 20% increase of the emission value along the middle reaches at New Hope.

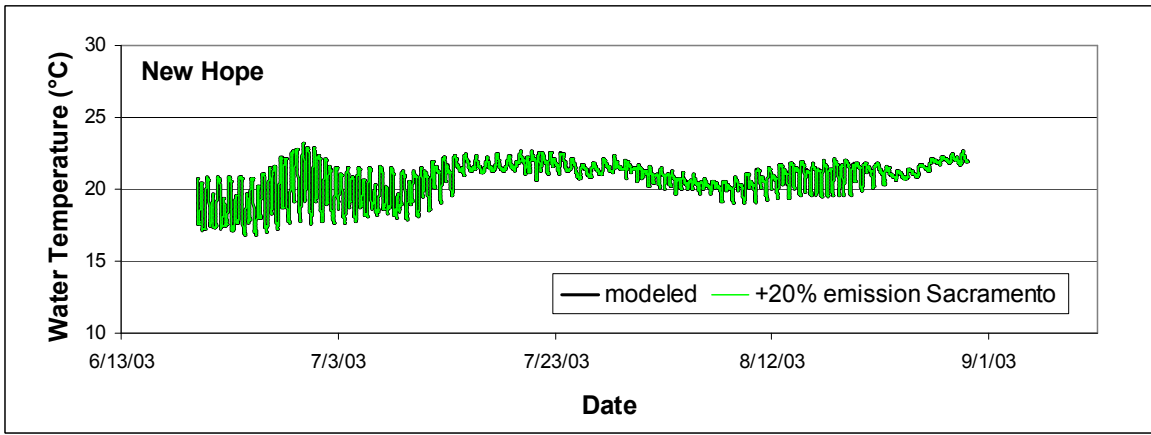
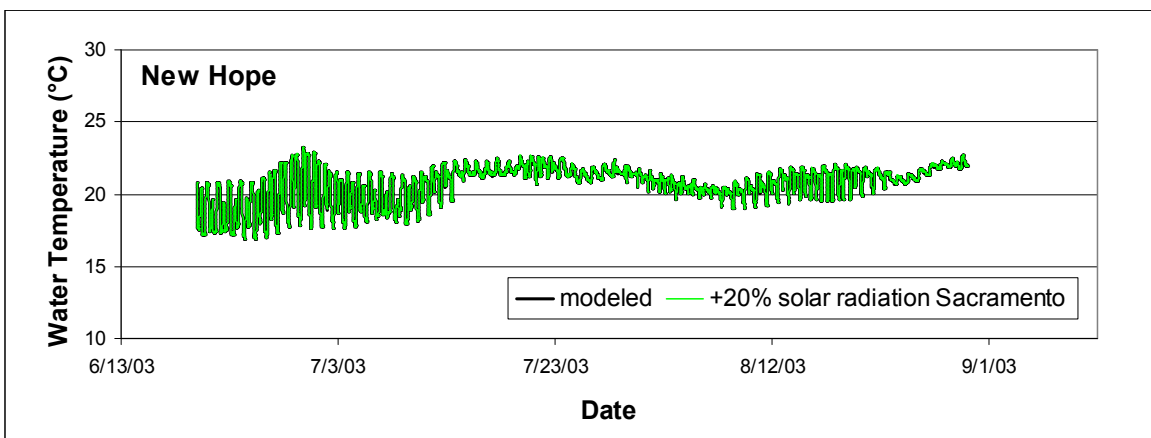
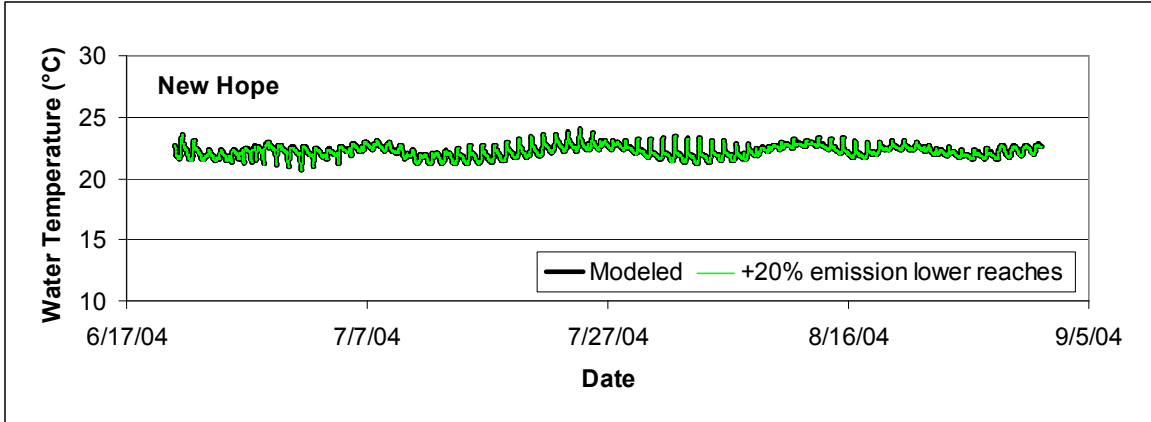


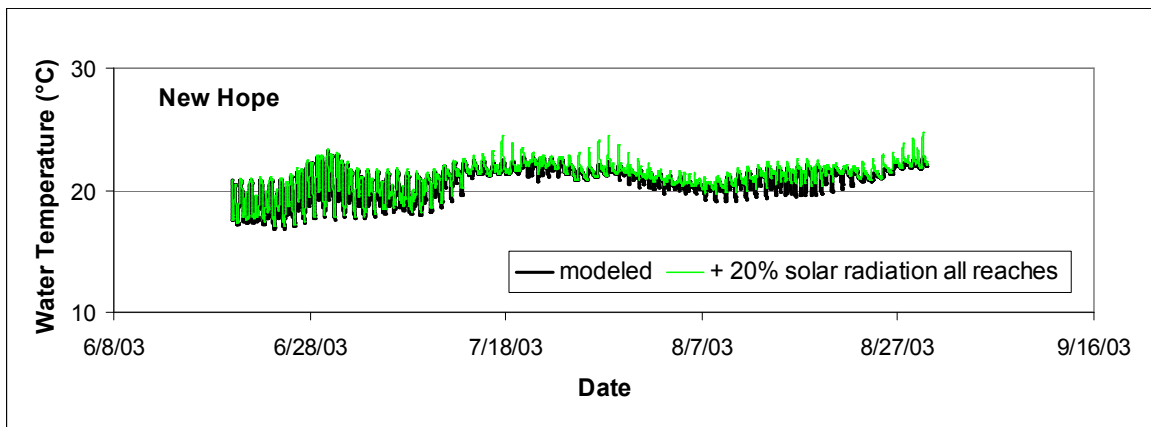
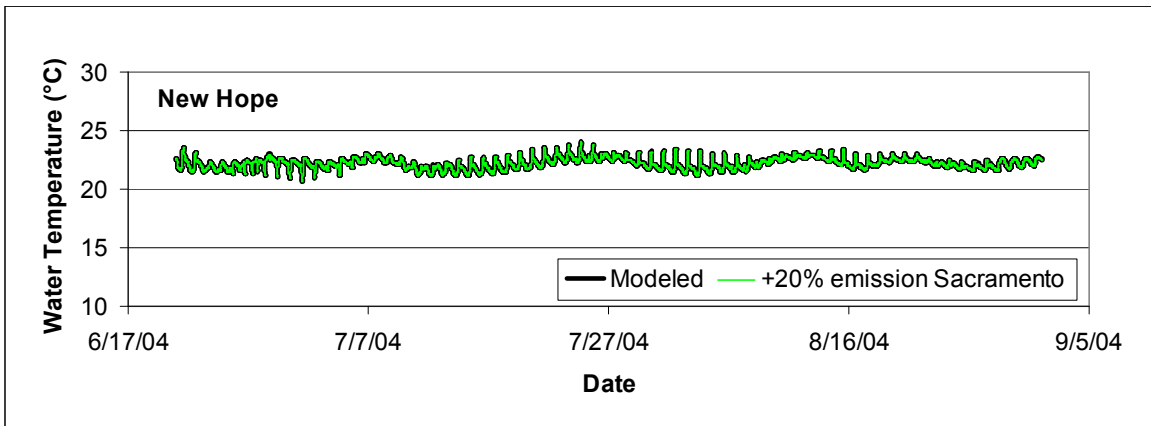
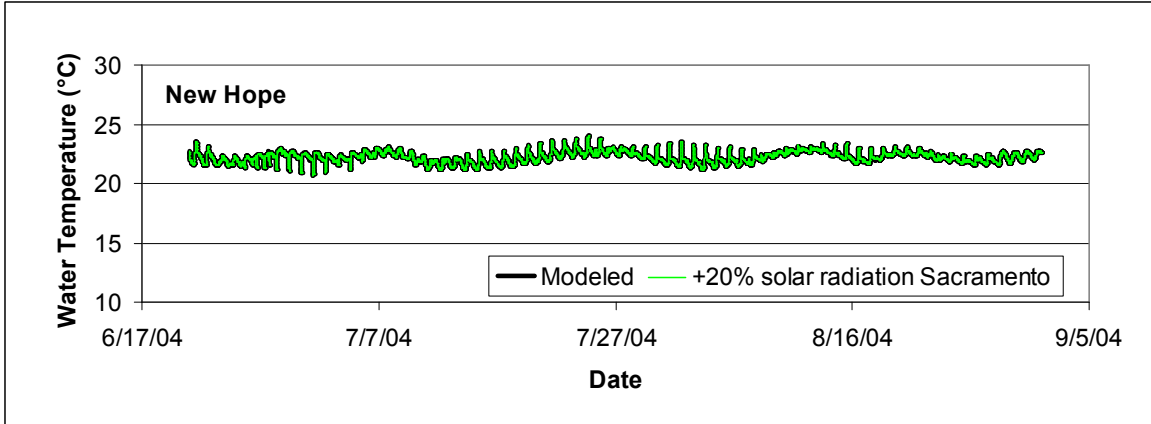
**Figure C-7:** Calibrated 2004 water temperature run plotted with 2004 water temperature run that has a 20% increase of the maximum solar radiation value along the middle reaches at New Hope

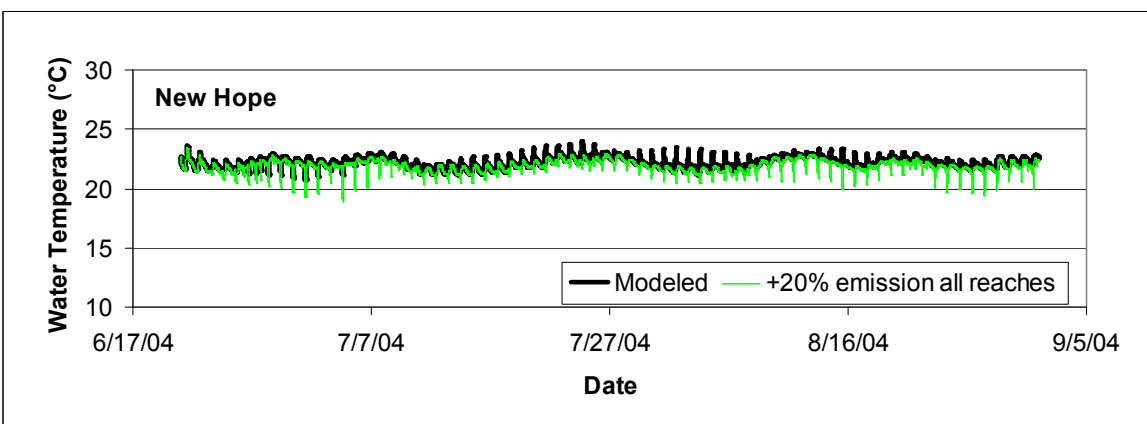
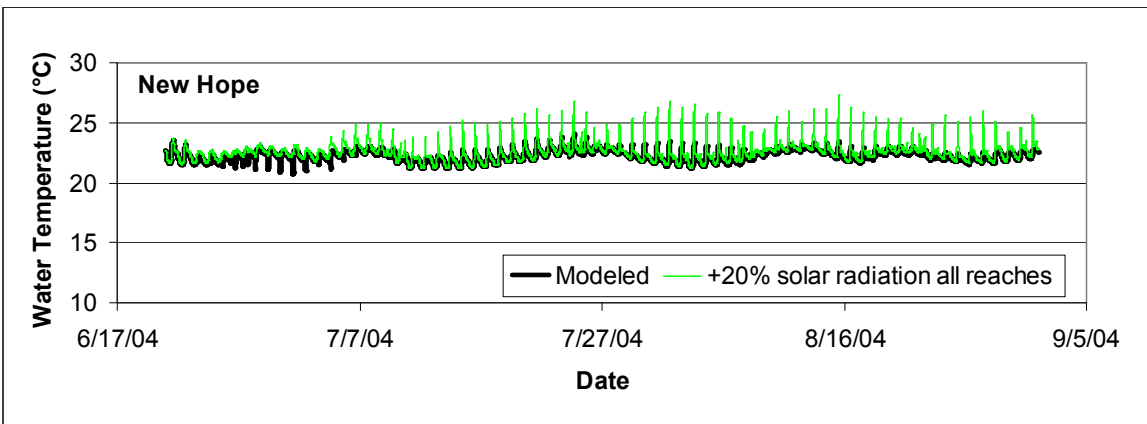
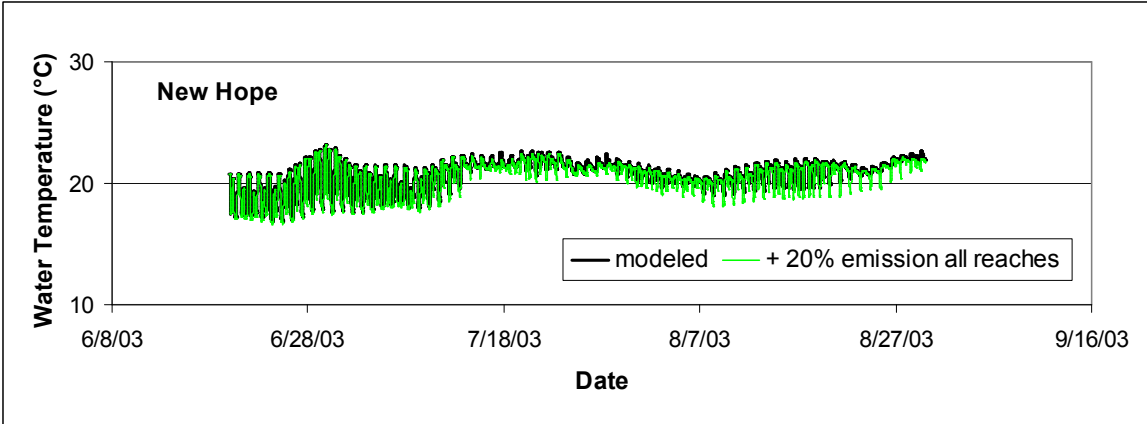


**Figure C-8:** Calibrated 2004 water temperature run plotted with 2004 water temperature run that has a 20% increase of the emission value along the middle reaches at New Hope.



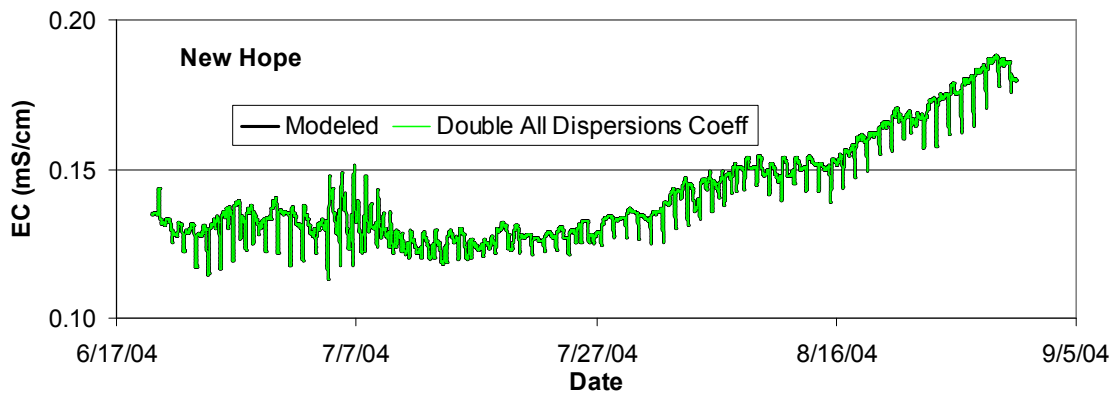




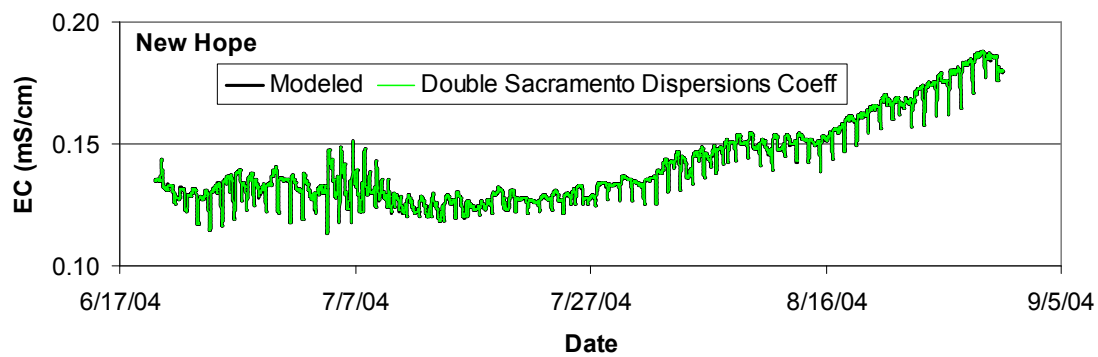


## APPENDIX D

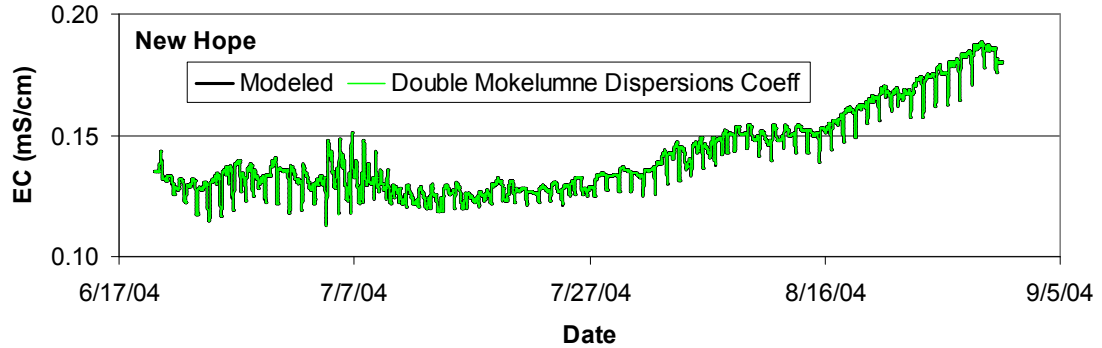
This appendix contains graphs which plot the results from the electrical conductivity sensitivity analysis when the dispersion coefficients were varied.



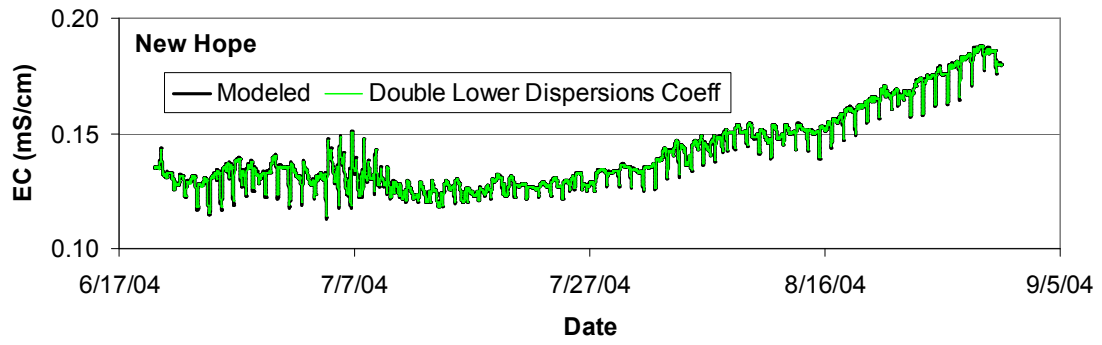
**Figure D-1:** Calibrated 2004 electrical conductivity run plotted with 2004 electrical conductivity run at New Hope with double dispersion coefficient values in all reaches.



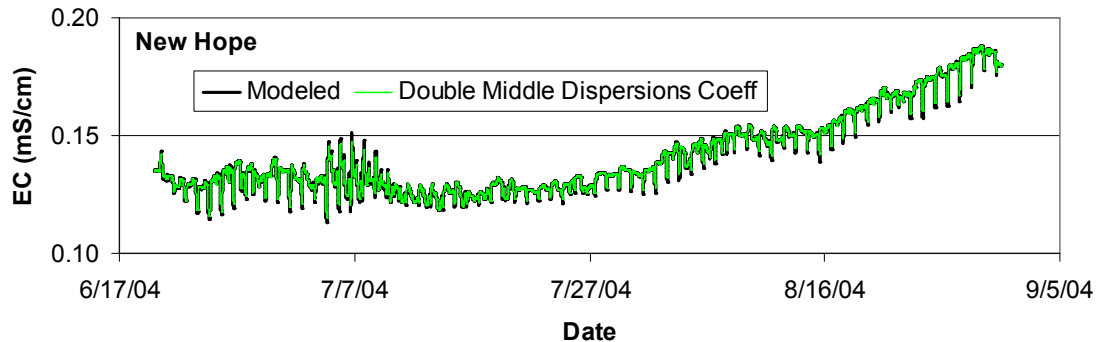
**Figure D-2:** Calibrated 2004 electrical conductivity run plotted with 2004 electrical conductivity run at New Hope with double dispersion coefficient values along the Sacramento River.



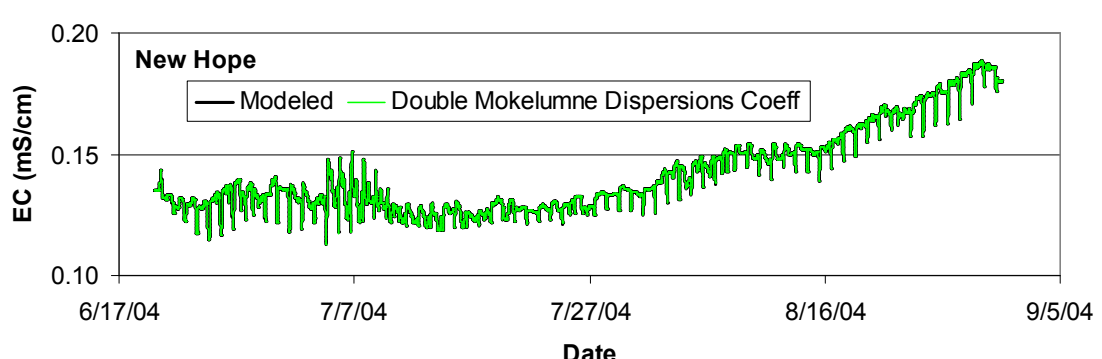
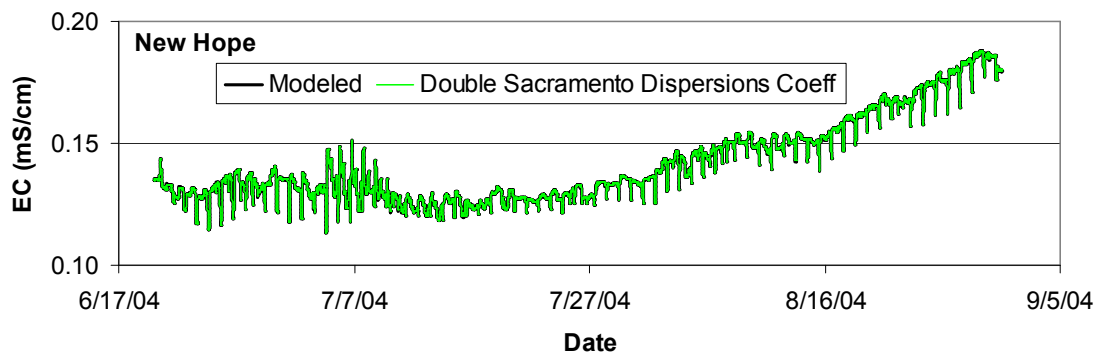
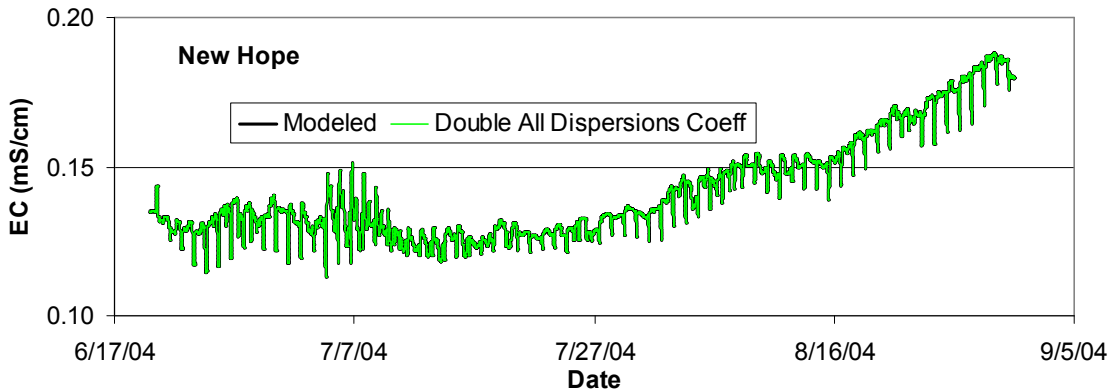
**Figure D-3:** Calibrated 2004 electrical conductivity run plotted with 2004 electrical conductivity run at New Hope with double dispersion coefficient values along the Mokelumne River.



**Figure D-4:** Calibrated 2004 electrical conductivity run plotted with 2004 electrical conductivity run at New Hope with double the dispersion coefficient values in the lower reaches.



**Figure D-5:** Calibrated 2004 electrical conductivity run plotted with 2004 electrical conductivity run at New Hope with double the dispersion coefficient values in the middle reaches.



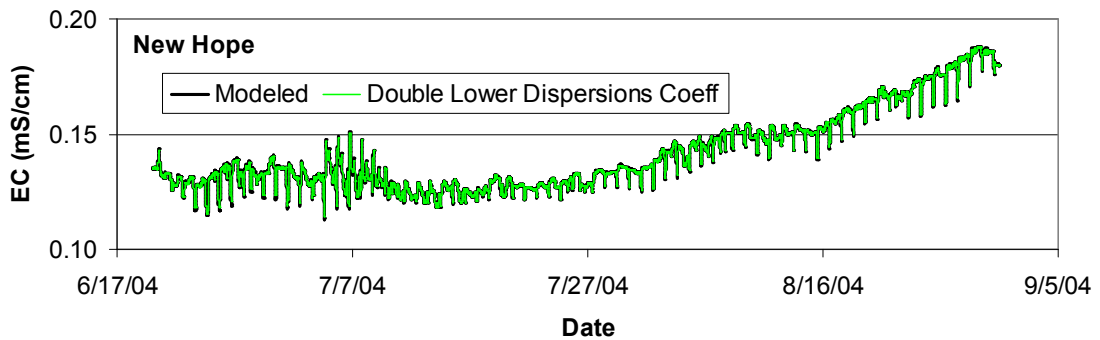


**Figure D-9:** Calibrated 2004 electrical conductivity run plotted with 2004 electrical conductivity run at South Staten with double the dispersion coefficient in the lower reaches.

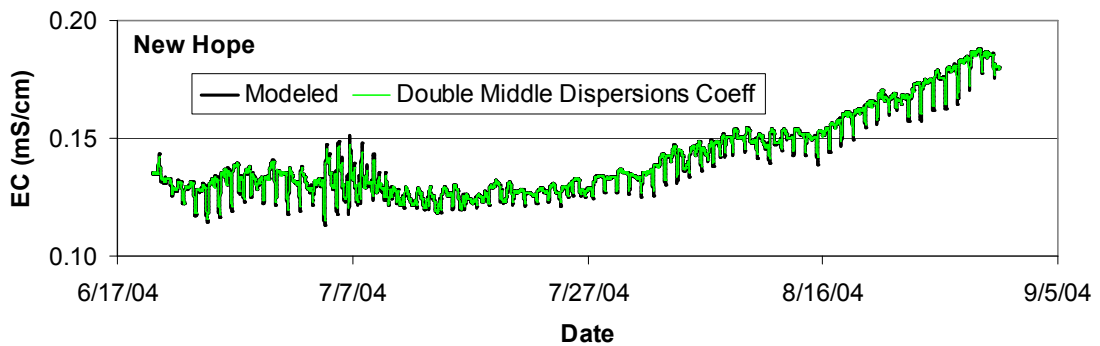


**Figure D-9:** Calibrated 2004 electrical conductivity run plotted with 2004 electrical conductivity run at South Staten with double the dispersion coefficient in the middle reaches.

## APPENDIX E

This appendix presents graphs, which plot the results when the flow on the Sacramento and Mokelumne Rivers were increased by twenty percent.

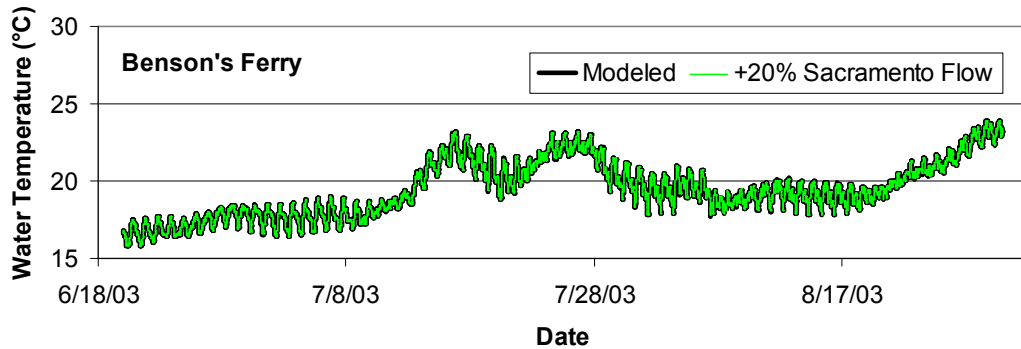


**Figure E-1:** Calibrated 2003 water temperature run plotted with the 2003 water temperature run with a 20% increase of Sacramento River flow at Benson's Ferry.

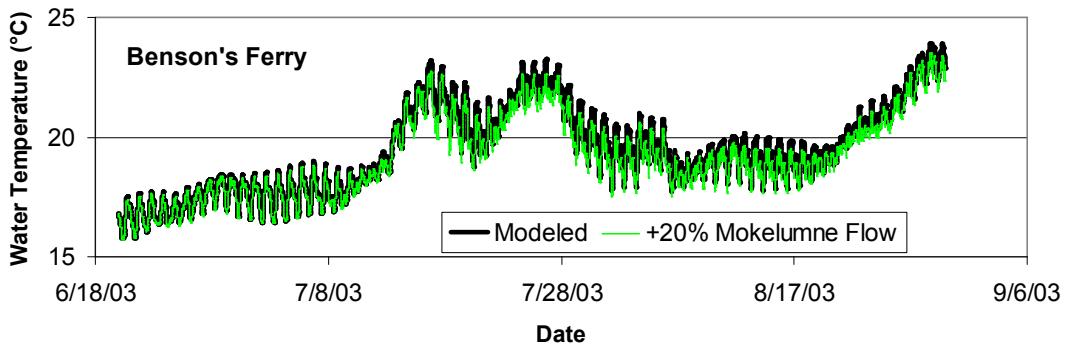


**Figure E-2:** Calibrated 2003 water temperature run plotted with the 2003 water temperature run with a 20% increase of Moklumne River flow at Benson's Ferry.

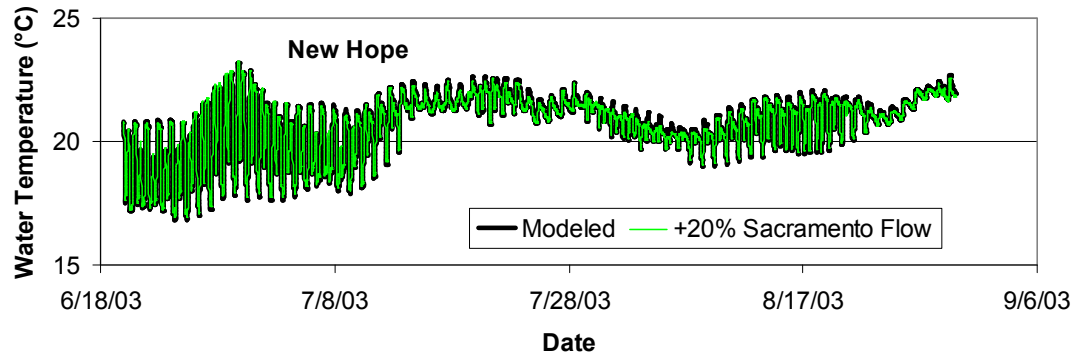


**Figure E-3:** Calibrated 2003 water temperature run plotted with 2003 water temperature run with a 20% increase of Sacramento River flow at New Hope.

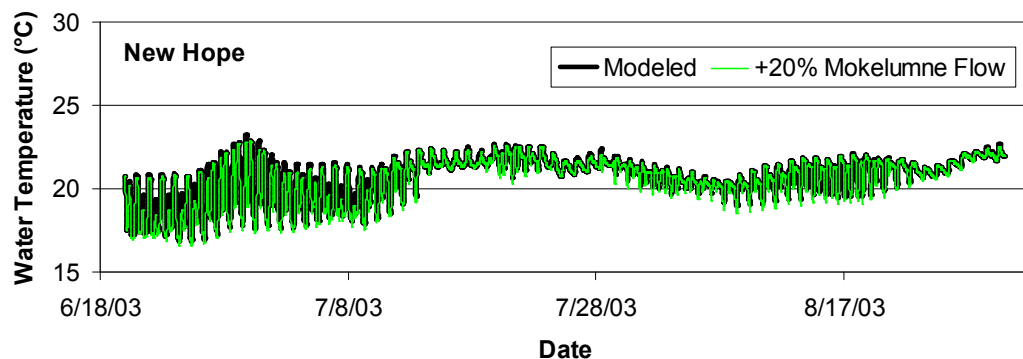


**Figure E-4:** Calibrated 2003 water temperature run plotted with 2003 water temperature run with a 20% increase of Mokelumne River flow at New Hope.

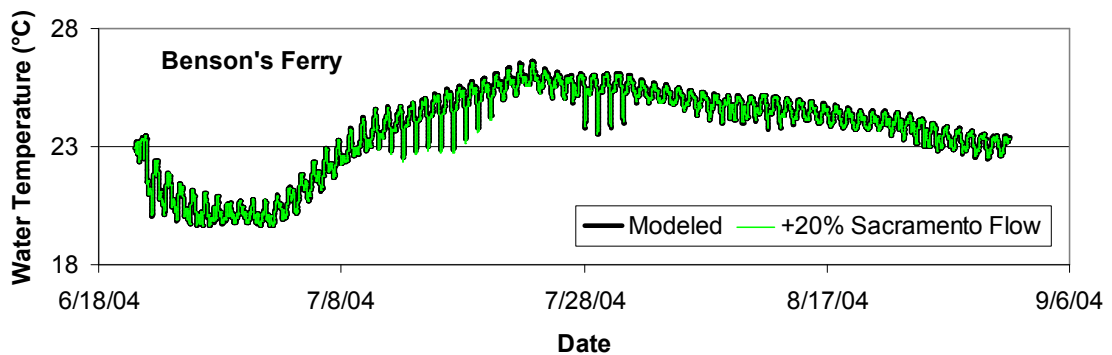


**Figure E-5:** Calibrated 2004 water temperature run plotted with 2004 water temperature run with a 20% increase of Sacramento River flow at Benson's Ferry.

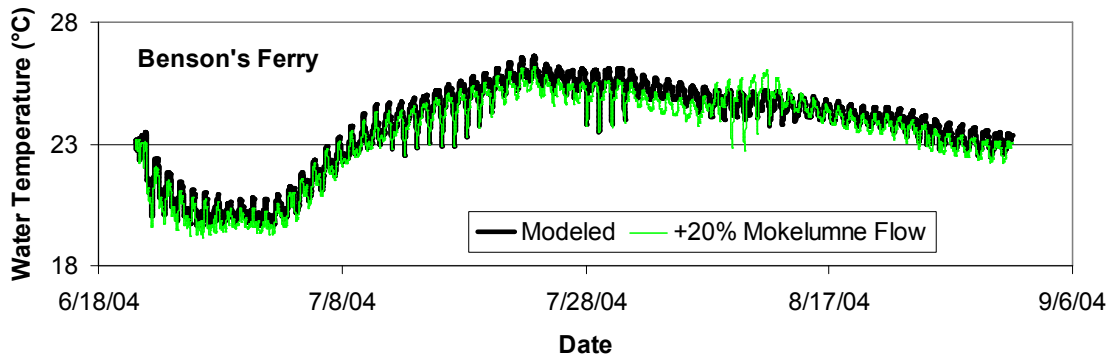


**Figure E-6:** Calibrated 2004 water temperature run plotted with 2004 water temperature run with a 20% increase of Mokelumne River flow at Benson's Ferry.

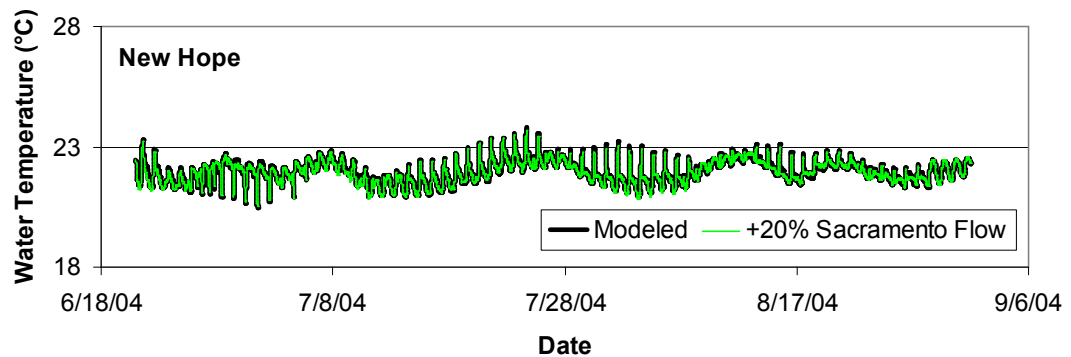


**Figure E-7:** Calibrated 2004 water temperature run plotted with 2004 water temperature run with a 20% increase of Sacramento River flow at New Hope.

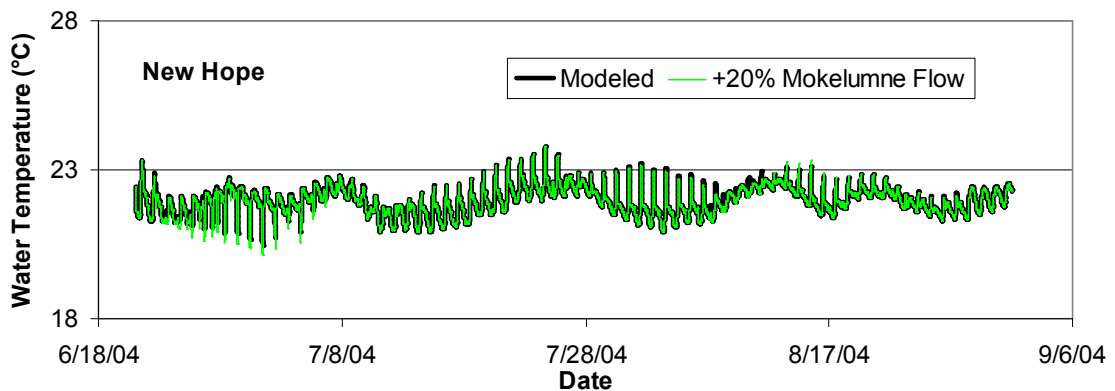


**Figure E-8:** Calibrated 2004 water temperature run plotted with 2004 water temperature run with a 20% increase of Mokelumne River flow at New Hope.

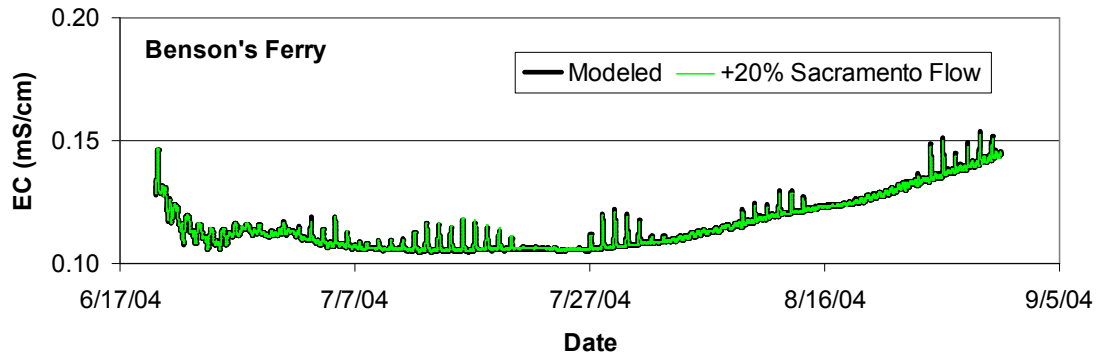


**Figure E-9:** Calibrated 2004 electrical conductivity run plotted with 2004 electrical conductivity run with a 20% increase of Sacramento River flow at Benson's Ferry.

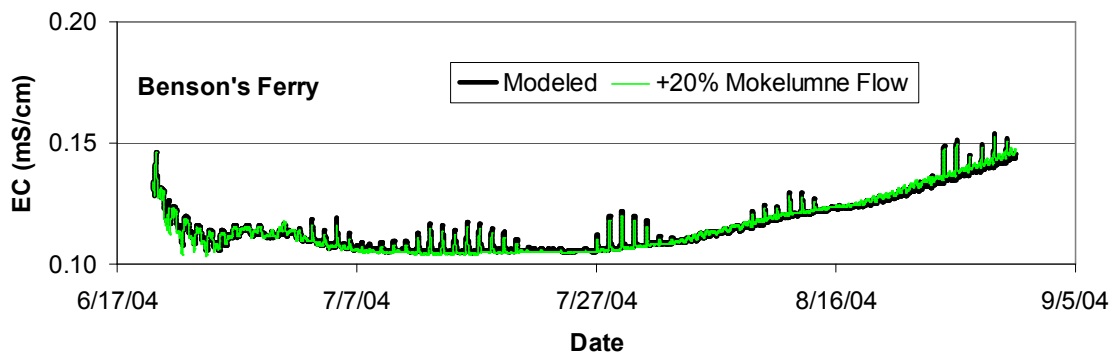


**Figure E-10:** Calibrated 2004 electrical conductivity run plotted with 2004 electrical conductivity run with a 20% increase of Mokelumne River flow at Benson's Ferry.

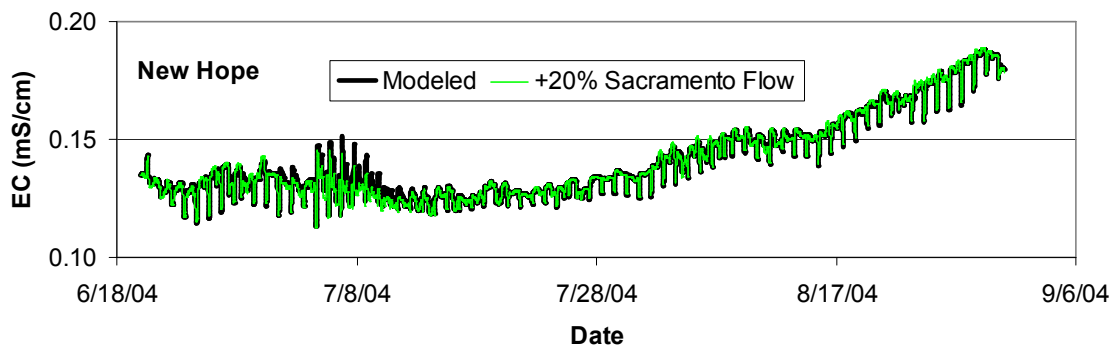


**Figure E-11:** Calibrated 2004 electrical conductivity run plotted with 2004 electrical conductivity run with a 20% increase of Sacramento flow at New Hope.

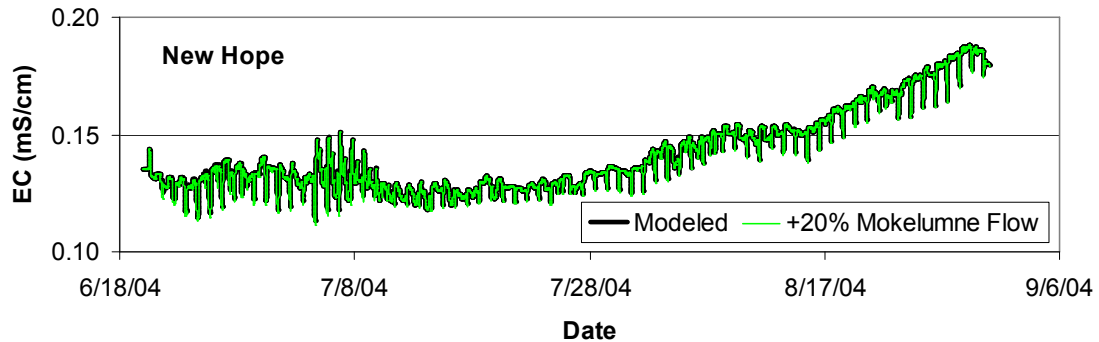


**Figure E-12:** Calibrated 2004 electrical conductivity run plotted with 2004 electrical conductivity run with a 20% increase of Mokelumne River flow at New Hope.

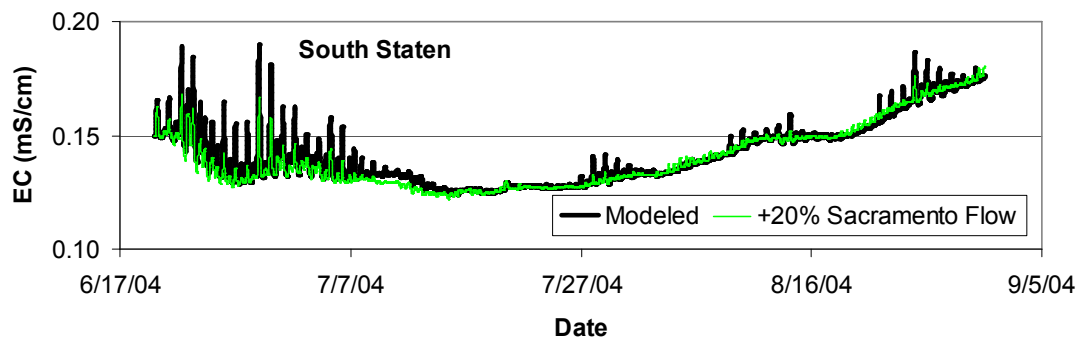


**Figure E-13:** Calibrated 2004 electrical conductivity run plotted with 2004 electrical conductivity run with a 20% increase of Sacramento River flow at South Staten.

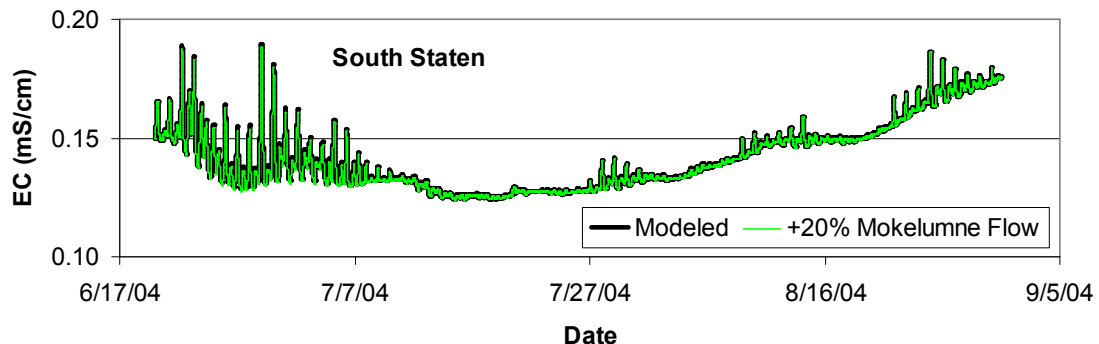


**Figure E-14:** Calibrated 2004 electrical conductivity run plotted with 2004 electrical conductivity run with a 20% increase of Mokelumne River flow at South Staten.

## APPENDIX F

This appendix presents graphs, which plot the results of all the management scenarios.

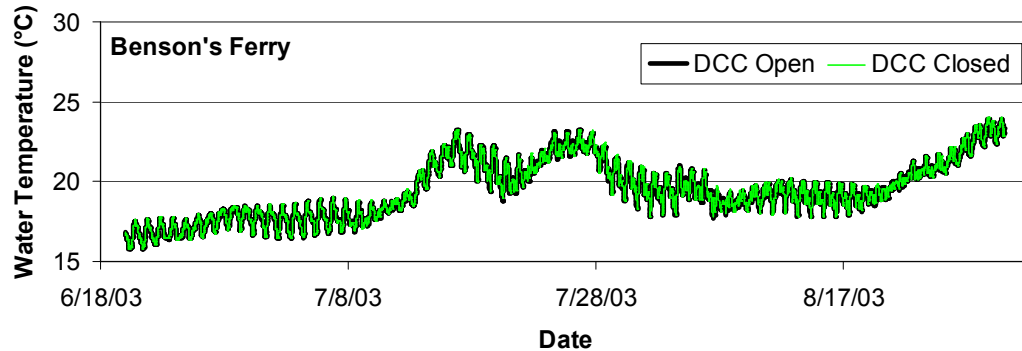


**Figure F-1:** Comparison of water temperatures at Benson's Ferry when DCC is open (calibrated base case) to when DCC is closed in 2003.

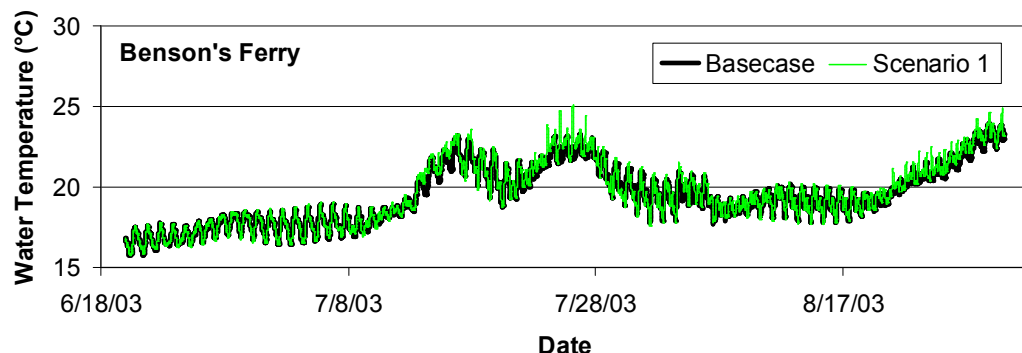


**Figure F-2:** Comparison of calibrated base case plotted with the application of scenario 1 to 2003 at Benson's Ferry.

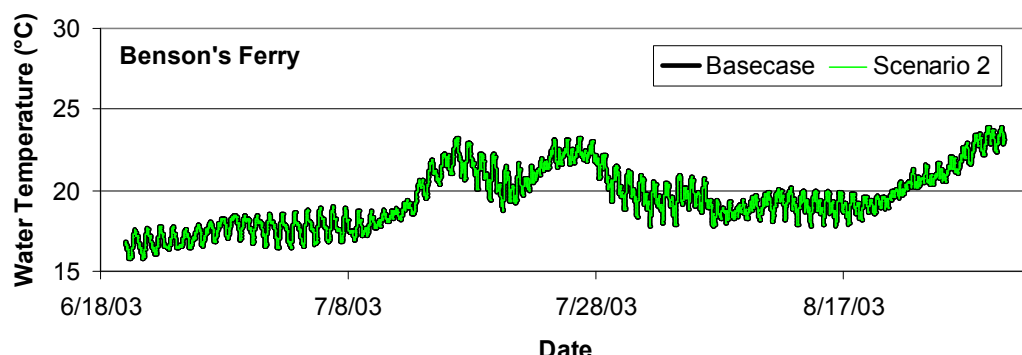


**Figure F-3:** Comparison of calibrated base case plotted with the application of scenario 2 to 2003 at Benson's Ferry.

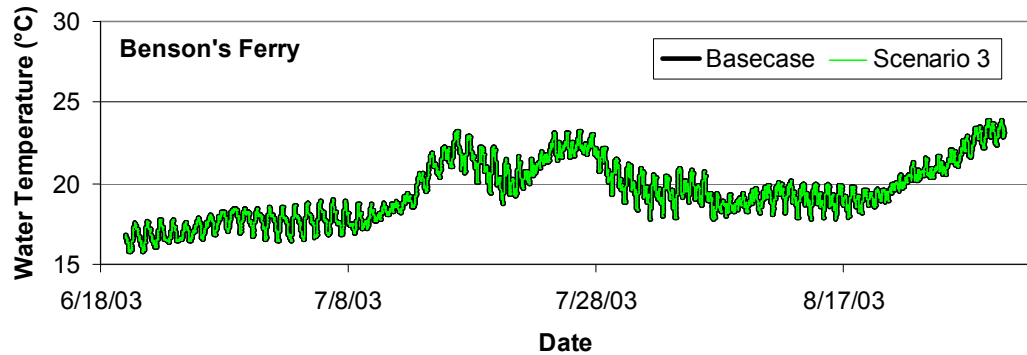


**Figure F-4:** Comparison of calibrated base case plotted with the application of scenario 3 to 2003 at Benson's Ferry.

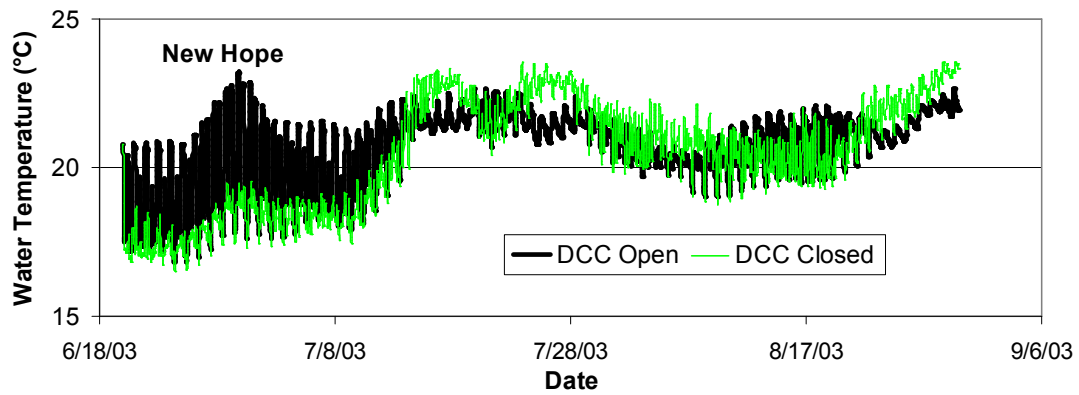


**Figure F-5:** Comparison of water temperatures at New Hope when DCC is open (calibrated base case) to when DCC is closed in 2003.

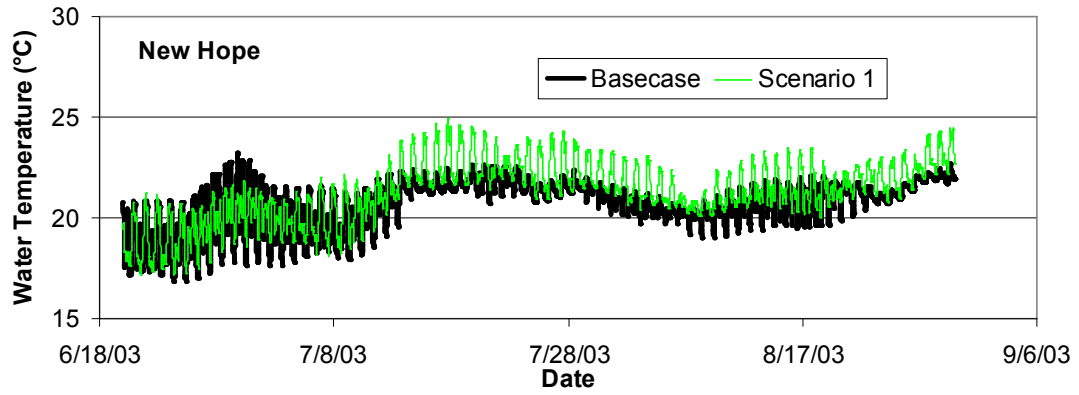


**Figure F-6:** Comparison of calibrated base case plotted with the application of scenario 1 to 2003 at New Hope.

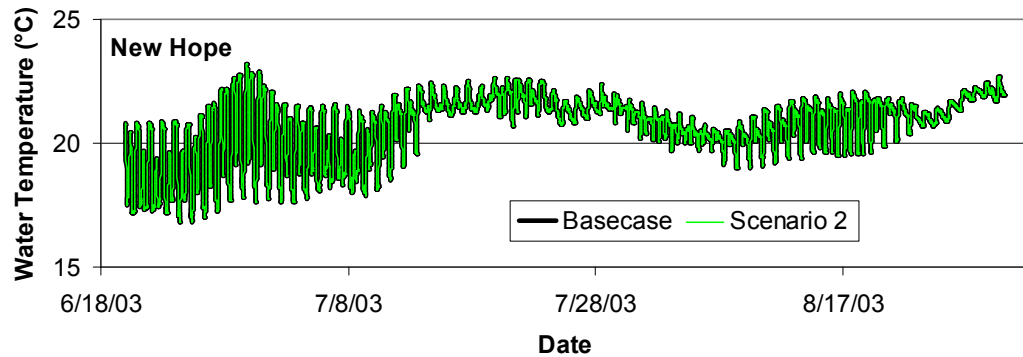


**Figure F-7:** Comparison of calibrated base case plotted with the application of scenario 2 to 2003 at New Hope.

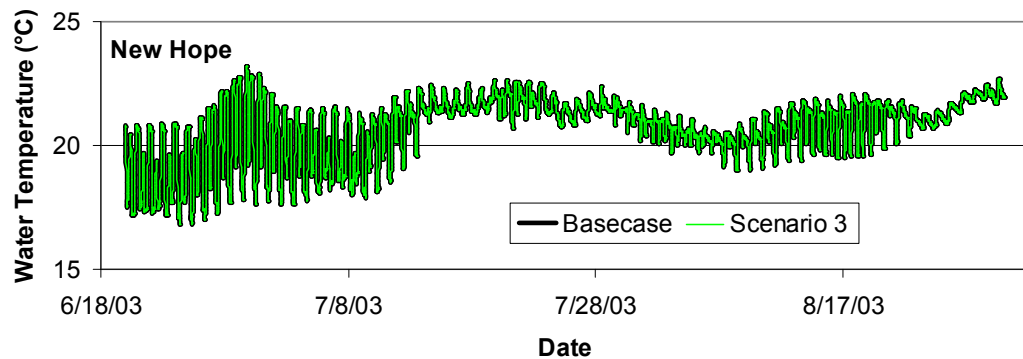


**Figure F-8:** Comparison of calibrated base case plotted with the application of scenario 3 to 2003 at New Hope.

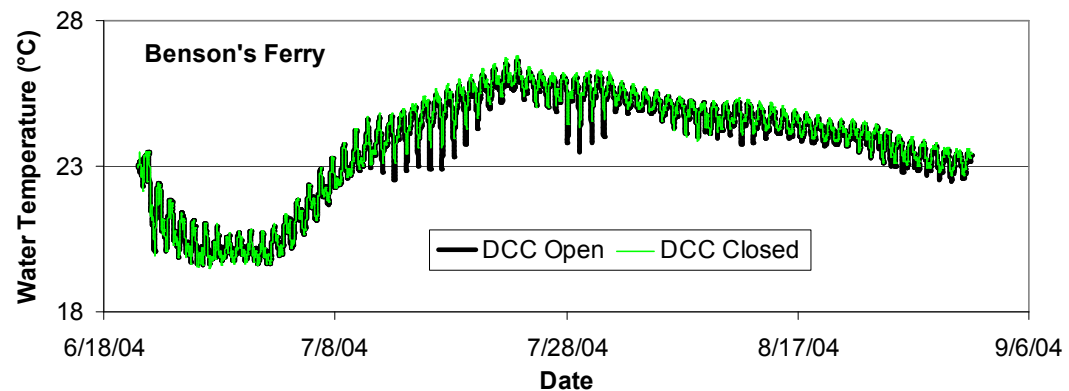


**Figure F-9:** Comparison of water temperatures at Benson's Ferry when DCC is open (calibrated base case) to when DCC is closed in 2004.

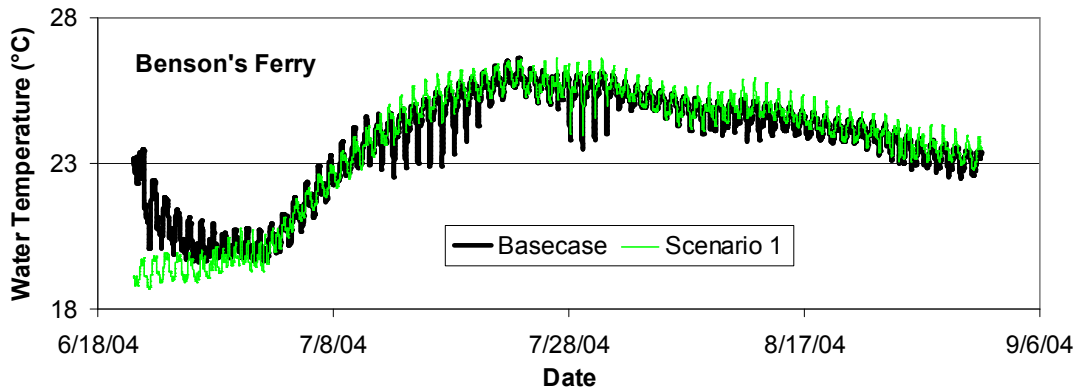


**Figure F-10:** Comparison of calibrated base case plotted with the application of scenario 1 to 2004 at Benson's Ferry.

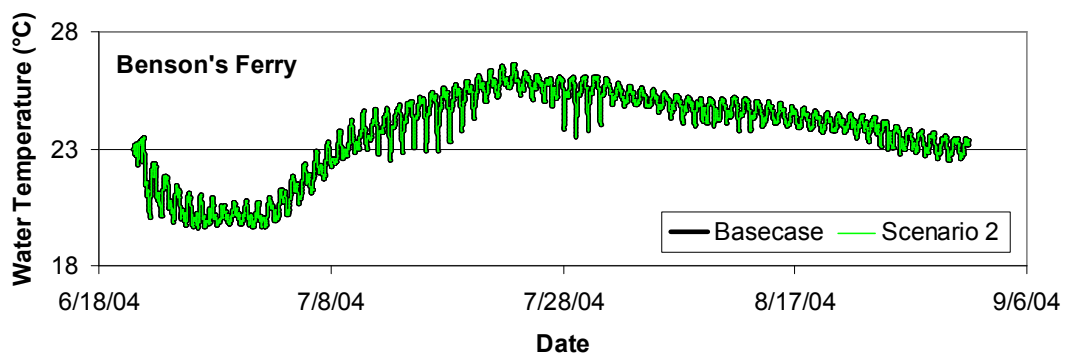


**Figure F-11:** Comparison of calibrated base case plotted with the application of scenario 2 to 2004 at Benson's Ferry.

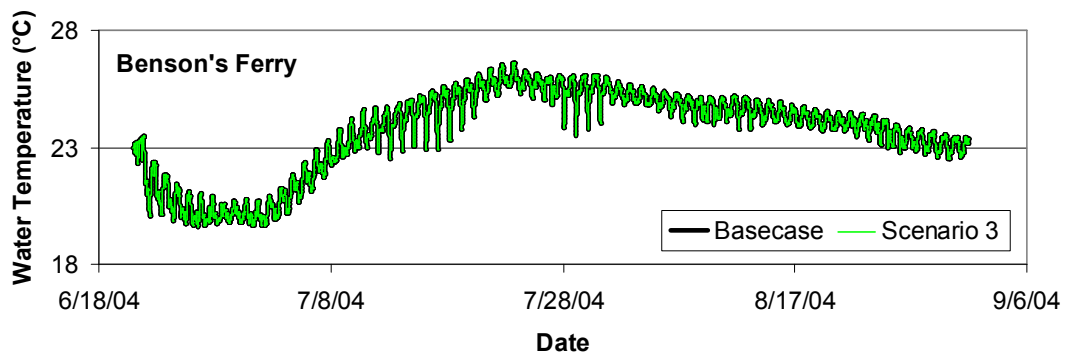


**Figure F-12:** Comparison of calibrated base case plotted with the application of scenario 3 to 2004 at Benson's Ferry.

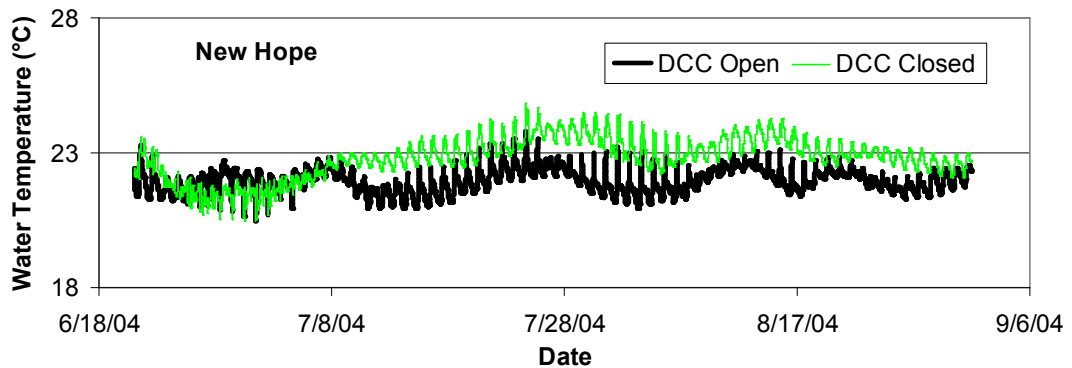


**Figure F-13:** Comparison of water temperatures at New Hope when DCC is open (calibrated base case) to when DCC is closed in 2004.

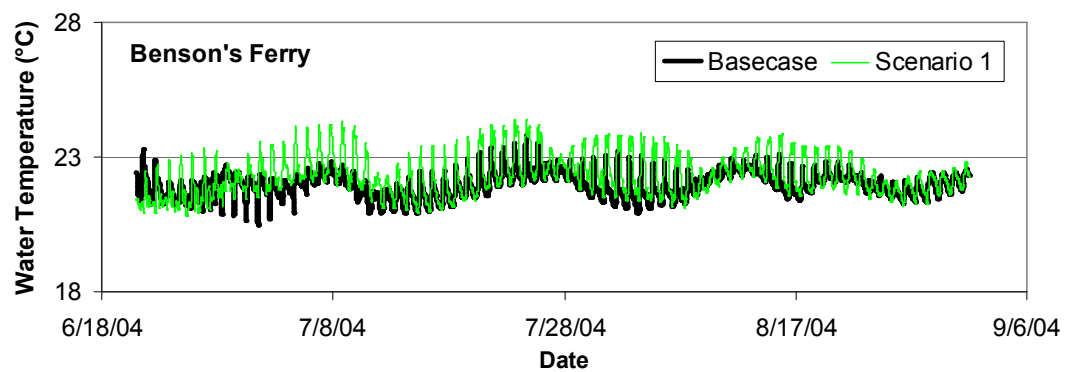


**Figure F-14:** Comparison of calibrated base case plotted with the application of scenario 1 to 2004 at New Hope.

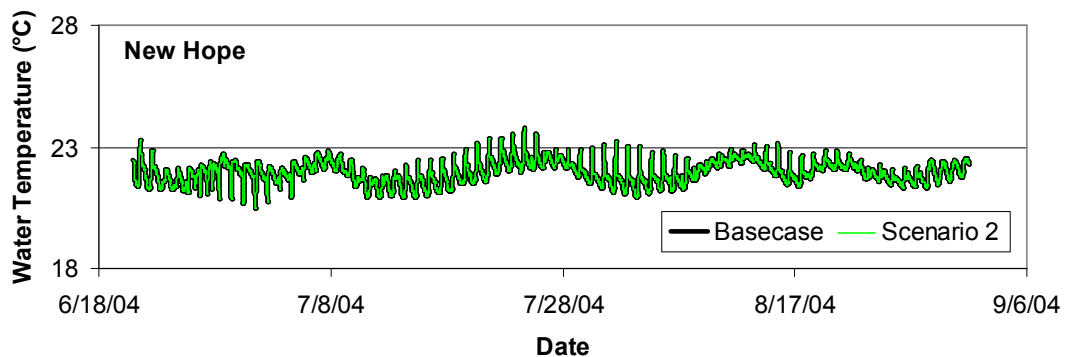


**Figure F-15:** Comparison of calibrated base case plotted with the application of scenario 2 to 2004 at New Hope.

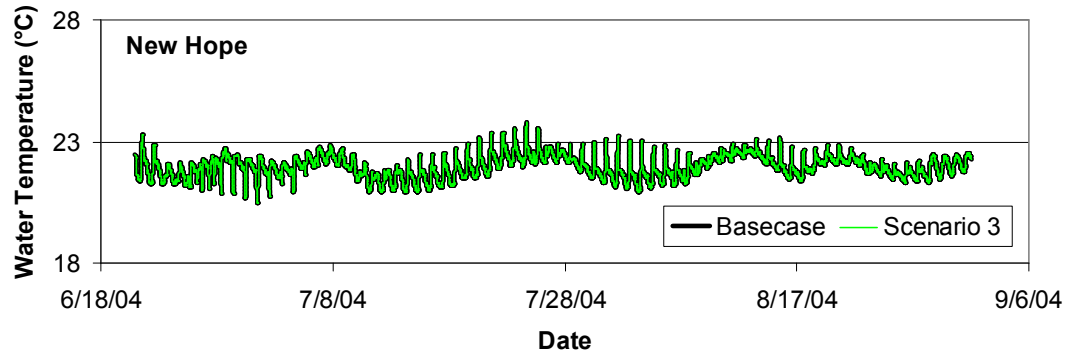


**Figure F-16:** Comparison of calibrated base case plotted with the application of scenario 3 to 2004 at New Hope.

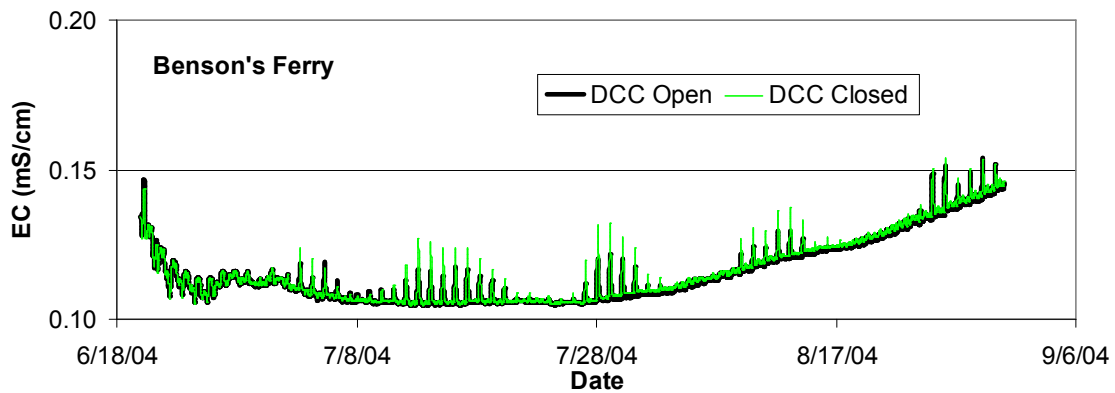


**Figure F-17:** Scenario four at Benson's Ferry where the Delta Cross Channel (DCC) is closed with the calibrated base case that has the DCC open.

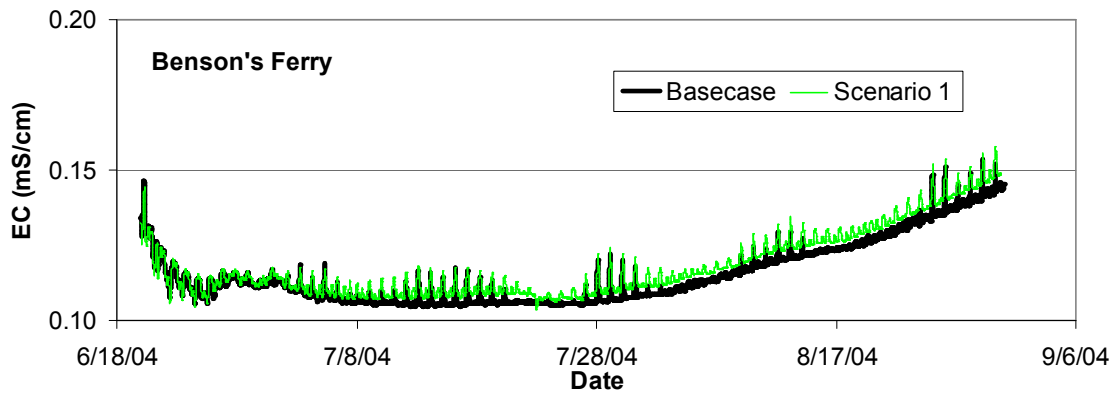


**Figure F-18:** Comparison of calibrated base case plotted with scenario 1 for 2004 electrical conductivity at Benson's Ferry.

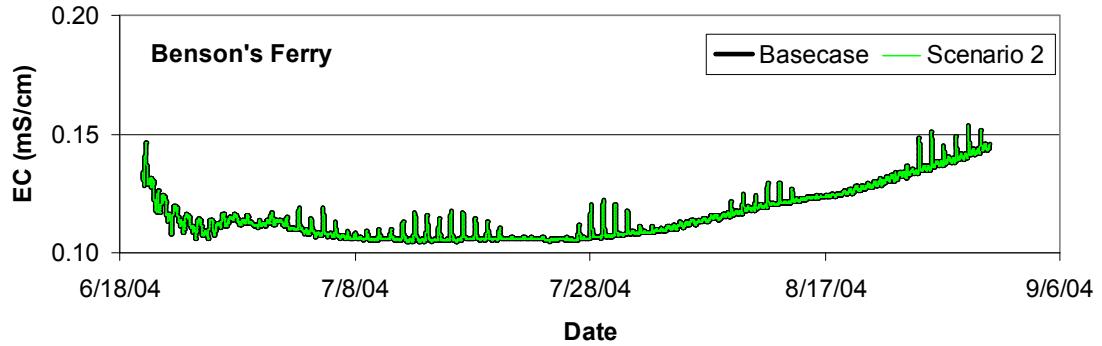


**Figure F-19:** Comparison of calibrated base case plotted with scenario 2 for 2004 electrical conductivity at Benson's Ferry.

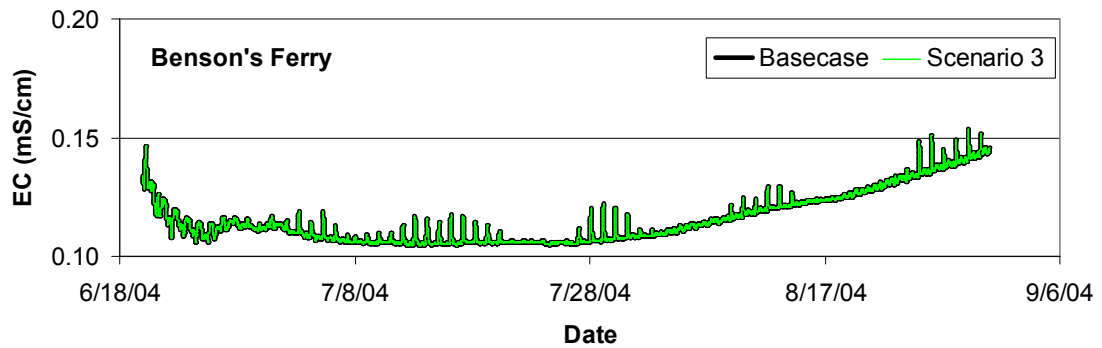


**Figure F-20:** Comparison of calibrated base case plotted with scenario 3 for 2004 electrical conductivity at Benson's Ferry.

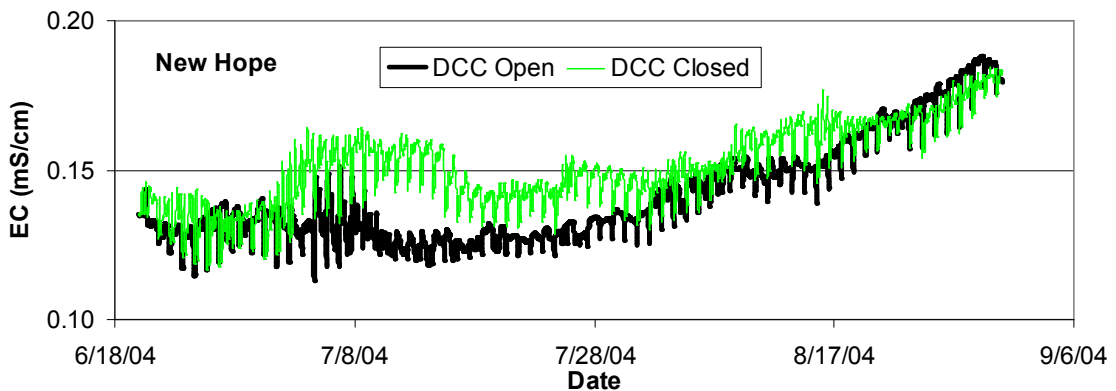


**Figure F-21:** Scenario four at New Hope where the Delta Cross Channel (DCC) is closed with the calibrated base case that has the DCC open.

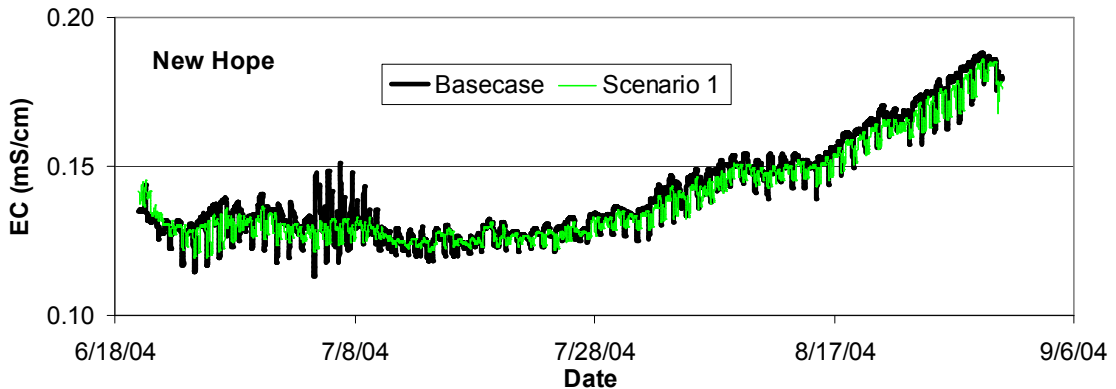


**Figure F-22:** Comparison of calibrated base case plotted with scenario 1 for 2004 electrical conductivity at New Hope.

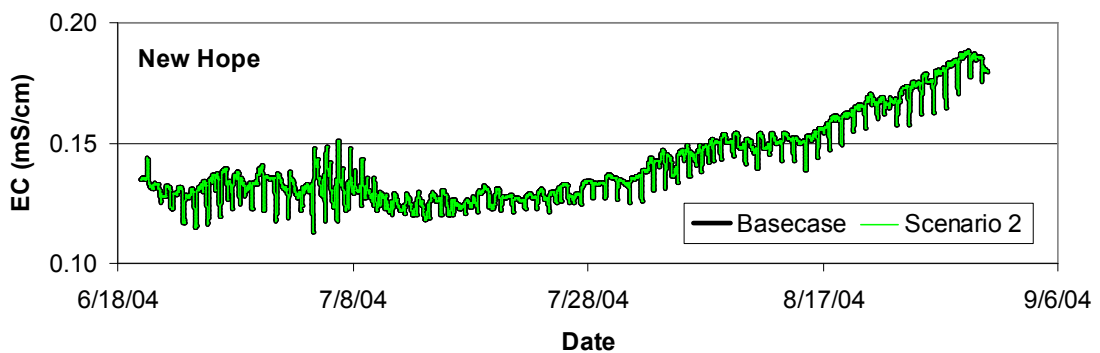


**Figure F-23:** Comparison of calibrated base case plotted with scenario 2 for 2004 electrical conductivity at New Hope.

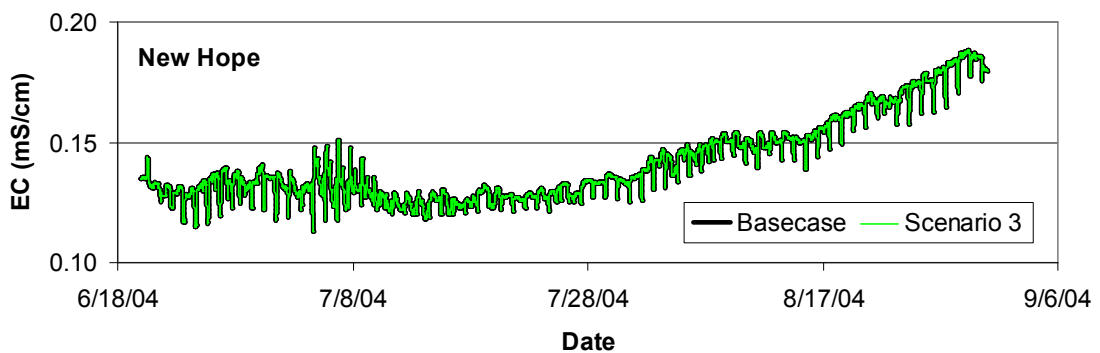


**Figure F-24:** Comparison of calibrated base case plotted with scenario 3 for 2004 electrical conductivity at New Hope.

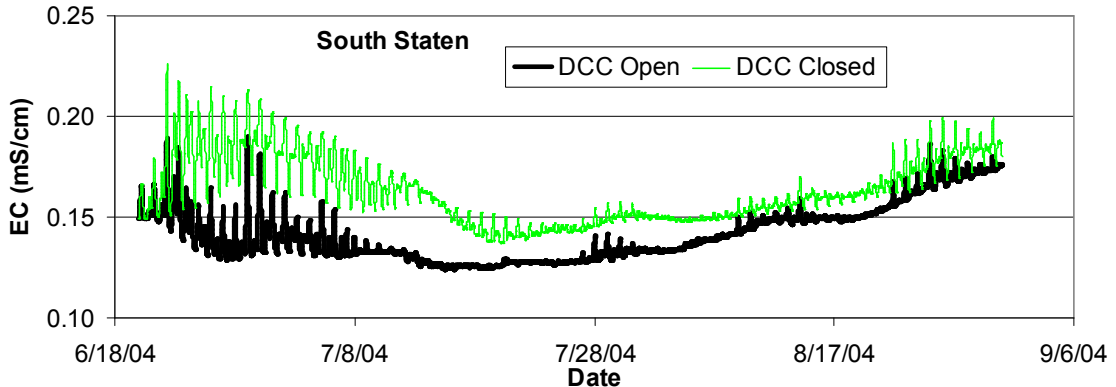


**Figure F-25:** Scenario four at South Staten where the Delta Cross Channel (DCC) is closed with the calibrated base case that has the DCC open.

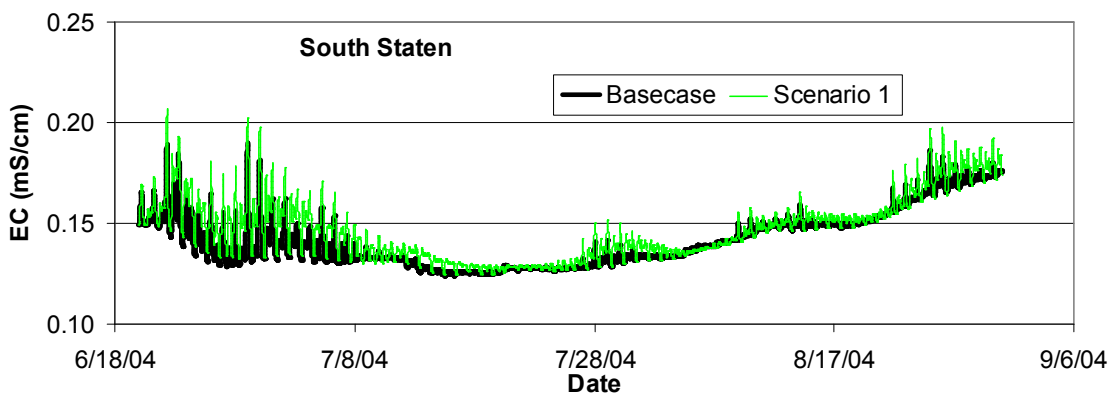


**Figure F-26:** Comparison of calibrated base case plotted with scenario 1 for 2004 electrical conductivity at South Staten.

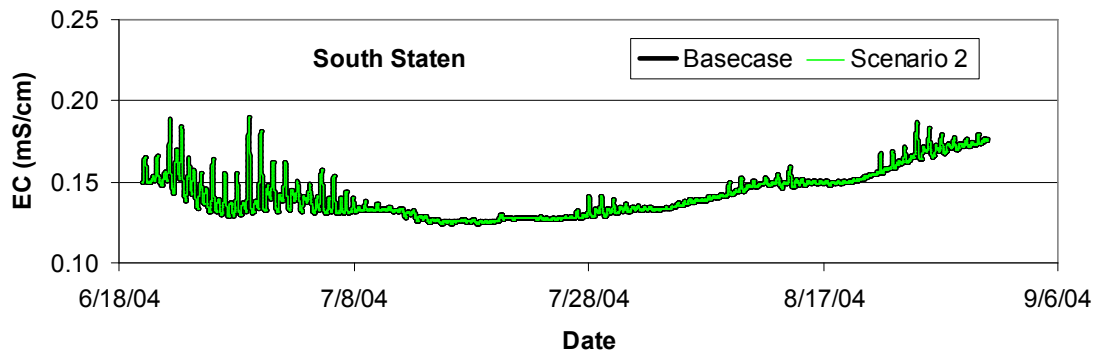


**Figure F-27:** Comparison of calibrated base case plotted with scenario 2 for 2004 electrical conductivity at South Staten.

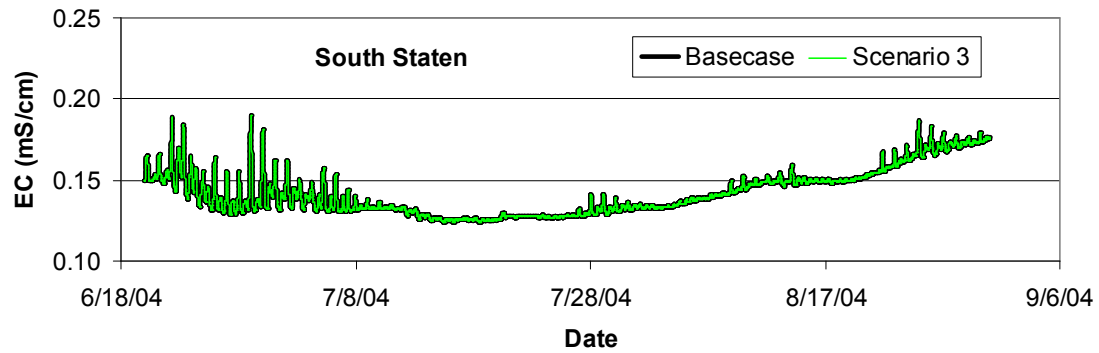


**Figure F-28:** Comparison of calibrated base case plotted with scenario 3 for 2004 electrical conductivity at South Staten.

## APPENDIX G

This appendix contains graphs that plot all the input data which was required for the 2003 water quality model simulation.

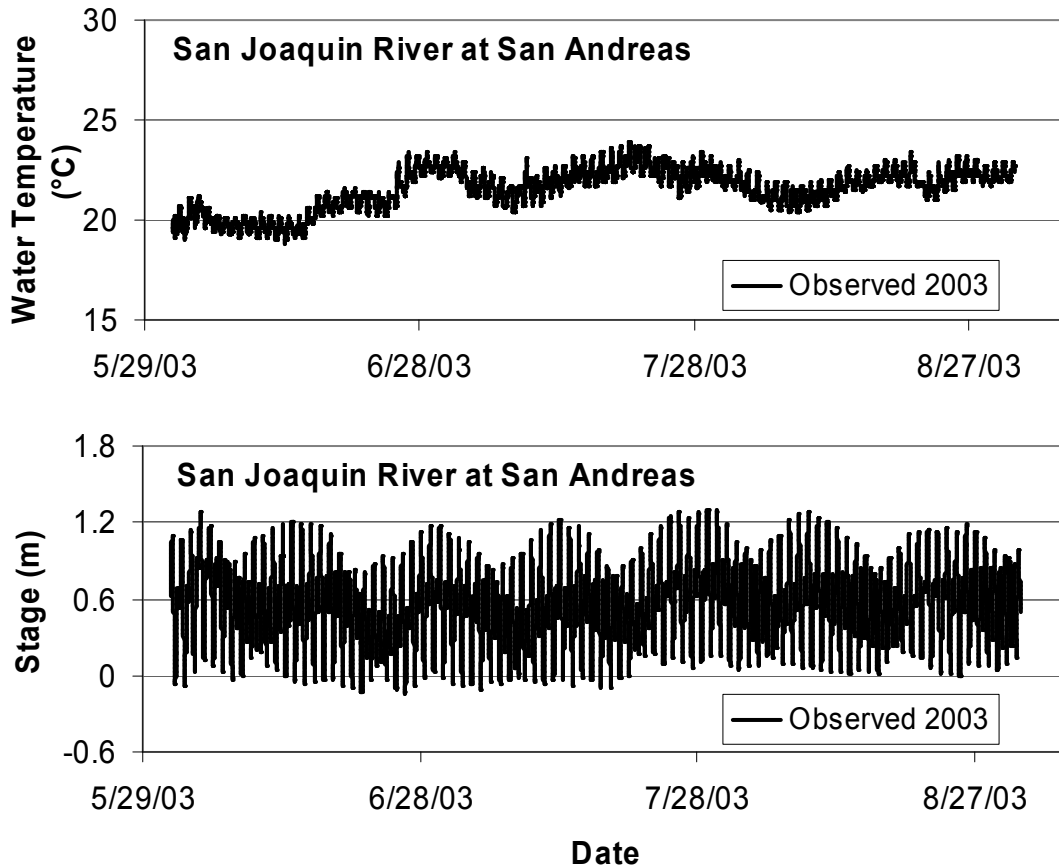


**Figure G-1:** Water temperature and stage measured data that was input in the model for the 2003 simulations at the boundary point along the San Joaquin River at San Andreas Landing.

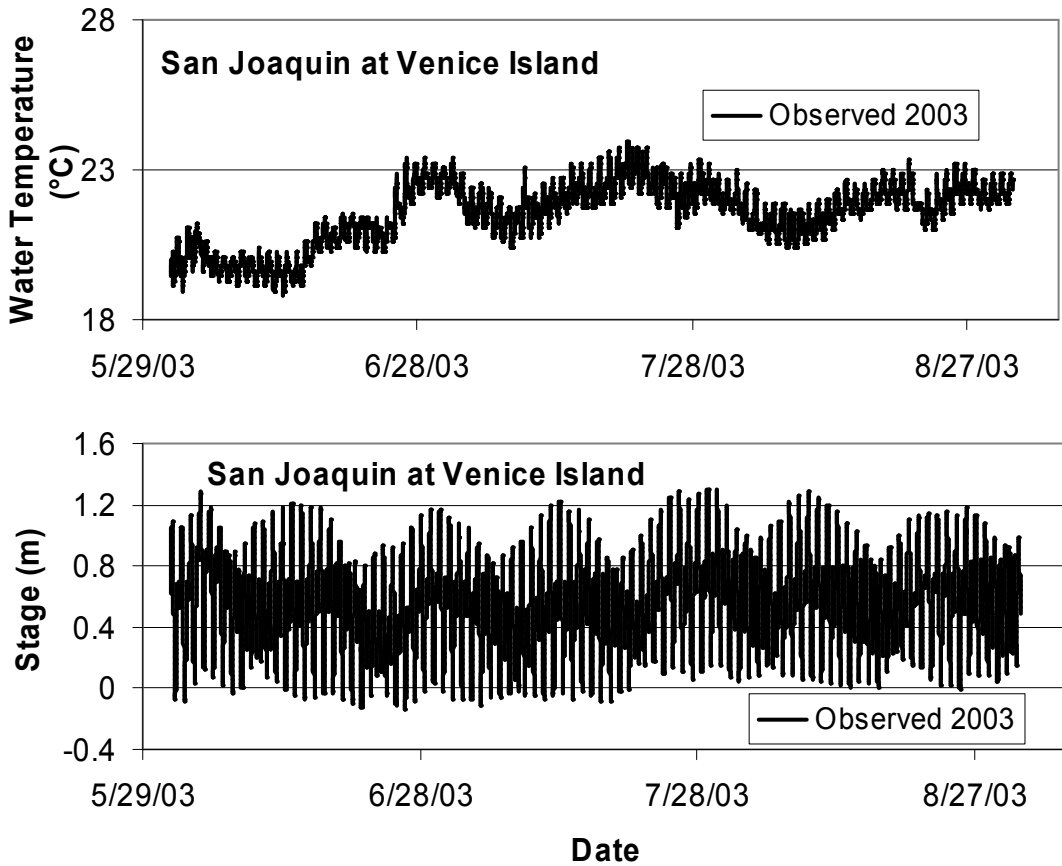


**Figure G-2:** Water temperature and stage measured data that was input in the model for the 2003 simulations at the boundary point along the San Joaquin River near Venice Island.

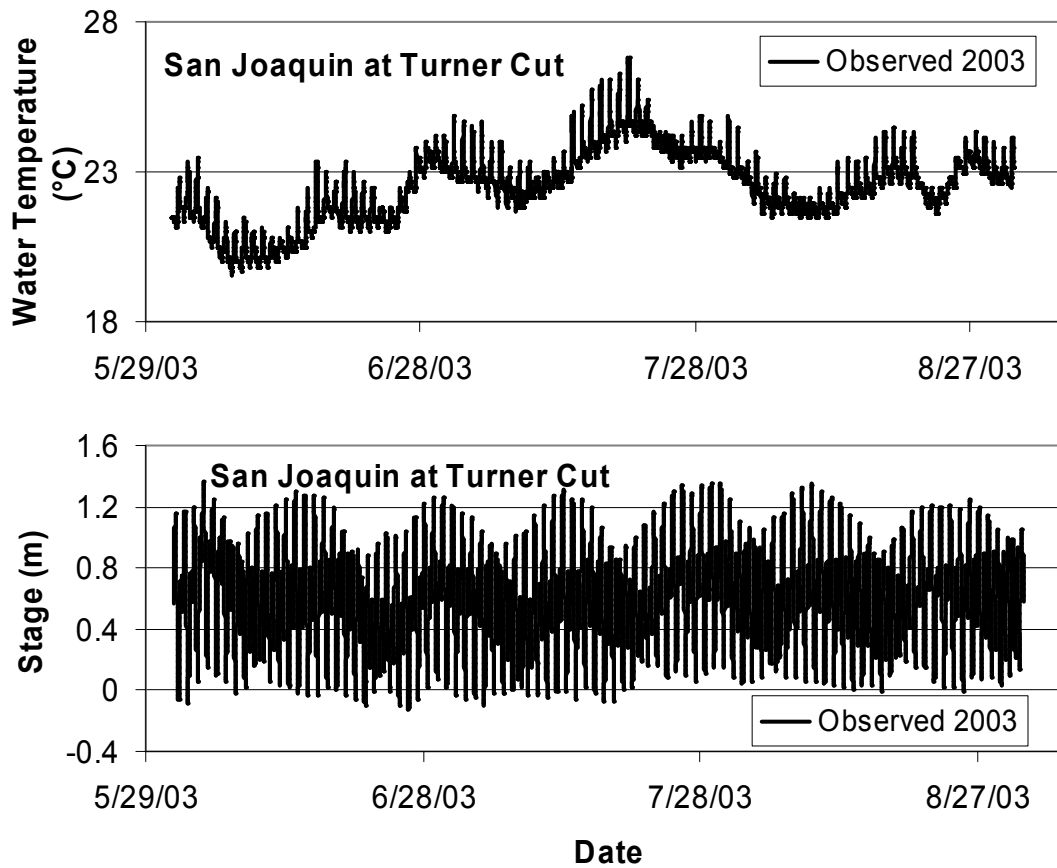


**Figure G-3:** Water temperature and stage measured data that was input in the model for the 2003 simulation at the boundary point along the San Joaquin River near Turner Cut.

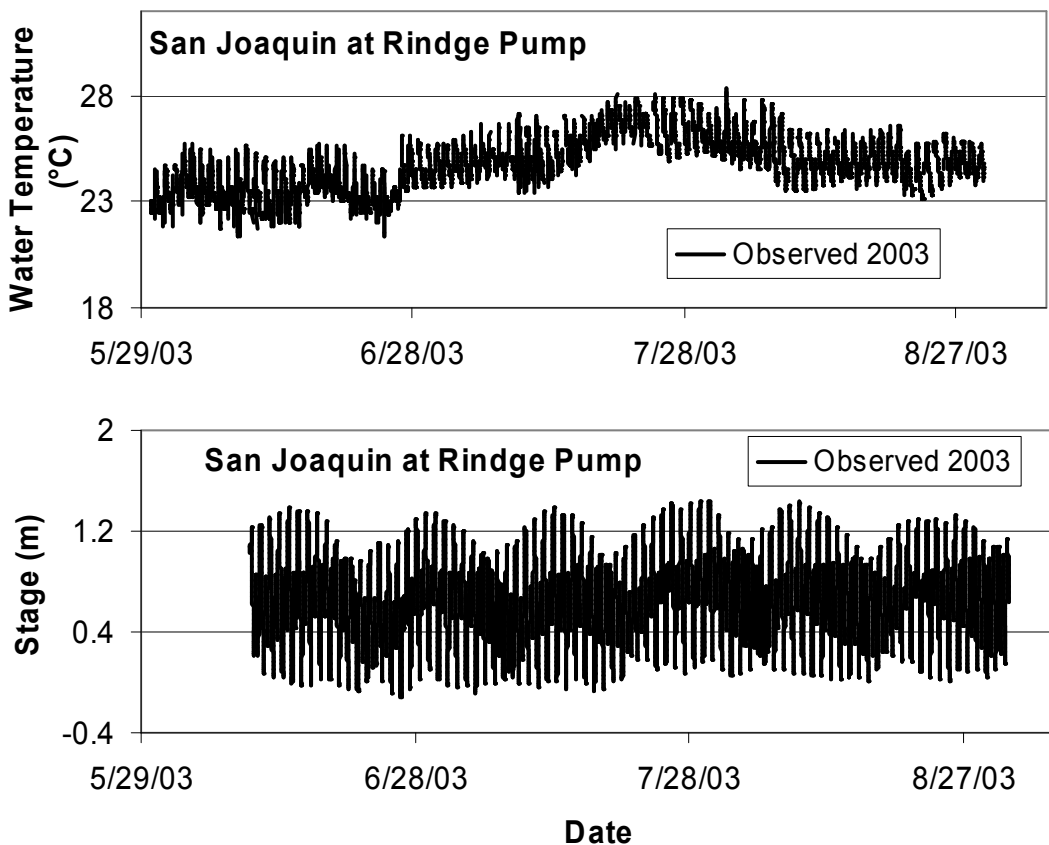


**Figure G-4:** Water temperature and stage measured data that was input in the model for the 2003 simulation at the boundary point along the San Joaquin River near Rindle Pump.

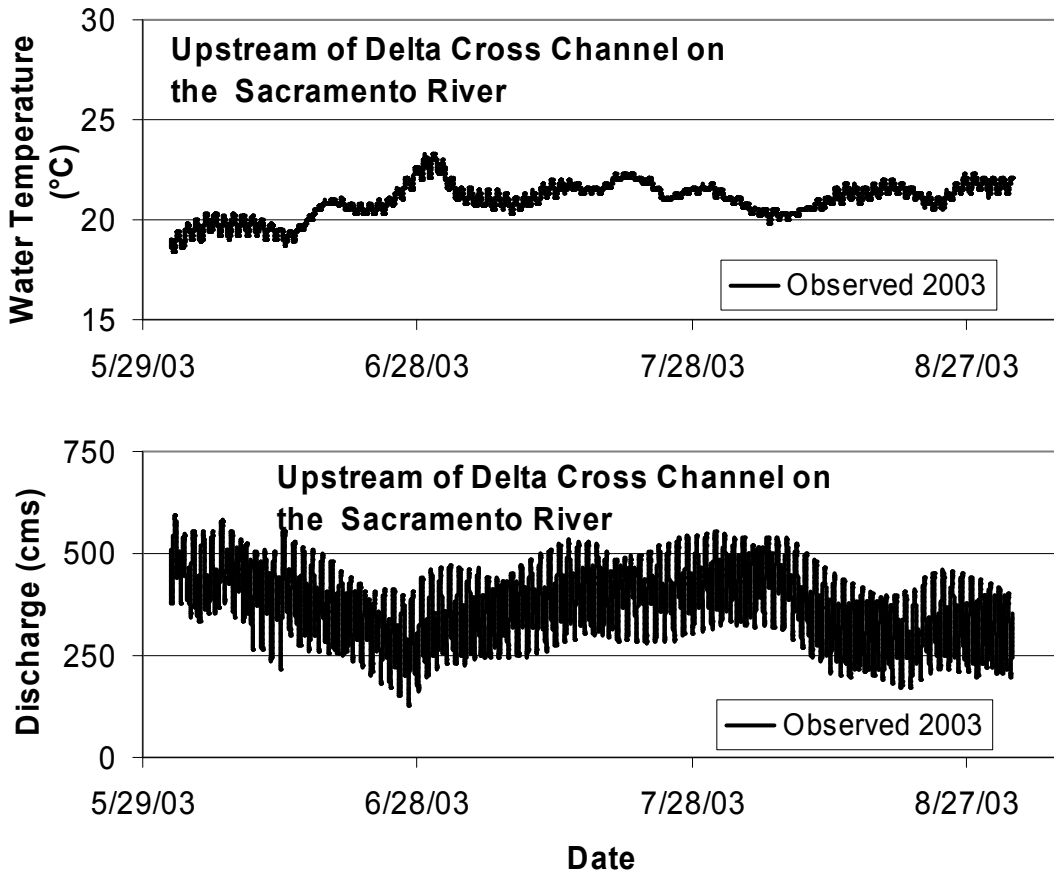


**Figure G-5:** Water temperature and discharge measured data that was input in the model for the 2003 simulation at the boundary point along the Sacramento River upstream of the Delta Cross Channel.

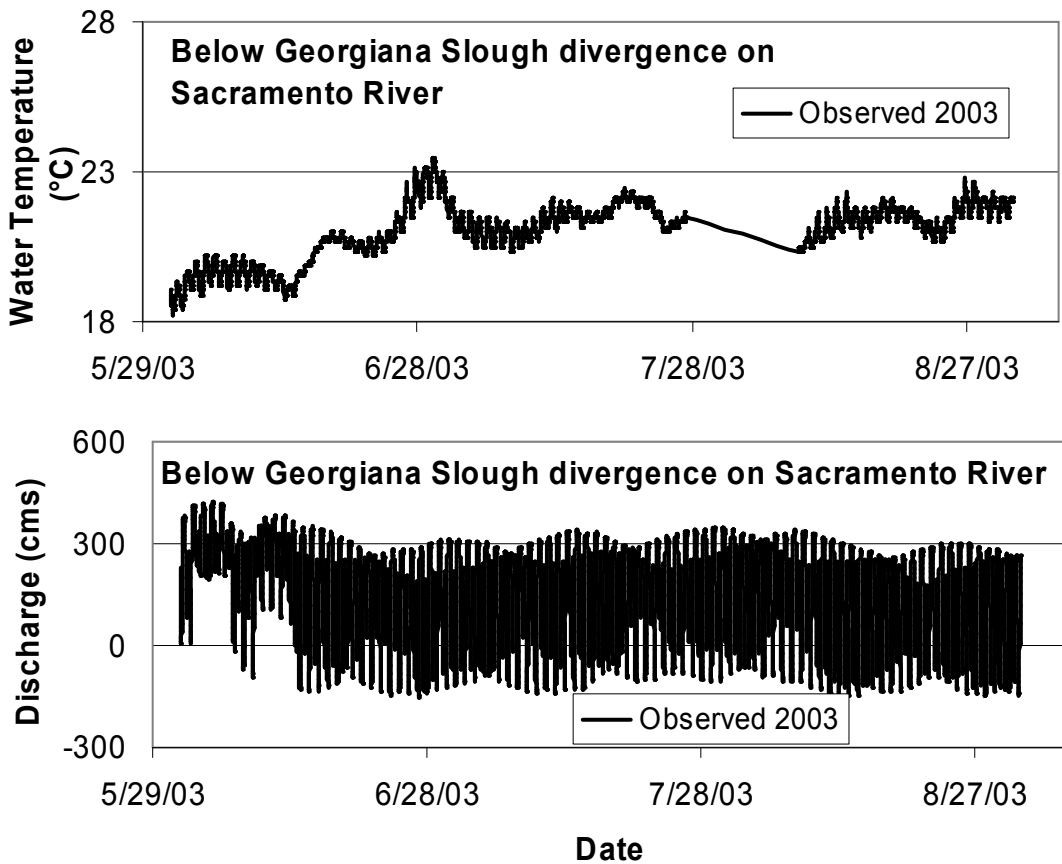


**Figure G-6:** Water temperature and discharge measured data that was input in the model for the 2003 simulations at the boundary point along the Sacramento River below the Georgiana Slough divergence.

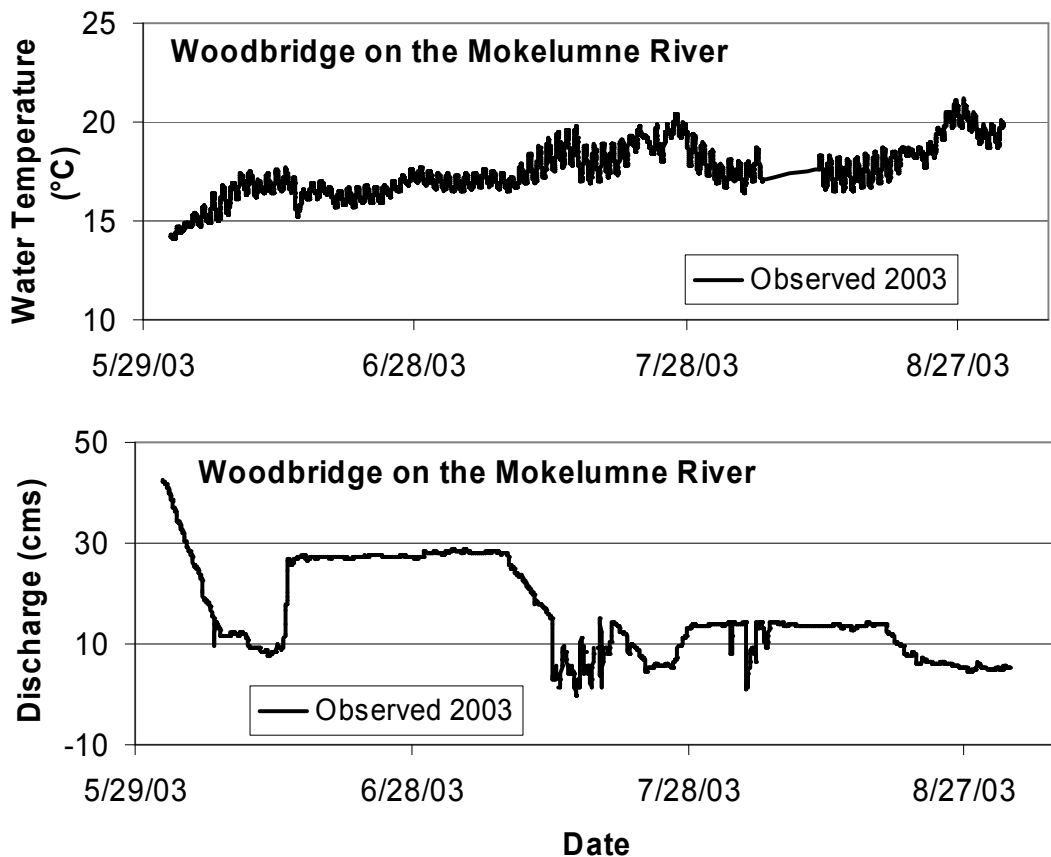


**Figure G-7:** Water temperature and discharge measured data that was input in the model for the 2003 simulations at the boundary point along the Mokelumne River below the Woodbridge Dam.

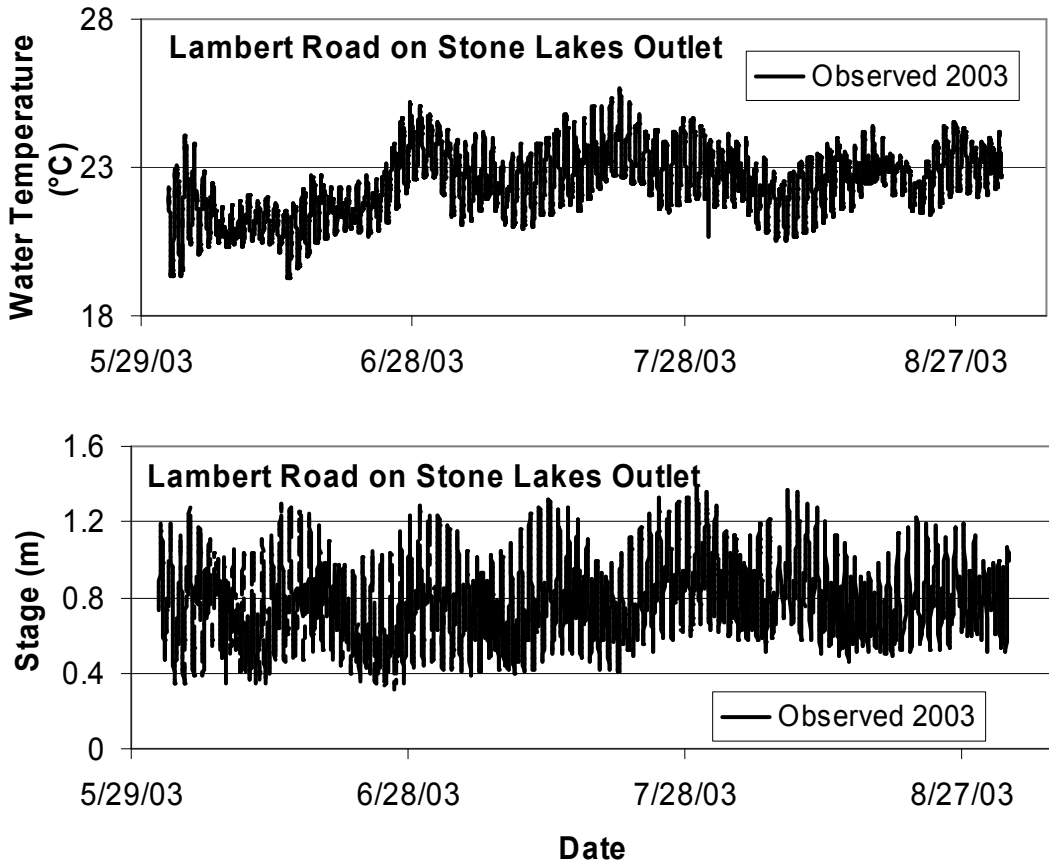


**Figure G-8:** Water temperature and stage measured data that was input in the model for the 2003 simulations at the boundary point at the Stone Lake Outlet just north of Lambert Road.

## APPENDIX H

This appendix contains graphs that plot all the input data which was required for the 2004 water quality model simulation.

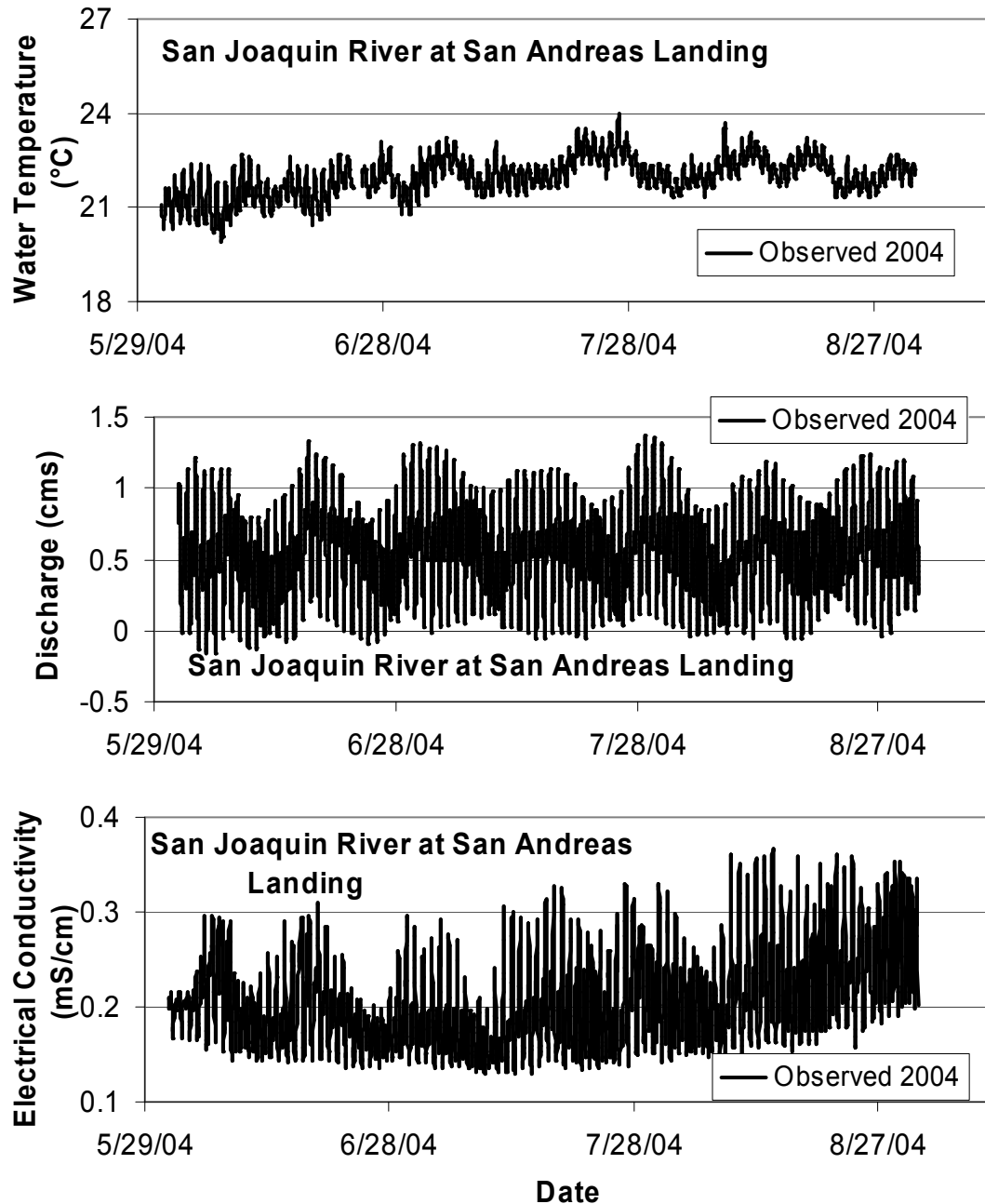


**Figure H-1:** Water temperature, discharge, and electrical conductivity measured data that was input in the model for the 2004 simulations at the boundary point along the San Joaquin River at San Andreas Landing.

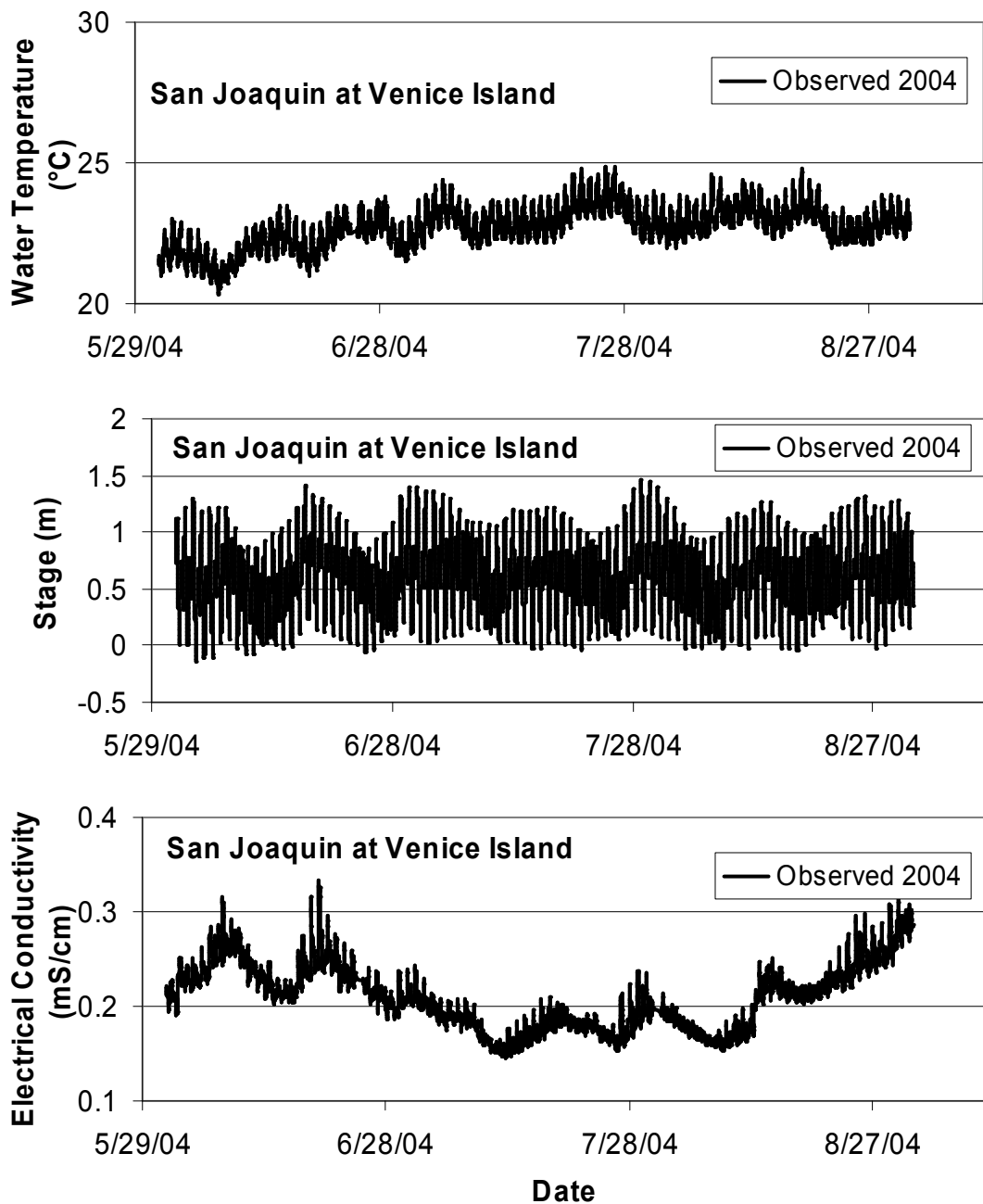


**Figure H-2:** Water temperature, stage, and electrical conductivity measured data that was input in the model for the 2004 simulations at the boundary point along the San Joaquin River near Venice Island.

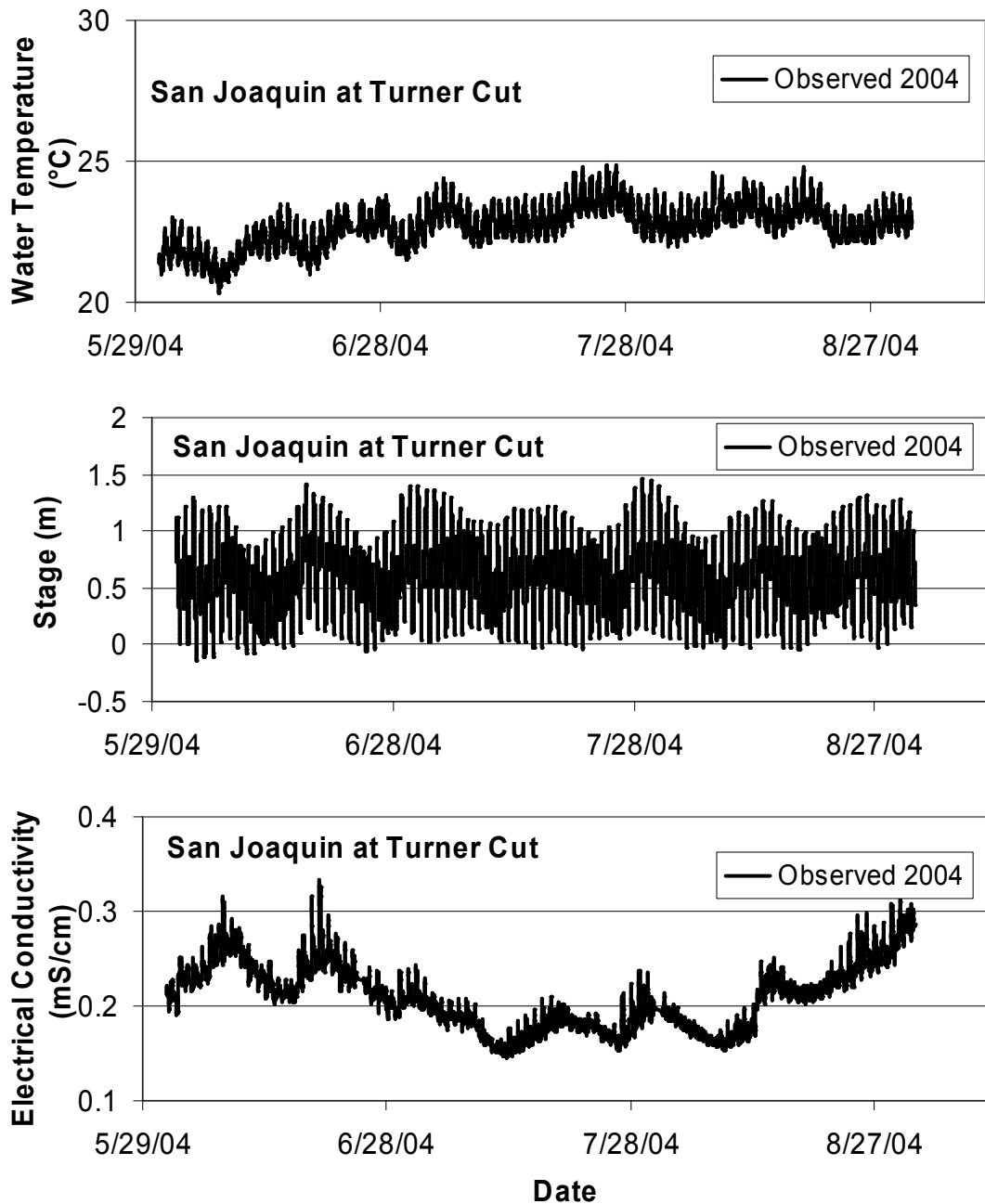


**Figure H-3:** Water temperature, stage, and electrical conductivity measured data that was input in the model for the 2004 simulation at the boundary point along the San Joaquin River near Turner Cut.

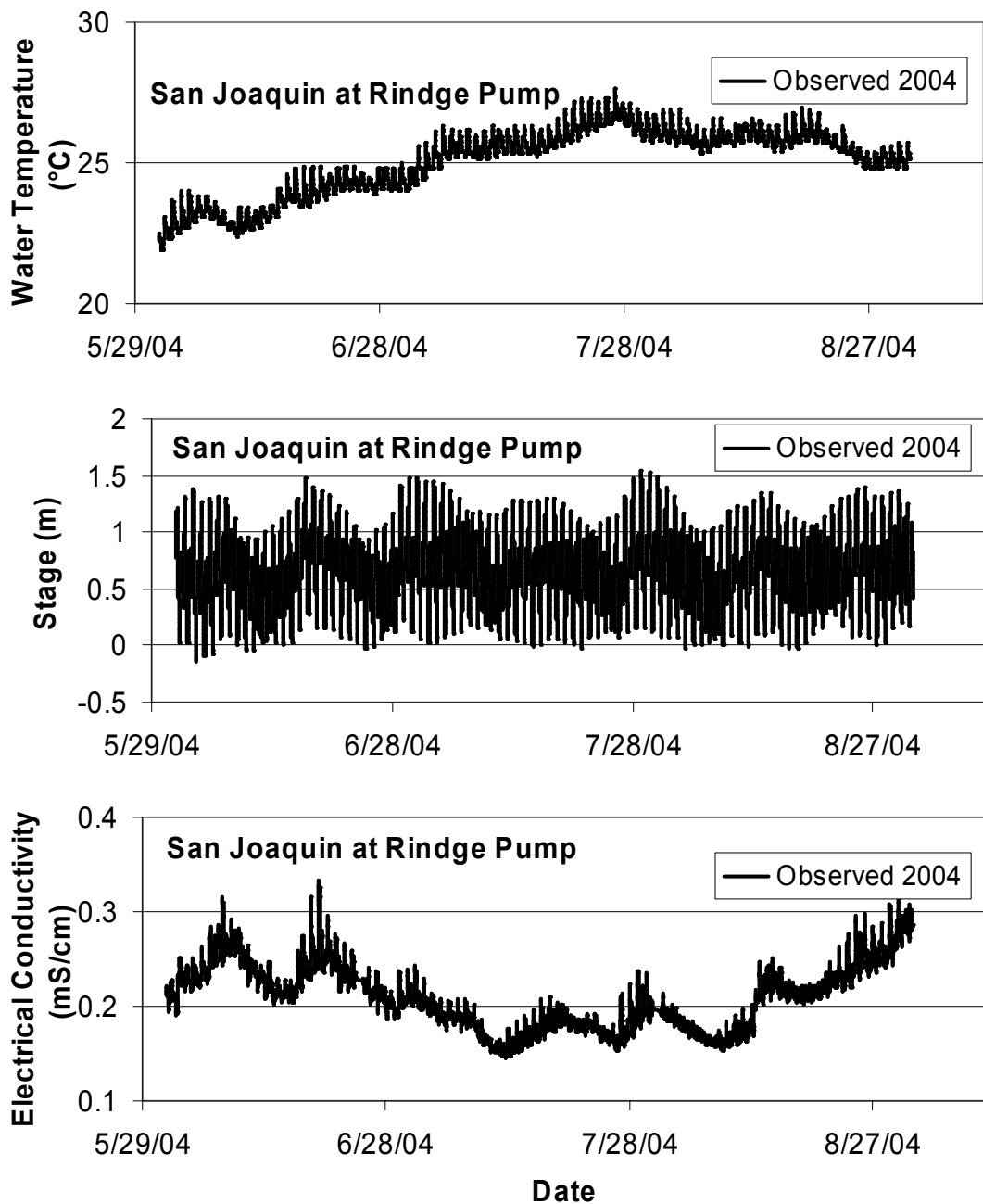


**Figure H-4:** Water temperature, stage, and electrical conductivity measured data that was input in the model for the 2003 simulation at the boundary point along the San Joaquin River near Rindle Pump.

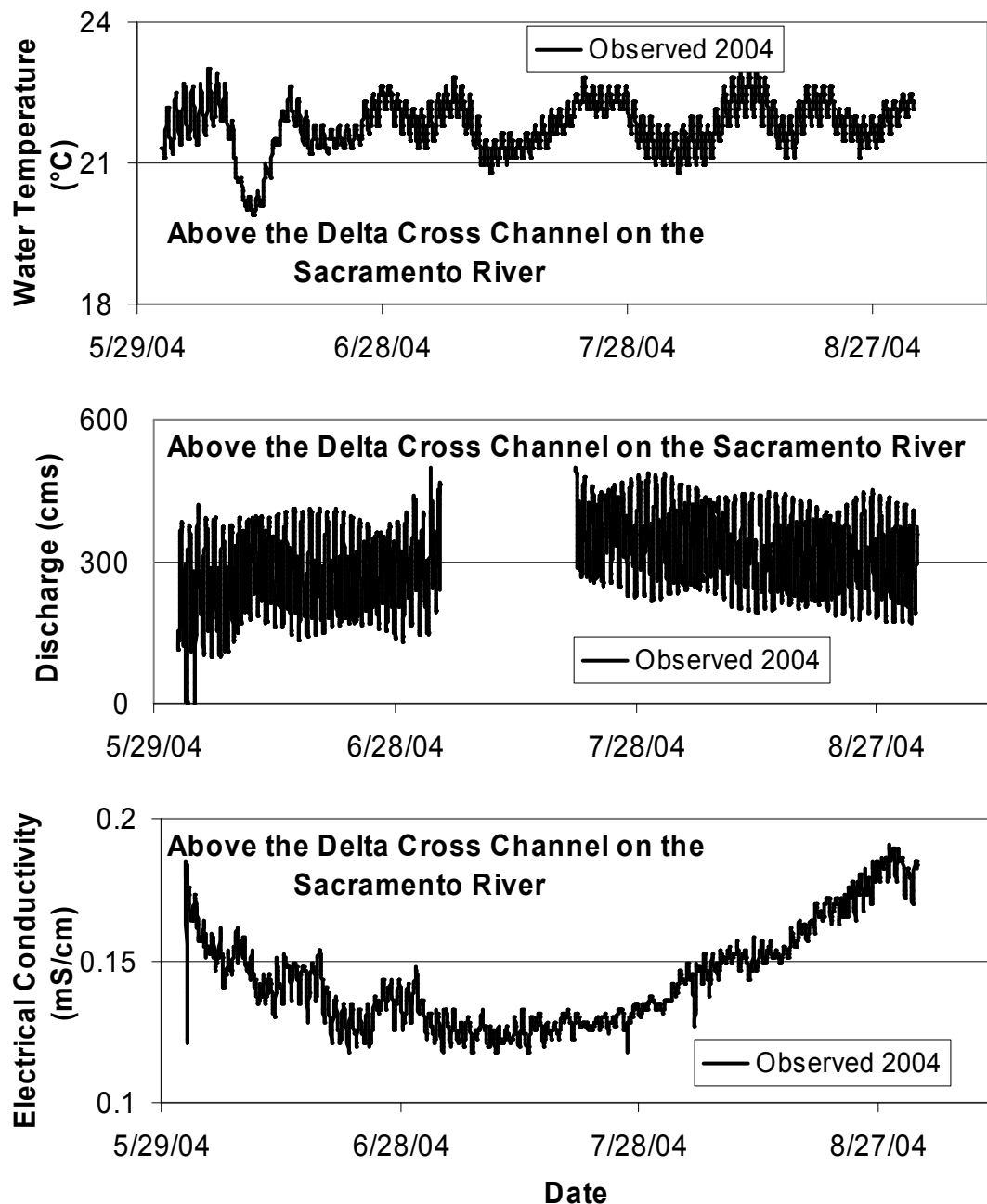


**Figure H-5:** Water temperature, discharge, and electrical conductivity measured data that was input in the model for the 2004 simulation at the boundary point along the Sacramento River upstream of the Delta Cross Channel.

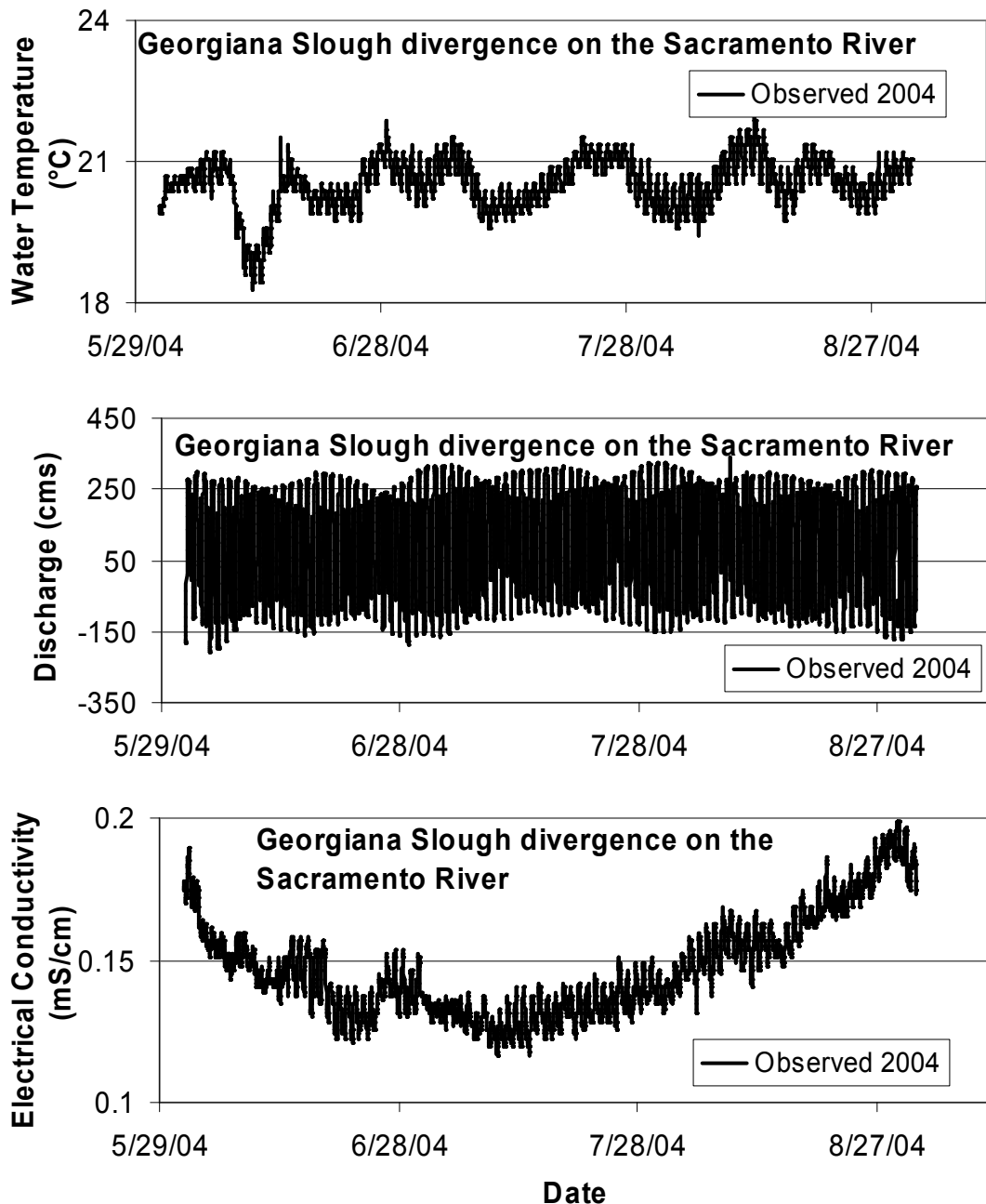


**Figure H-6:** Water temperature, discharge, and electrical conductivity measured data that was input in the model for the 2004 simulations at the boundary point along the Sacramento River below the Georgiana Slough divergence.

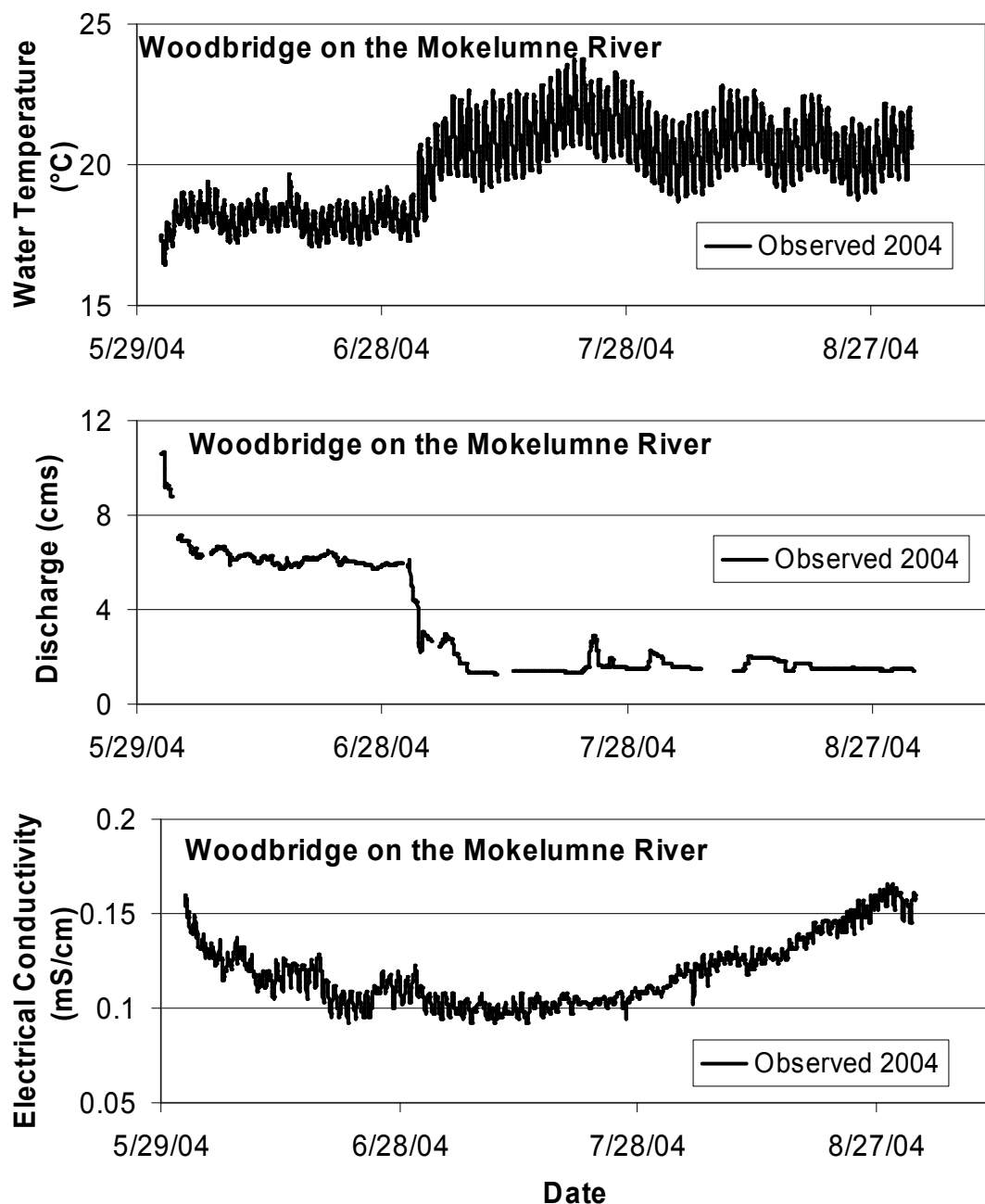


**Figure H-7:** Water temperature, discharge, and electrical conductivity measured data that was input in the model for the 2004 simulations at the boundary point along the Mokelumne River below the Woodbridge Dam.

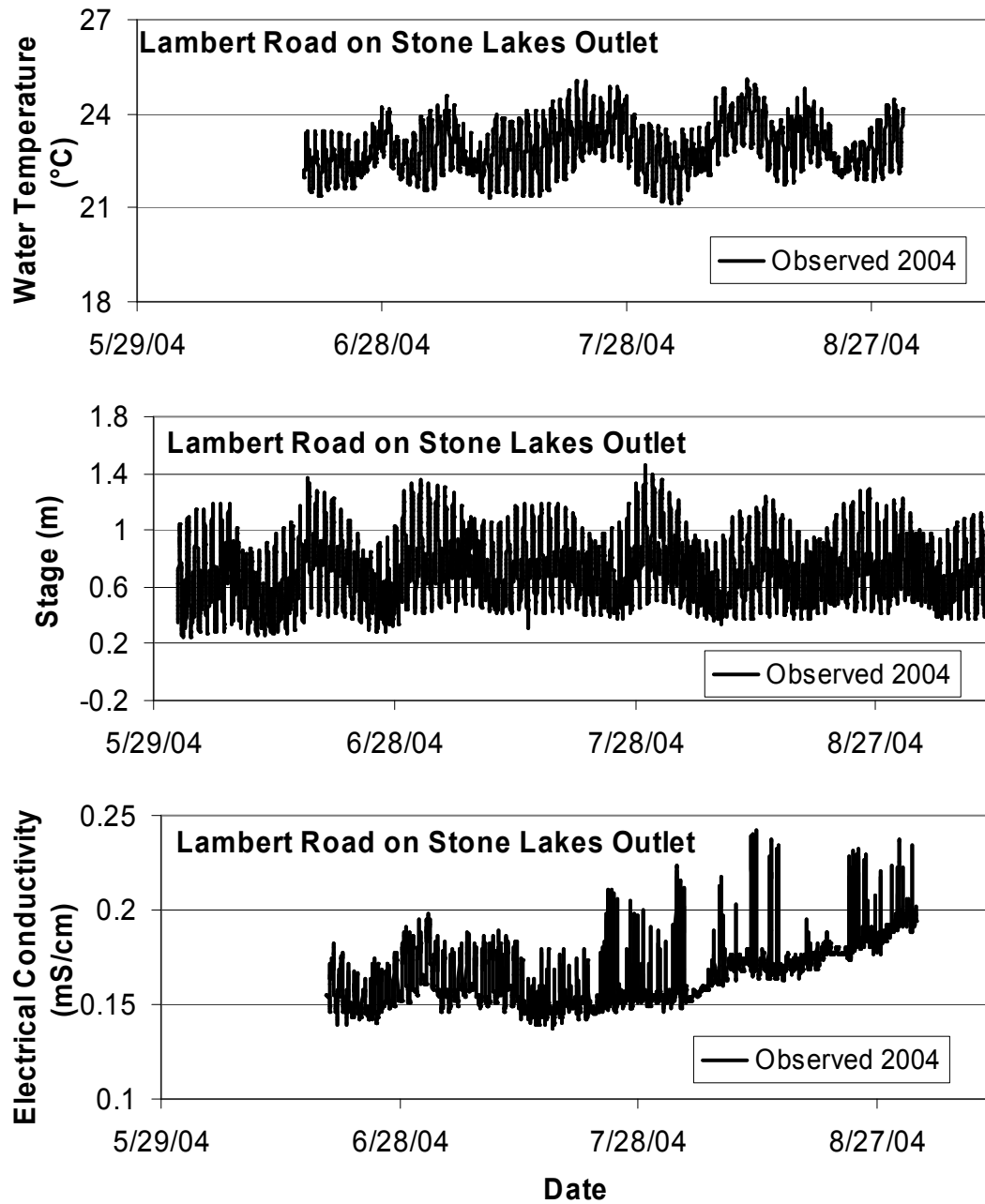


**Figure H-8:** Water temperature, stage, and electrical conductivity measured data that was input in the model for the 2004 simulations at the boundary point at the Stone Lake Outlet just north of Lambert Road.